Hydrological Drought

A Study across Europe

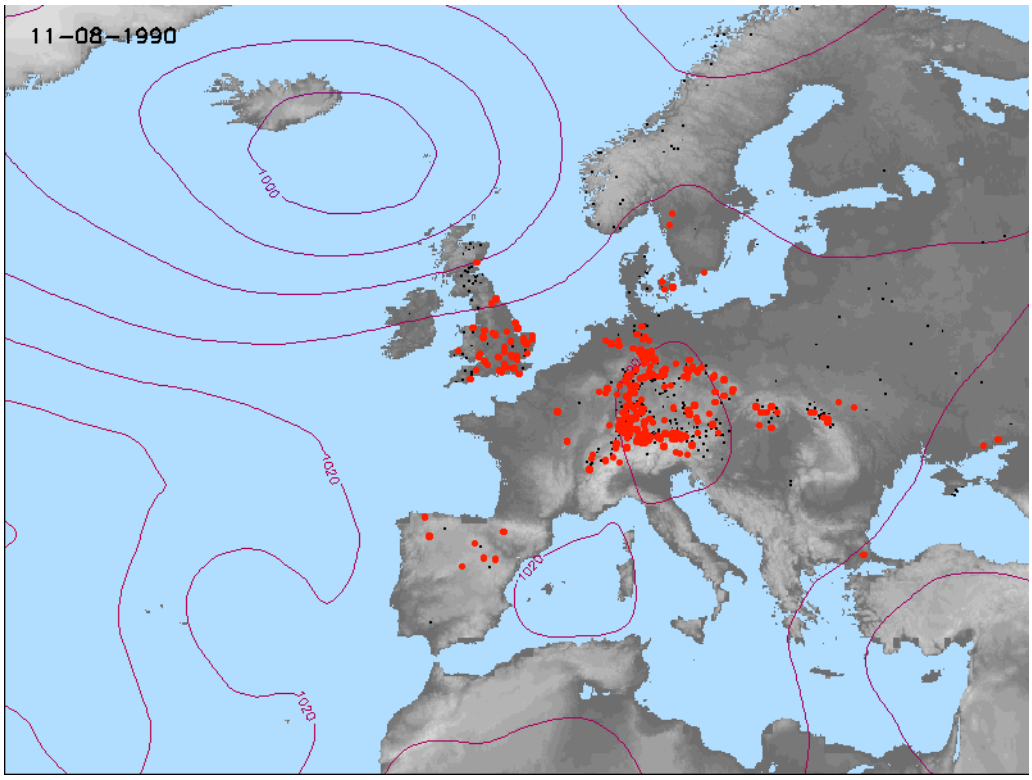

Kerstin Stahl

Hydrological Drought

A Study across Europe

Dissertation
zur Vergabe des Doktorgrades
der
Geowissenschaftlichen Fakultät
der
Albert-Ludwigs-Universität Freiburg i. Br.

vorgelegt von
Kerstin Stahl
aus Offenburg
Mai, 2001

Dekan: Professor Dr. Jan Behrmann

Referent: Professor Dr. Siegfied Demuth

Korreferent: Professor Dr. Lena Tallaksen

Tag der Beschlussfassung des Promotionsausschusses: 28.06.2001

Contents

List of Figures

List of Tables

Abbreviations

ACD	Annual cumulated duration of all drought events (days)
ACV	Annual cumulated deficit volume standardised by seasonal mean flow (days)
AMD	Annual maximum drought duration (days)
AMHY	Alpine and Mediterranean HYdrology FRIEND project
AMV	Annual maximum deficit volume standardised by seasonal mean flow (days)
ARIDE	Assessment of the regional impact of drought in Europe
BMDI	Bhalme-Mooley Drought Index
CDAS	Climate Data Assimilation System
CEH	Centre for Ecology and Hydrology, Wallingford (formerly Institute of Hydrology)
CP	Atmospheric circulation pattern
CPgx	CP group number x
CRED	Centre of Research on the Epidemiology of Disasters
CRU	Climate Research Unit at the University of East Anglia
Cx	Cluster number x
EEA	European Environment Agency
ElektrA	Electronic drought Atlas
EM-DAT	Emergency Events Database
EWA	European Water Archive
fdc	Flow duration curve
FRIEND	Flow Regimes from International Network Data
GCM	Global Circulation Models
GPCC	Global Precipitation Climate Centre
GRDC	Global Runoff Data Centre
IPCC	Intergovernmental Panel on Climate Change
ITCZ	Inner tropical convergence zone
Med-HYCOS	Mediterranean Hydrological Cycle Observing System
MSLP	Mean sea level pressure

NAO	North Atlantic Oscillation
NCAR	National Center for Atmospheric Research
NCEP	National Centers for Environmental Prediction
ND	Number of drought events per year (-)
NDMC	National Drought Mitigation Center.
NOAA	National Oceanic and Atmospheric Administration
OFDA	Office of US Foreign Disaster Assistance
PDSI	Palmer drought severity index
PNA	Pacific North America Index
USGS	United States Geological Survey

Symbols

a	coefficient of agreement
α	significance level
b_i	weight factor for CP group i
D	distance
d_i	drought duration
DI	deficiency/drought indicator
E	expectation
G	gauging station
O	observed values
p	percentile from the flow duration curve
P	predicted values
Q	discharge (m^3/s)
q_0	threshold level (streamflow in m^3/s)
Q70	flow exceeded for 70% of the time (rep. Q90, Q80 etc.)
r	Pearson product moment correlation coefficient
RDI	regional streamflow deficiency index
$RDIarea$	cluster homogeneity parameter (deviation of RDI distribution from optimum)
RDI_{sim}	simulated RDI
s_i	drought severity of event i
t	time
T	test statistic
Var	variance
Y	model state for regional streamflow deficiency
y_0	threshold for onset of RDI_{sim} from Y
Z	occurrence of CP group

Abstract

The occurrence of droughts in the 1980s and 1990s has raised the awareness of the impact of this natural hazard across Europe. With climate change studies even predicting more severe hydrological extremes for the future, already competing demands for water resources may further aggravate. On this background, the ARIDE (Assessment of the Regional Impact of Droughts in Europe) project, in the framework of which this study was carried out, addressed different aspects of hydrological drought at the pan-European scale. Aiming at a better understanding of drought causes and processes, the present study investigated drought characteristics in space and time and their large-scale atmospheric driving forces.

From the European Water Archive, the database of the FRIEND (Flow Regimes from International Network Data) project, daily streamflow data of more than 600 European rivers were available for a common reference time period from 1962 to 1990. The catchments of this dataset cover a great part of western, northern, central, and eastern Europe, and Spain, thus representing several different climatic zones and diverse environments. Consequently, the river flow regimes and the low flow seasons in the study area vary strongly. Two different types of events were therefore defined from the European streamflow dataset: *streamflow drought*, defined by a classic seasonally constant threshold level method and *streamflow deficiency*, defined by a new varying threshold level method. Streamflow deficiency events were defined as periods when the streamflow is below a varying threshold describing a typically expected annual cycle of low flows by the Q90 values of daily flow duration curves.

Time series analyses on the available streamflow drought and deficiency series characterised the persistency and stationarity of the dataset for the reference period, as well as for smaller datasets covering longer periods. Considerable within-year and even inter-annual persistency was detected and trends across Europe were found. The results depend strongly on the analysed time period. For the reference period, increasing trends of drought severity were found in Spain, southeastern UK and Slovakia. Another initial analyses explored the synoptic meteorological causes for the spatial and temporal dynamics of major streamflow deficiency events, which affected Europe in the early 1960s, the mid-1970s and the late 1990s. The method, a new visualisation application, which allows to simultaneously display animated sequences of maps of contoured mean sea level pressure and streamflow deficiency conditions across Europe, generally demonstrated a strong regional response of surface hydrology

to the synoptic situation. Similarities concerning the causes and regional development of the major events, but also differences between the events were found.

By the means of cluster analysis, the 602 streamflow deficiency series across Europe were classified into 19 groups, which resulted in spatially coherent regions despite the purely statistical method. The introduction of a regional streamflow deficiency index (*RDI*) for each cluster provided a daily parameter, which describes how strong a region is affected by streamflow deficiency. Hence, the index allowed a first regional assessment of the space-time characteristics of the major dry spells in the reference period 1962-90. Regions such as Spain, southeastern UK, southern Scandinavia and northern Germany show a tendency to persistent dry spells while the index fluctuates more strongly in other regions.

The regional index further provided a suitable basis to analyse the influence of synoptic meteorology on streamflow deficiencies across Europe. Typical circulation patterns causing dry spells were detected based on anomalies of the occurrence frequencies of atmospheric circulation patterns (*Europäische Großwetterlagen*) during times of severe regional streamflow deficit. The 30 different circulation patterns (CPs) were grouped according to their seasonal forcing. These CP-groups finally provided an adequate input for a new model, which predicts the regional streamflow deficiency index on the occurrence of the circulation patterns. To model the link, a basic recursive approach conditioning the *RDI* on the *RDI* of the previous day and the occurring CP-group was applied. Good model fits were obtained for most clusters using a 17-year calibration period. In particular seasonally aggregated values of extreme events are well comparable with the observed series.

Finally, two different applications of the CP-*RDI* link model were tested: historic reconstruction and scenario prediction of regional streamflow deficiency indices. Regional streamflow deficiency indices were reconstructed for the whole period 1881-1998, for which the circulation patterns are available. As a comparison with documented historic droughts gave strong confidence in the reconstruction, some tentative conclusions on the impact of climatic changes on the drought situation across Europe were drawn. The trend towards drier conditions in the end of the 20th century in Spain was confirmed and regions in northern Germany and southern Scandinavia exhibit a shift in the variability of the index series towards longer dry spells after the 1960s. This shift might be a consequence of the widely reported change to more persistent synoptic meteorological conditions. The response to a scenario, which was motivated by changes in circulation patterns attributed to climate change, are basically in line with common findings. Most of Europe will be exposed to generally wetter conditions, however rare and severe drought events are likely to increase, particularly in vulnerable regions such as Spain, southeastern UK and northern Germany.

It can be concluded that droughts have a considerable impact on several regions in Europe. As demonstrated in this study, forecasting and prediction of the regional drought conditions based on the relationship to atmospheric circulation patterns yield a great potential for a valuable accomplishment of discussed drought watch systems and improved drought management for Europe.

Zusammenfassung

Das Auftreten von Dürreperioden in verschiedenen Regionen Europas in den 80iger und 90iger Jahren sowie die Vorhersagen verstärkter hydrologischer Extreme bei einer Klimaänderung haben die Themen Trockenheit und Wassermangel wieder stärker in den Blickpunkt gerückt. Als eine der ersten europaweiten hydrologischen Untersuchungen, beschäftigte sich das EU Projekt ARIDE (Assessment of the Regional Impact of Droughts in Europe), in dessen Rahmen die Forschungsarbeiten zu dieser Dissertation durchgeführt wurden, mit verschiedenen Aspekten des Themenkreises. Die hier vorgestellte Arbeit behandelt die räumlich-zeitlichen Ausprägungen hydrologischer Trockenperioden sowie deren meteorologische Ursachen in Europa. Ein besseres Verständnis der großräumigen Prozesse ist Voraussetzung sowohl für die direkte Vorhersage als auch für die Planung nachhaltiger Wasserbewirtschaftungsaspekte auf überregionaler Ebene.

Mittlere Abflüsse von über 600 Pegeln aus der FRIEND-Datenbank, die eine gemeinsame Zeitreihe von 1962 bis 1990 umfassen, stellt die Datengrundlage für die Untersuchung dar. Verteilt über West-, Nord-, Mittel- und Osteuropa sowie Spanien, umfasst das Untersuchungsgebiet verschiedene Klimazonen und Naturräume. Dementsprechend vielfältig sind auch die Abflussregime und das jahreszeitliche Auuftreten von Niedrigwasser. Um der daraus resultierenden hydrologischen Vielfalt gerecht zu werden, wurden zwei verschieden Ereignistypen aus den Abflusszeitreihen gewonnen: Hydrologische Dürre, definiert als Unterschreitung eines konstanten Schwellenwertes und Abflussdefizite, definiert mittels eines neuen variablen Schwellenwertkonzeptes. Der variable Schwellenwert stellt hierbei einen Jahreszyklus der zu erwartenden Niedrigwasserabflüsse dar und bestimmt somit relative Niedrigwasserperioden gemessen am typischen Jahresgang des Abflusses.

Durchgeführte Zeitreihenanalysen erlaubten die Charakterisierung des zeitlichen Persistenzverhaltens und der Stationarität der Trockenperioden im Untersuchungsraum. Dabei lassen sich regionale Unterschiede im Persistenzverhalten zum Teil mit vorherrschenden Einzugsgebietseigenschaften erklären. Trends zu stärkeren und anhaltenderen Trockenperioden von 1962 bis 1990 konnten für Spanien, Südostengland und die Slovakei gefunden werden, während insbesondere der Norden und Osten Europas eher Trends zu schwächeren und kürzereren Trockenperioden zeigt. Eine weitere explorative Untersuchung des Datensatzes behandelte die räumlich-zeitliche Dynamik der Trockenperioden im Spiegel der synoptischen meteorologischen Situation. Mittels einer neuen Visualisierungsanwendung zur zeitlichen

Animation von täglichen Karten der Bodenluftdruckverteilung und der farbcodierten Abflussbedingungen, konnte eine starke Reaktion der Hydrologie auf Veränderungen im Zirkulationsgeschehen gezeigt und analysiert werden. Die detaillierte Beschreibung der räumlich ausgeprägten europäischen Trockenperioden Anfang der 60iger, Mitte der 70iger und Ende der 80iger Jahre demonstriert sowohl Gemeinsamkeiten als auch Unterschiede bezüglich der Ursachen und der Dynamik der Ereignisse.

Mittels einer Clusteranalyse wurden die 602 Abflussdefizit-Zeitreihen in 19 homogene Gruppen klassifiziert. Durch die starke räumliche Ausprägung von Trockenperioden ergaben sich hierbei räumlich zusammenhängende Regionen, obwohl die Klassifikation rein statistische Zusammenhänge des simultanen Auftretens der Abflussdefizitereignisse an den Pegeln verwendet. Um die zeitliche Entwicklung der Defizitereignisse innerhalb einer Region zu beschreiben, wurde ein regionaler Index, der sich aus den einzelnen Pegelreihen errechnet, eingeführt. Dieser regionale Abflussdefizitindex (*RDI*) erlaubte eine erste Bewertung der unterschiedlichen regionalen Ausprägung von Trockenperioden. Regionen wie Spanien, Südostengland und Norddeutschland tendieren zur Ausbildung langer persistenter Ereignisse, während der Index in anderen Gegenden stärker schwankt.

Desweiteren bildet der regionale Index eine geeignete Basis zur Untersuchung des Einflusses synoptischer Meteorologie auf regionale Trockenperioden. Starke Anomalien der relativen Auftrittshäufigkeiten der Europäischen Großwetterlagen während Perioden mit starker Trockenheit demonstrieren die Stärke des schon bei der Visualisierungsstudie vermuteten Zusammenhangs. Die 30 Großwetterlagen (CP) wurden daraufhin bezüglich ihrer saisonalen Assoziation mit Trockenperioden gruppiert, so dass die erhaltene neue Zeitreihe der Grosswetterlagengruppen eine geeignete Eingabegröße für ein neues Modell zur Simulation des regionalen Abflussdefizitindizes darstellt. Für die Modellierung wurde ein rekursiver Ansatz gewählt, der den *RDI* durch denjenigen des vergangen Tages und eine Modifikation durch das Auftreten einer Grosswetterlage darstellt. Nach Eichung der Modellparameter an einer 17-jährigen Kalibrierperiode, konnte für die meisten Regionen eine gute Simulation der beobachteten Werte erreicht werden. Ein Vergleich saisonal aggregierter Werte, für hydrologische Trockenperioden eine durchaus interessante Zeitskala, schneidet sogar noch besser ab.

Im letzten Teil der Arbeit wurden zwei mögliche Anwendungen des CP-*RDI* Modells getestet. Zum einen wurden historische Trockenperioden seit Beginn der Großwetterlagenzeitreihe im Jahr 1881 rekonstruiert. Zum anderen wurden die Eigenschaften regionaler Abflussdefizitserien unter veränderter Klimabedingungen, die durch ein Großwettterlagenszenario dargestellt wurden, simuliert. Große Ereignisse der rekonstruierten langen Zeitreihen konnten durch einen Vergleich mit dokumentierten historischen Dürreereignissen erfolgreich validiert werden. Dies erlaubt eine erste vorläufige Einschätzung des Einflusses von, Klimaänderungen zugeschriebenen Änderungen der Häufigkeiten und Andauern von Grosswetterlagen, auf hydrologische Trockenperioden. So zeigt sich die Änderung zu längeren Wetterlagenandauern ab Mitte der 60er Jahre in einer Veränderung der Variabilität der *RDI* Zeitreihen zu längeren Trockenperioden, insbesondere in Norddeutschland und Südskandinavien. Weiterhin

bestätigt sich der vielfach genannte Trend zu trockeneren Bedingungen in Spanien und feuchteren Bedingungen im Nordwesten Europas als Folge erhöhter zonaler Zirkulation im Winter in den letzten zwei bis drei Jahrzehnten des 20. Jahrhunderts. Die Reaktion auf ein Szenario, das auf diesen in der Literatur dokumentierten Veränderungen aufbaut, unterstützt die Einschätzung anderer Untersuchungen. Europa wird wahrscheinlich größtenteils feuchteren Bedingungen ausgesetzt sein, jedoch können trotzdem die Spitzenwerte regionaler Abflussdefizite durch anhaltendere Trockenperioden erhöht werden. Dies gilt insbesondere für Regionen, die durch ihre klimageographische Lage (Spanien) oder eine große Grundwasserbeeinflussung des Abflusses (Südostengland, Norddeutschland) zur Ausbildung langer persistenter Trockenperioden tendieren.

Aus der Untersuchung kann gefolgert werden, dass der Einfluss von Trockenperioden auf die Wasserressourcen in einigen Regionen Europas durchaus ernstzunehmen ist. Somit sollte dringend eine Verbesserung der Vorhersage und Planungsgrundlagen für ein nachhaltiges Management der Wasserressourcen während Trockenperioden angestrebt werden. Der gezeigte direkte Einfluss synoptisch meteorologischer Situationen stellt hierfür vielversprechende Ansätze zur Verfügung.

1 Introduction

1.1 Background

Drought is a natural hazard temporarily affecting almost every region in the world. The temporary shortage of water poses a great threat on nature, quality of life and economy. As drought is a slowly developing phenomenon, only indirectly affecting human life, its impacts are often underestimated in financially well off regions such as Europe. Historically, water use and management practices had been well adapted to the natural water availability of the specific regions. With the rising water demand and competition for water resources, the natural availability and in particular its seasonal variation has sometimes been neglected in water use and management practices. The increased demand has made even wetter parts of Europe susceptible to droughts (Bradford, 2000). The European Commission (1998) estimated that some 84 million people living in cities with more than 100 000 inhabitants already experience occasional limitations in water supply. EU countries are, on average, abstracting around 21% of their renewable freshwater resources each year which is regarded as a sustainable position, although significant water loss occurs in southern countries, where around 18% of the resource is lost each year in irrigation (EEA, 1999). These percentages however are averages. Water availability across Europe varies considerably in time and space.

Recent years have shown how vulnerable countries can be to low precipitation, when periodic droughts in several European countries have caused major environmental, social and economic problems (EEA, 1999). Figure 1.1 shows a summary of the drought records in the international disaster database EM-DAT, kept by the Office of US Foreign Disaster Assistance (OFDA) and the Centre of Research on the Epidemiology of Disasters (CRED). EM-DAT contains essential core data on the occurrence and effects of over 12 000 mass disasters in the world from 1900 to present. The database is compiled from various sources, including UN agencies, non-governmental organisations, insurance companies, research institutes and press agencies (OFDA/CRED, 2001). A more detailed list of recent drought events obtained from various information sources compiled by Bradford (2000) shows that many other severe events have recently occurred across Europe. As the problems were solved without international aid, they were not recorded in the disaster database.

Despite these severe events, research on low flows and drought was rare compared to other continents. Little is known on the development, extent and spatial characteristics of droughts

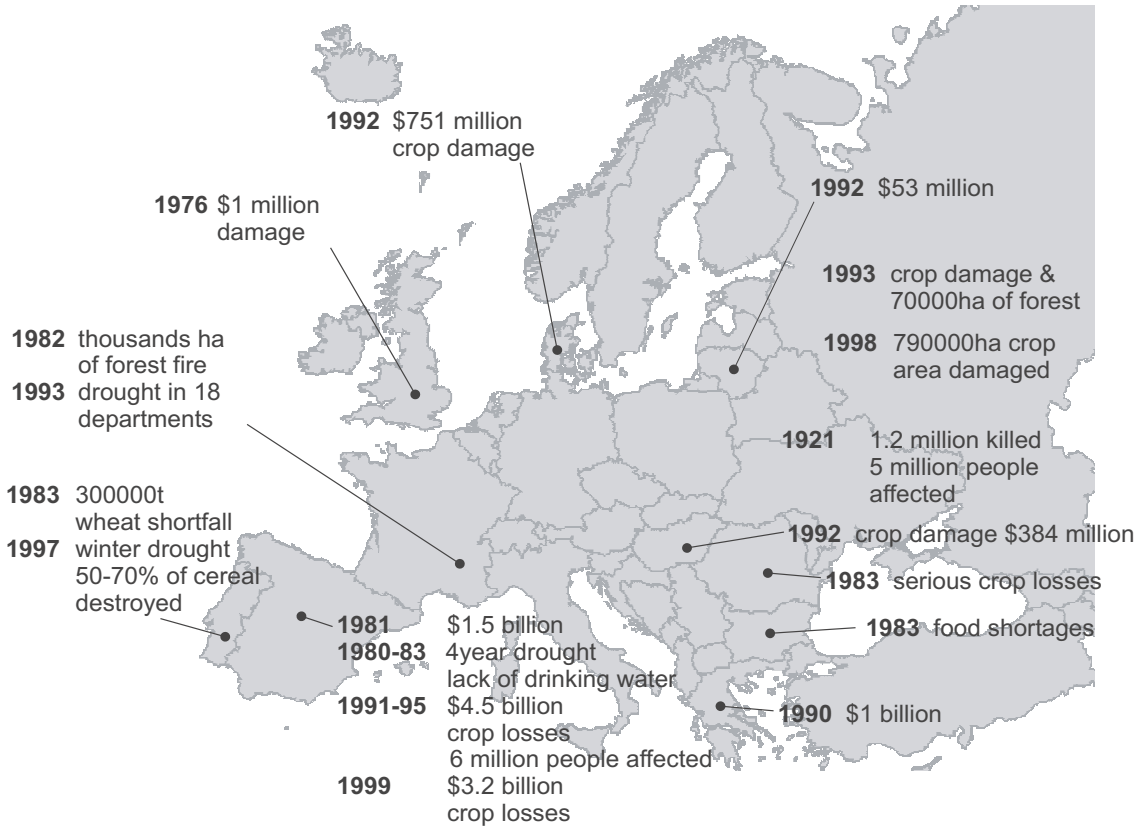

Fig. 1.1 *Selection of important droughts in Europe from 1900 to present (source: OFDA/CRED, 2001)*

in Europe. One of the few research initiatives considering this topic at an international level is the European FRIEND project, in particular the Northern European FRIEND Low Flow group and the Mediterranean group (AMHY). With the damages of the severe water deficits in the nineties and the climate change research results predicting an intensification of the hydrological cycle with more extreme hydrological conditions such as summer droughts and winter floods, the issue has recently gained more attention. The ARIDE (Assessment of the Regional Impact of Droughts in Europe) project, in which the research work presented in this thesis was carried out, addressed many different aspects of drought in Europe. Funded by the Fourth European Community Framework Programme for Research and Technical Development in the Climate Change and Impact on Natural Resources, European Water Resources programme, the ARIDE project assembled a database for hydrological studies at a pan-European scale, reviewed drought definitions for use across Europe, studied space-time characteristics of drought occurrence, drought severity, and recurrence frequency, investigated small and large scale drought causing processes and finally developed a pilot monitoring system for Europe (Demuth and Stahl, 2001).

Drought is a normal, recurrent feature of climate, which occurs in virtually all climatic zones, although its characteristics vary significantly from one region to another (NDMC, 2001). The

water deficit resulting from this climatic anomaly propagates through the hydrological cycle, finally causing streamflow and groundwater reservoirs to deplete. In the research presented, mainly streamflow deficiency and low flows, drought indicators visible for everyone, are investigated. Most European countries actually rely more on surface water than on groundwater. In Lithuania and Finland more than 90% of the abstracted water is surface water, and out of 27 European countries, only Denmark, Iceland, Slovenia, Belgium and Austria abstract more groundwater than surface water (EEA, 1999). Furthermore, dilution of chemicals is low during drought situations and therefore water quality often becomes a problem.

1.2 Objectives

The review of drought events in Europe shows a considerable impact of these spatially and temporally extended events. However, not many aspects of hydrological drought situations have been studied at a pan-European scale. From a planning perspective, the spatial characteristics of droughts have serious implications (Wilhite et al., 2000). Within the European Union there are not only direct interdependencies on agricultural products but also considerable economic interactions, which might be influenced by regional hazards such as drought. Through a gain in knowledge on the space-time characteristics and the drought causing processes, this study aims to contribute to a better basis for international drought planning and prediction, which is also an important part of a sustainable water resources management.

The objectives for this thesis work can therefore be summarised in three key objectives elaborated by several specific tasks:

- With the availability of pan-European hydrological data, the first objective in the present study was to elaborate event definitions, which allow the investigation of dry periods and droughts across the entire continent. A definition had to be found, which
  - → is applicable to the available time-series data and
  - → allows a comparison of the identified events across the different geographic and climatic regions.
- Then, the spatial and temporal characteristics of historic events defined by this event definition were to be analysed to
  - → investigate, whether the historic series show a trend towards an increased drought severity and frequency, as some recent studies on climate change suggest.
  - → study the regional extent of specific events, their dynamics and their recurrence.
  - → classify and characterise regions typically experiencing water deficit at the same time to enhance planning possibilities.

- Finally, a major task for hydrologists is to work on methods for regional drought forecasting and for the investigation and prediction of the influence of climate change on regional drought occurrence. For large-scale European regions,
  → Synoptic meteorological situations causing droughts were to be investigated and
  → a relationship was to be deducted to study the impact of climatic variability.

2 Data and Study Area

2.1 Introduction

Pan-European hydrological studies depend on available pan-European datasets of suitable resolution and quality. The issue of collating and harmonising large scale datasets has been given a lot of attention in the last few years. International data centres like the Global Runoff Data Centre (GRDC) and the Global Precipitation Climate Centre (GPCC) were established and provide global hydrological data from large river basins and global gridded hydro-climatological data to the user. Research projects like the FRIEND project (Flow Regimes from International Experimental and Network Data, CEH, 2001) and the Mediterranean Hydrological Cycle Observing System (Med-HYCOS, Morell, 2001) have been able to build up hydrological databases. Some national research centres like the Climate Research Unit at the University of East Anglia (CRU) or the United States Geological Survey (USGS) provide climatological, hydrological and topographical data, usually obtained from various sources and assembled to harmonized national, continental or global datasets. Several international agencies like EUROSTAT and the European Environment Agency have put great effort in making GIS data available to research projects in particular. Altogether, availability and accessibility of datasets has considerably improved during the past years. Nevertheless, these international datasets often have a low spatial and temporal resolution. Station data is difficult to obtain as the responsibility and pricing policy varies between countries. If climatological data are available free for research purposes, they are usually derived values like gridded monthly precipitation, etc. Depending on the study, these data might not be detailed enough.

For a pan-European drought study, long-term climatological and hydrological series are a prerequisite, in particular if typical drought characteristics are to be determined or changes through time (Chapter 4) and teleconnections (Chapter 5 and Chapter 7) are to be studied. Sufficient spatial coverage is an advantage for the study of regional patterns (Chapter 5 and Chapter 6). Thematic maps and catchment information become important when hydrological parameters are to be regionalised (Demuth et al., 2000). As this study was carried out within the ARIDE project, the ARIDE project database, which provided a considerable update to the FRIEND database, could be used (Rees, 2001). The data obtained for the project, especially the updated hydrological database, which is now one of the largest in the world, gives a unique opportunity to investigate and assess hydrological droughts across Europe.

2.2 Database

2.2.1 A streamflow dataset for European drought analysis

As a contribution to the FRIEND Project, the ARIDE Project had full access to the European Water Archive (EWA), a database of river flows maintained at the Centre for Ecology and Hydrology (CEH) in Wallingford, UK. Only data from rivers whose flow regimes approximate to natural conditions is included in the EWA (Roald et al., 1993). Therefore, the European Water Archive has been the source for many pan-European hydrological studies, e.g. regionalisation of flow characteristics (e.g. Demuth, 1993, Gustard et al., 1997), the description of the variability in European annual and seasonal river runoff (Arnell, 1994), the classification of river flow regimes in Europe (Krasovskaia et al., 1994), and for the analysis of the link between river flow and the North Atlantic Oscillation (Shorthouse & Arnell, 1997).

The database currently contains daily flow data from 4400 gauging stations from 29 European countries, of which 40% have records in excess of 30 years (Rees and Demuth, 2000). Unfortunately, those 40% of records do not necessarily cover the same 30-year time period and many of the stations also have long gaps. The influence of the selected period on statistical parameters of the hydrograph used in drought studies is considerable (Chapter 4). To ensure the best possible comparability, datasets with common time periods were analysed. The catchments were selected according to the following criteria:

- Only catchments with an area less than 1000 km² were included in order not to have a superposition of different river flow regimes in the hydrograph.
- Records with jumps, inconsistencies and errors, detected on a visual check of the hydrographs were excluded.
- Records with gaps of more than ten consecutive days were removed, smaller gaps were linearly interpolated.

Finally, the period 1962-90 (Period 1) was found the best compromise between a long record and an adequate pan-European coverage. The 612 stations cover most of northern, central and eastern Europe, and Spain. Consequently, this dataset is used as ’reference period’ to determine the drought threshold and other statistical parameters describing the hydrology of the catchments (Chapter 3.2 and Chapter 4). Period 1 is also used for the studies of spatial patterns and teleconnections (Chapter 5 to Chapter 7). However, due to some gaps in winter, only 602 record were available for this part of the study. Two additional sets of stations, one with more recent data (Period 2: 1962-95, 365 stations) and one with longer time series but poorer spatial coverage (Period 3: 1930-95, 54 stations), were chosen to investigate longer-term trends (Chapter 4.3). Two of the longest series in the EWA were specially selected to study how trends depend on the period analysed (Period 4: 1911-95). The location of the stations of the four datasets are shown in Figure 2.1

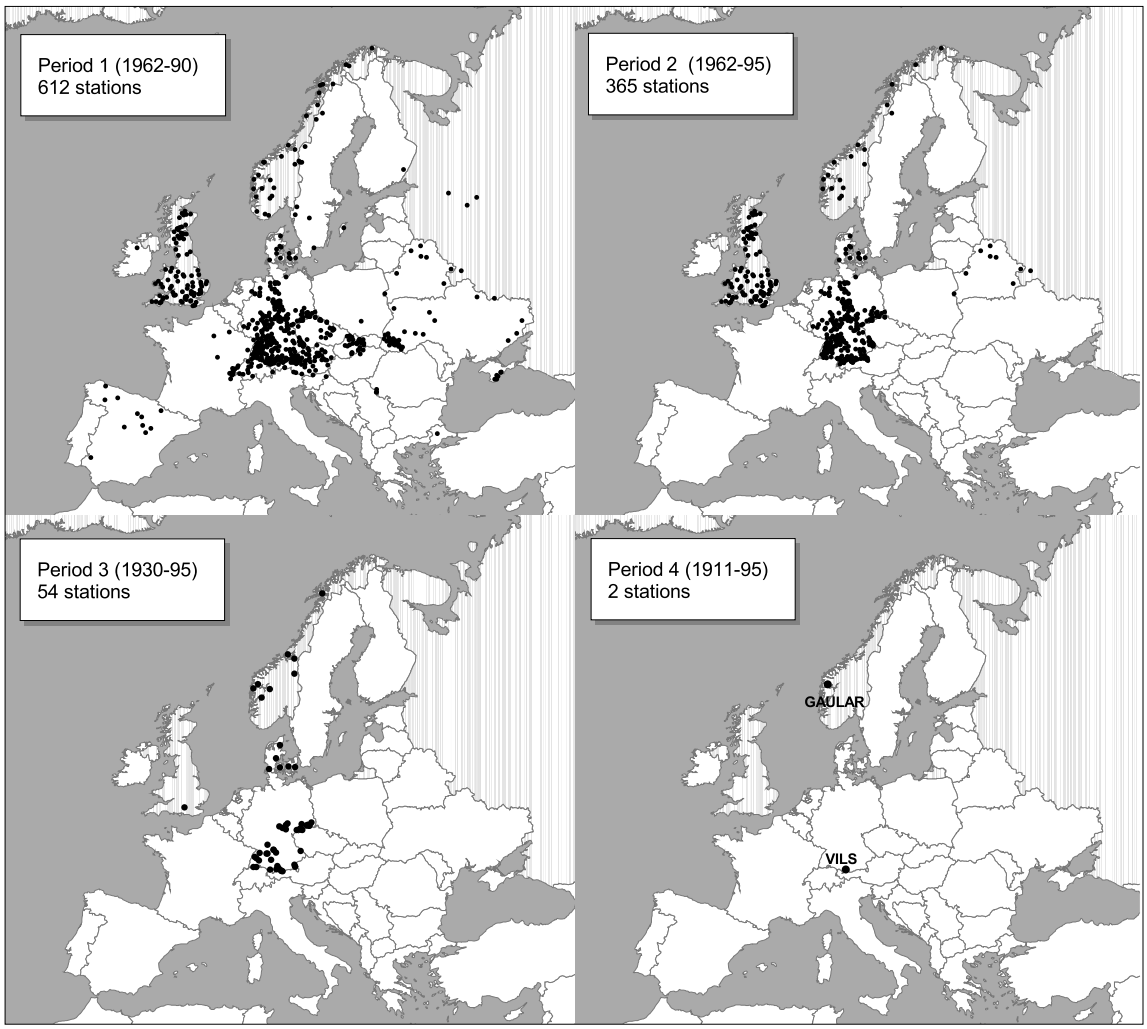

Fig. 2.1 *Locations of the stations with streamflow records covering Period 1 to Period 4*

2.2.2 Synoptic meteorological data

Synoptic meteorology describes weather map features such as high and low pressure areas and fronts over a large region. Gridded values of mean sea level pressure (MSLP) or pressure at the 500 hPa or 750 hPa level are usually the basis to derive synoptic meteorological parameters. Classified atmospheric circulation patterns (CPs) and circulation indices have proved to be a valuable tool to establish a direct link with hydrologic parameters (Chapter 7.2), an approach also followed in this study. The chosen parameters as described in the following section, consider the large-scale meteorological situation over entire Europe. All the data are freely available via the Internet.

Mean Sea Level Pressure

Gridded MSLP (mean sea level pressure) at a resolution of 2.5° is available to the public from NOAA (National Oceanic and Atmospheric Administration), through their 'reanalysis project', which is a joint project between the National Centers for Environmental Prediction (NCEP) and the National Center for Atmospheric Research (NCAR). The goal of this joint effort is to produce new atmospheric analyses using historical data (1948 onwards) and as well to produce analyses of the current atmospheric state (Climate Data Assimilation System, CDAS) (NOAA, 2001).

The data have been widely used in climate and weather forecast models, for classifying atmospheric circulation patterns, for the calculation of synoptic indices and for other applications. In this study, contour maps of the mean sea level pressure with the maximum high and low pressure centres in the chosen region are included in the dynamic visualisation of drought events in Chapter 5.

North Atlantic Oscillation Index

The North Atlantic Oscillation (NAO) is a large-scale mode of natural climate variability in the Northern Hemisphere and has important impacts on the weather and climate of the North Atlantic region and surrounding continents, especially Europe. Put simply, the NAO measures the strength of the westerly winds blowing across the North Atlantic Ocean between 40° N and 60° N (Greatbatch, 2000). Although the NAO occurs in all seasons, it is during winter that it is particularly dominant (Osborn, 2000). The NAO can be measured as an index (NAOI) defined as the normalized pressure difference between Stykkisholmur/Reykjavik on Iceland and Ponta Delgada on the Azores. The NAOI is not directly used in this study. However, since the available information on its influence on European climate influenced the analysis in Chapter 8, this short documentation is included in this section.

Many studies have addressed interdecadal variability and trends of the NAOI. Recent changes in and warming of wintertime climate across Europe can be related to the NAO, which has tended to persist in one extreme phase since 1980 (Hurrel & van Loon, 1997). A strong influence of the NAOI on regional climatic parameters such as temperature and precipitation was shown by Hurrel (1995) and Hurrel & van Loon (1997). Shorthouse & Arnell (1997) found correlations of NAOI to seasonal streamflow in some regions across Europe. The relation to the North Atlantic Sea surface temperatures and the prediction of the NAOI within Global Circulation Models (GCMs) and Ocean/Atmosphere Models are further topics of research addressed in many publications (Greatbach, 2000).

Circulation and Weather Patterns

Many different classifications of atmospheric circulation patterns (CPs) exist. For Europe, one of the well known classifications are Lamb's weather types, which subjectively classified

each day's weather over the British Isles from 1861 to February 1997 (Lamb, 1972). Later, an objective scheme to classify the daily circulation according to the Lamb weather-typing scheme was developed. The similarly derived and also well known ’European Grosswetterlagen’ after Hess & Brezowsky (1977) are used in this study to describe the relationship of drought to synoptic meteorology (Chapter 7 and Chapter 8). These circulation patterns (CPs) are defined daily by the German Weather Service. Based on the mean air pressure distribution (sea level and 500 hPa level) over Europe and the Northern Atlantic Sea, the classification initially distinguishes zonal, meridional and mixed circulation. Subtypes specify the movement direction of frontal zones and the location of high and low pressure area centres as well as cyclonic or anticyclonic rotation. This scheme leads to the definition of 29 circulation pat-

Table 2.1 *Circulation Patterns after Hess & Brezowsky (1977)*

Circulation type		**Description**		
major type	**subtype**	**no.**	**name**	**CP**
zonal circulation	W	1	West anticyclonic	Wa
		2	West cyclonic	Wz
		3	Southern West	WS
		4	Angleformed West	WW
mixed circulation	SW	5	Southwest anticyclonic	SWa
		6	Southwest cyclonic	SWz
	NW	7	Northwest anticyclonic	NWa
		8	Northwest cyclonic	NWz
	HM	9	Central European high	HM
		10	Central European ridge	BM
	TM	11	Central European low	TM
meridional circulation	N	12	North anticyclonic	Na
		13	North cyclonic	Nz
		14	North, Iceland high, anticyclonic	HNa
		15	North, Iceland high, cyclonic	HNz
		16	British Isles high	HB
		17	Central European trough	TRM
	NE	18	Northeast anticyclonic	NEa
		19	Northeast cyclonic	NEz
	E	20	Fennoscandian high anticyclonic	HFa
		21	Fennoscandian high cyclonic	HFz
		22	Norwegian Sea -Fennoscandianhigh, anticyclonic	HNFa
		23	Norwegian Sea -Fennoscandianhigh, cyclonic	HNFz
		24	Southeast, anticyclonic	SEa
		25	Southeast, cyclonic	SEz
	S	26	South, anticyclonic	Sa
		27	South, cyclonic	Sz
		28	British Isles low	TB
		29	Western Europe trough	TRW
unclassified	U	30	classification not possible	U

terns (and one undefined CP) that belong to three major circulation types and ten subtypes (Table 2.1).

A circulation pattern generally persists for several days while the entailed weather features remain constant. The transition to the following circulation pattern takes place rapidly. Revised and quality controlled time series are available since 1881 (Gerstengarbe & Werner, 1999). Analyses of the frequencies and seasonality of the particular CPs as well as a description of the typically associated weather for Germany are provided with the catalogue.

The European Grosswetterlagen have been used to study climatic trends and changes across Europe (Klaus, 1993). The change in wintertime climate shown for the NAOI was also detected in the classified circulation patterns (Bardossy & Caspary, 1990, Werner et al., 2000). The topic is treated in more detail in Chapter 8. Furthermore the link to different surface hydroclimatological variables was investigated. Stahl & Demuth (1999) studied the influence of the occurrence of the certain CPs on drought in southern Germany.

2.3 The study area

2.3.1 Delineation

Data availability limits the area covered by this pan-European drought study. Since the main hydrological parameter to be studied is streamflow, the spatial coverage of the analyses is defined by the dataset for Period 1 (1962-1990) introduced in Chapter 2.2.1. It covers most countries in northern, western central and eastern Europe, whereas southern Europe is not very well represented. Only a few Spanish stations are included. Unfortunately, no daily streamflow records for the same period were available for southern and western France or the Mediterranean countries from Italy to Greece. Through all the analyses it has to be kept in mind that the station density of the database varies strongly across the study area with most stations in Germany, Switzerland, Austria, and the UK. Station densities in Denmark and Norway are a little bit lower, but still very good. There is a clustering of stations along the Carpathian Mountains from the Czech Republic to Ukraine. Farther east, in Russia, Belarus and the Ukraine, station density is low. Poland and the Baltic states are also not or not well represented in the dataset. The next sections discuss the climatology, physical geography, and hydrology of the study area as defined by the streamflow dataset.

2.3.2 Climatology

Circulation

Within the global circulation system, Europe is located between the centres of action of the subtropical high pressure belt and the polar low pressure belt. This pressure difference strongly triggers the extratropical circulation of the lower and middle troposphere in these latitudes. Due to the coriolis effect, in the northern mid-latitudes, the air flow is diverted to the right, which results in the general extratropical westwind drift (zonal circulation). The temperature difference between the warm southern air masses and cold northern airmasses cause a north-south directed (meridional) circulation to achieve an energy balance. As a consequence, the frontal zone meanders and often cyclonic eddies develop on the polar side and anti-cyclonic eddies develop on the southern side of the frontal zone and move along with it.

The high and low pressure centres responsible for Europe's weather are the Azores High and the Icelandic Low. Within the fourfold pressure field of the Mexico Low, Canada High, Iceland Low and Azores High, cyclones along the meandering frontal zone are generated over the Atlantic Ocean, where the pressure and temperature gradients are highest. These frontal cyclones are meso-scale low pressure systems moving eastwards to Europe, with their tracks depending on the location of the Azores High and Icelandic Low and the movement of the frontal zone.

Extratropical cyclones are most active over the Oceans. The zone of maximum cyclonic activity crosses the North Atlantic from west-south-west to north-north-east (Weischet, 1991). When the cyclones hit the continent they slow down due to friction. How far they can advance into the continent strongly depends on the topography. In winter, polar low pressure and subtropical high pressure are stronger. The pressure difference (measured with the NAOI, Chapter 2.2.2) within the mid latitudes during winter time causes stronger upper-air westerlies, which finally results in higher rainfall amounts across Europe. Moving with the ITCZ, the subtropical high pressure belt with large-scale cells like the Azores High are shifted southwards during winter. The westerlies can then influence the southern part of Europe, where the annual climatic regime is consequently characterised by cyclonic rainfall in winter and summer dryness due to subtropical high pressure centres being located farther north again.

Circulation Patterns over Europe and the North Atlantic Ocean vary strongly and the Azores High and the Iceland Low do not always have their centres over the Azores or Iceland. However, this is the most frequent situation. Figure 2.2a shows an example of the Circulation Pattern West cyclonic (Wz) after Hess and Brezowsky, which occurs during 15% of the time and illustrates the zonal circulation with cyclones moving into Western Europe. Circulation over Europe has mixed zonal and meridional components, when the anticyclonic centres of action are located further north (Gerstengarbe & Werner, 1999), as in the second most frequent CP Central European High (HM) shown in Figure 2.2b. Airflow in Europe still has a westerly

component and is usually north-west or south-west. The characteristics of meridional circulation are stationary blocking high pressure cells between 50° N and 65° N (Gerstengarbe & Werner, 1999). Depending on the exact location of the centre, airflow in Europe is from the north, east or south. The air masses carried to Europe with these circulation types strongly govern the weather patterns. Zonal and mixed circulation generally bring moist maritime airmasses from the tropic Atlantic into Europe, whereas meridional circulation can bring maritime polar airmasses or dry continental airmasses (polar or tropic source).

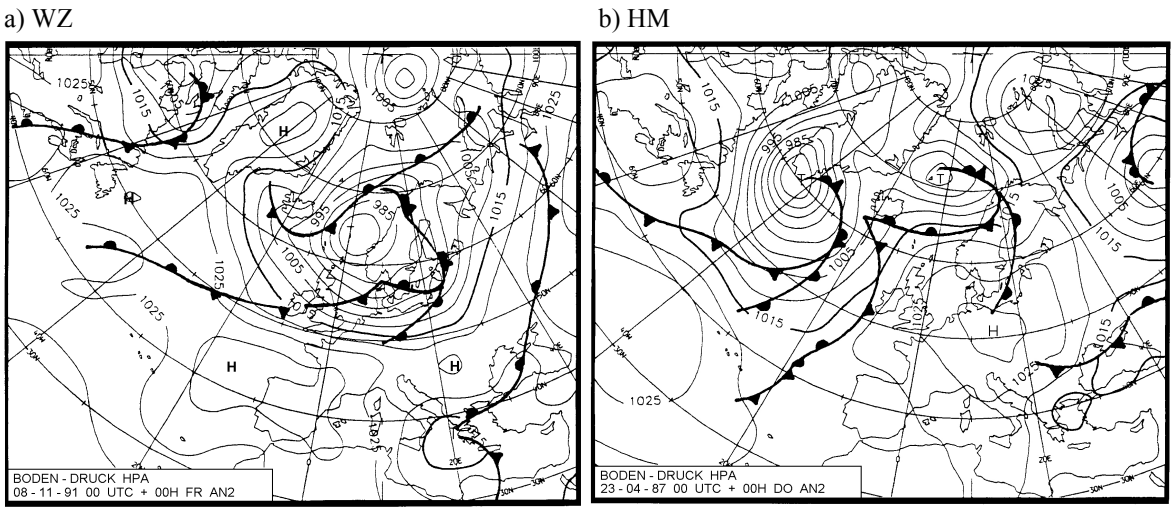

Fig. 2.2 *Examples of the mean sea level pressure distribution and location of fronts for two frequent circulation patterns over Europe (from Gerstengarbe and Werner, 1999)*

Precipitation and Temperature

From the discussion of the atmospheric circulation, it can be concluded that frontal rain mainly affects northern and western Europe. In the oceanic climate of northern Portugal and Spain, the UK, western France, the Benelux and southwestern Norway, winter precipitation is higher than summer precipitation due to the aforementioned stronger pressure differences. Along the coast snow is rare and temperatures are above zero all year with a monthly maximum in summer. The exposure to the frontal cyclones is responsible for Europe's maximum annual rainfall amounts of > 2000 mm/year in Scotland and Norway. Annual rainfall amounts in continental Europe generally decrease eastward from > 900 mm at the coast to < 600 mm in Warsaw, a pattern which can be locally modified by topography. From Cantabria to the Carpathian mountains, rainfall along the mountain ranges is higher than in the sourrounding plains. In central and eastern Europe, winter precipitation is lower and the precipitation maximum shifts to summer due to convective rainfall. The farther north and east, the lower are the temperatures in winter and the longer they remain below freezing. Only in the south east of the study area (Romania, Ukraine), is rainfall generally very low throughout the year. High summer temperatures cause an arid summer season, which classifies the region into the winter cold steppe climate zone. The rainy season in the mediterranean countries is concentrated

on the winter half year, due to the southward displacement of the subtropical high pressure belt. Annual rainfall is very low in southern Spain (< 300 mm) and on the eastern sides of southern Italy and Greece, where the western coasts receive considerably more rain (up to 800-1000 mm). Winter temperatures are moderate, summers are very hot causing a short arid summer season, typical for the Mediterranean climate zone.

2.3.3 Physical geography and geology

According to Ager (1980), Europe can be divided in four major physiographical regions.

The *North-west Highlands*, comprising western Scandinavia and the north west part of the British Isles. The region is composed of rugged country formed of complexly folded and faulted Precambrian and Paleozoic rocks. The landscape is dominated by boreal coniferous forest in Scandinavia (some mountain tundra in Norway) and heather and grassland in northern Britain.

The great *North European Plain* extends from the Aquitaine Basin and eastern England across Europe to the Russian steppes. The region is covered by great thicknesses of mesozoic and cainozoic sediments. Denmark, northern Germany, Poland, and the Baltic states are covered by quaternary tills and sands. The region is heavily cultivated, but there are also large forested areas.

The Old Massifs are isolated, uplifted blocks such as the Massif Central, the Black Forest, and the Bohemian Massif, predominantly composed of Precambrian and Paleozoic rocks. Topography, soils, vegetation, and landuse vary strongly and depend much on the climate and petrography.

Looking at physiographic maps of Europe, the fold belts of the *Alpine Mountains* from the Sierra Nevada, via the Pyrenees, the Alps, The Apennines, the Dinarides, the Carpathians, and the Caucasus dominate the European topography. They originate from the Alpine movements, which began in the Triassic and reached their climax in mid Cretaceous and again in the Tertiary. The sedimentary histories of these mountains are very complex. Also included in these regions are troughs in front of the Alpine mountains, the ancient massifs and cores and the intermontane basins filled with thick Neogene sediments.

2.3.4 Hydrology

River flow regimes

Europe exhibits a wide variety of typical annual streamflow distributions (regimes). They depend on the general regional climatic and physical factors discussed in the two previous sections and on the catchment's physiography. The catchment characteristics, especially the presence of large reservoirs like lakes, marshes, aquifers, etc. account for the variability

between basins exposed to similar climatic regimes (Krasovskaia et al., 1994). The knowledge of the streamflow regimes across Europe is an important prerequisite to define and understand drought and streamflow anomaly across the different climatic zones, because they define the normal and expected water availability throughout the year.

Traditionally river flow regimes have been defined by the monthly mean streamflow normalised by the mean flow of the period of record. These monthly indices are also known as Pardé-coefficients (Pardé, 1933). Most studies follow a subjective classification scheme that describes the maxima and minima for the investigated region. Few studies have classified regimes at a larger than the national scale. Schwarzmaier & Mayer (1992) used cluster analysis on global mean monthly streamflow to obtain groups of similar regimes. Eight out of the twelve distinguished patterns were found in Europe, the variability being particularly high in Scandinavia. Krasovskaia et al. (1994) defined flow regime types for western and northern Europe and automatically classified series from the EWA. They also investigated the stability of the regimes and discussed suitable mapping procedures.

As stations with catchments larger than 1000 km² were excluded in this study, the flow regimes should not be a superposition of regimes from different catchments with different influences. A few examples of monthly Pardé-Coefficients on the one hand illustrate the high variability across Europe but also regional clustering of similar regime types (Figure 2.3). The following description of the regime types uses the classification of Arnell et al. (1993) and Krasovskaia et al. (1994). The *Northern Scandinavian* regimes are characterised by a low flow period in winter, when precipitation is stored as snow and rivers are often ice-covered, and a maximum in June due to snowmelt. Further inland there is a tendency for a second minimum in autumn. *Mountain regimes* generally have the same character, however due to a catchment covering different zones of altitude, the start of the spring/early summer flood is more gradual. Regimes with the high flow season lasting through summer until the temperatures drop below zero are found in Norway and Sweden, at the high altitudes in the Alps (Switzerland, Germany, Austria) and in the High Tatras (Slovakia). Around these regions and in many other mountainous areas in Europe, the *mountain nival or transition* regime dominates with a snowmelt spring flood, a second low flow period in late summer and again higher flows due to autumn storms. Timing of the extremes and Pardé-coefficients vary strongly depending on the catchment characteristics. The dataset used in this study is biased towards mountain rivers due to the limit in the catchment size and human influence.

Regimes with two maxima, one resulting from snowmelt and one from autumn rain, and two minima, one in winter and one in summer, can also be found around the Baltic sea and in continental northern and central Europe. Generally, it can be seen that winter flow is higher closer to the Baltic sea and lower farther into the continent. The onset of the spring flood is earlier and not as abrupt farther south. Arnell et al. (1993) distinguish between *Northern Inland, Baltic, Baltic Inland* and *Southern Inland* regimes, however their dataset did not include eastern European stations. Due to the oceanic climate, western European *Atlantic* regimes strongly follow the annual precipitation distribution with a winter maximum and

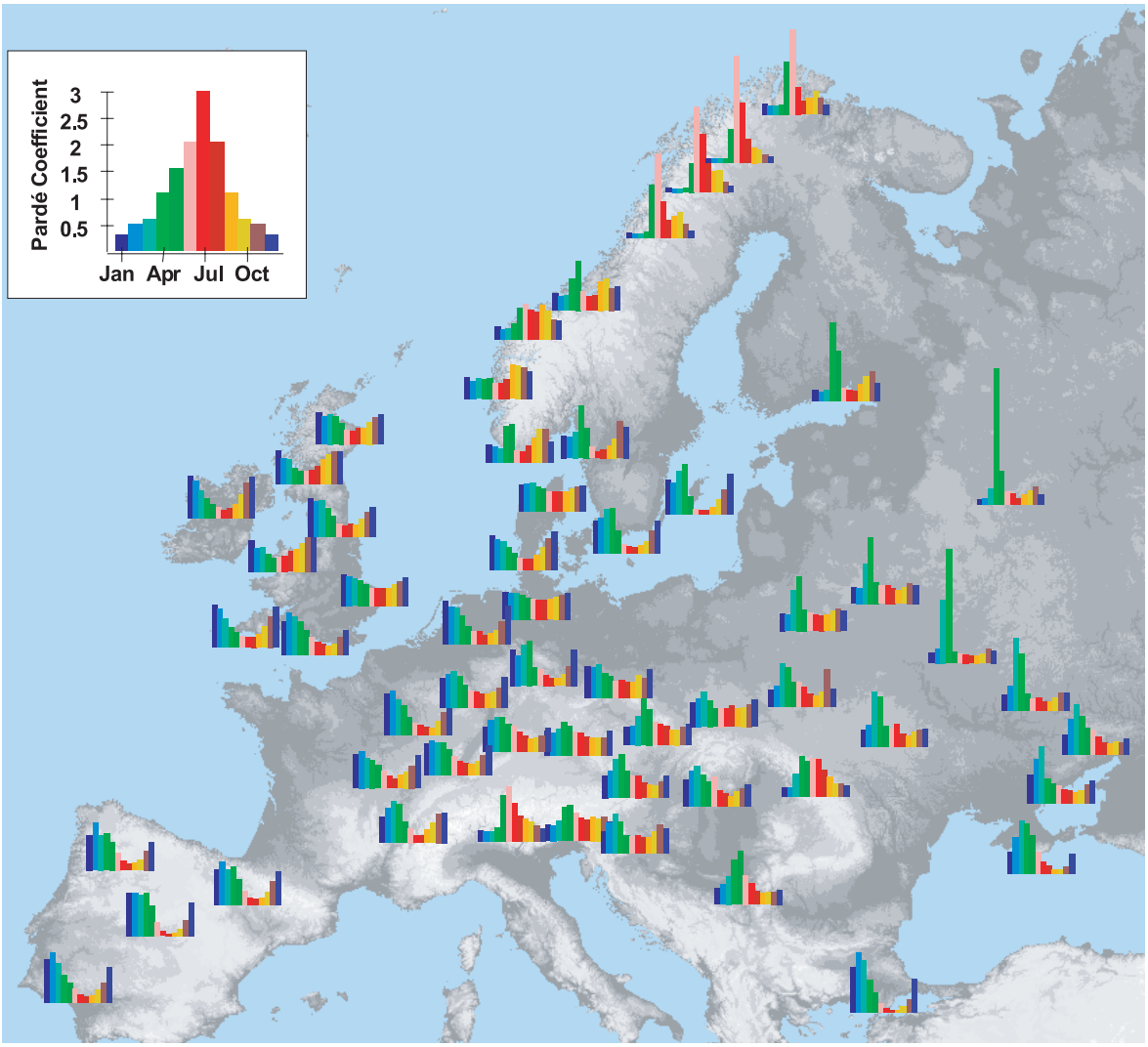

Fig. 2.3 *Pardé regimes of selected European rivers*

summer minimum. This regime type is characteristic for the coastal regions from Norway to France. The exact timing of the maxima and minima varies and strongly depends on catchment physiography and geology (Krasovskaia et al., 1994). If rainfall minus evapotranspiration is even throughout the year, and the reservoirs in a catchment have high storage capacity and drain continuously like in groundwater catchments, streamflow variablilty of the resulting *azonal* regimes may be hardly visible during the year using monthly mean values. *South European* Mediterranean like the Atlantic regimes are characterised by higher winter flows, but exhibit a more extreme and longer summer low flow season.

There are some limitations to the use of monthly mean flows for regime description. At the monthly time scale, the Atlantic and South-European flow regime types are difficult to distinguish, but flows in the South European regime tend to occur in fewer, more intense flood events (Arnell et al., 1993). The interannual variability is not included in the definition.

Krasovskaia et al. (1994) found that rainfall dominated regimes are less stable than snow dominated regimes.

Low flow

A closer look was taken at the low flow periods to be expected across Europe. In order to study the typical duration and timing of the low flow periods of a river, severals methods were tested. The following analysis was found most suited to describe these parameters:

- A daily regime in terms of the mean flow for each day of the year (Jan1, Jan2, ..., Dec31) was calculated from the series 1962-90).
- The values were normalised by the mean flow of the period.
- The daily regime was smoothed by a 21 day moving average
- The minimum of the daily regime was determined
- The *low flow season* was defined as days of the year, when the regime values are below 120% of the minimum.
- The low flow season is visualised in polar plots placed at each station in a map (Figure 2.4)

In the UK, the summer low flow seasons in Scotland and Wales are shorter and earlier (June, July) than in the other parts of the country. In the southwest, the low flow terminates by the end of August and farther east, stations show a low flow season from July through September. The same seasonality is demonstrated by Young et al. (2000), for the occurrence of Q95 across the UK. In Denmark and northern Germany, the low flow season lasts from June to September, sometimes to October. In southern Sweden and Norway, the summer low flow period is shorter. In Norway, the regimes described in the previous section are represented: the higher up in the mountains or the farther north, the longer is the wintertime low flow period. The method depicts the two low flow seasons of the Baltic and Baltic Inland regimes (Finland, Belarus and Russia), with the dominance of the summer low flow period increasing towards the south and the west. The stations in the south of Belarus and in the north of Ukraine even show a third short low flow season in May. Further south in Ukraine, summer low flow can continue into the winter low flow. The group of stations in the Carpathian mountains of Ukraine show either two short low flow seasons in winter and summer or only one winter low flow period. At the Black Sea, the summer low flow season lasts from July/ August to October.

In central Europe the low flow season shifts from a long June-October summer low flow (e.g. central Germany) to a shorter autumn low flow period from August to October the further south and east the station is located (e.g. France and Czech Republic). However this character is partly due to the bias to mountainous stations in the dataset. Along the Alps winter low flow periods dominate, some stations show an additional low flow season in summer. The stations in the French Jura all show a very similar short low flow season in July/August. In Spain, the lowest flows usually last from July to September.

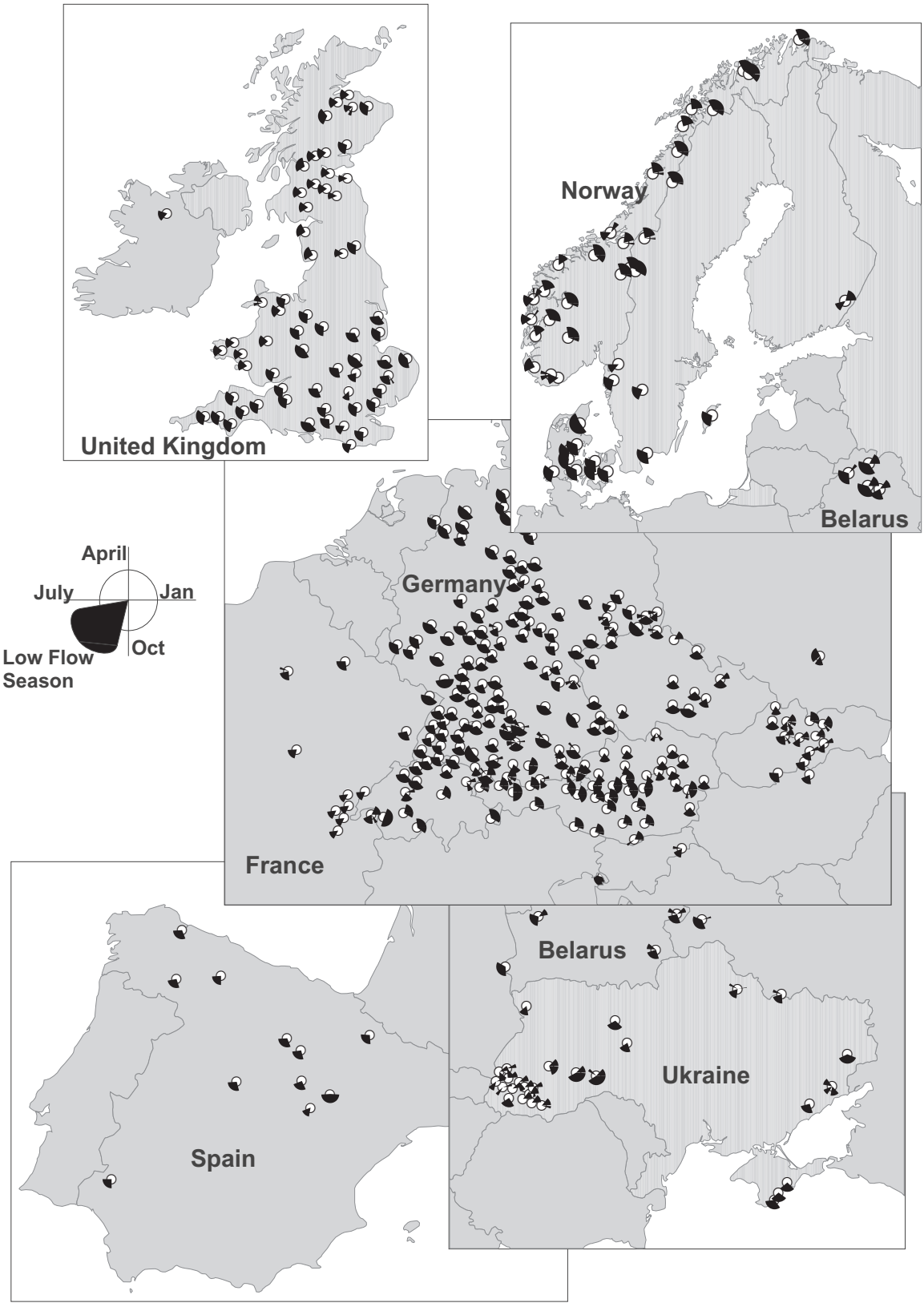

Fig. 2.4 *Timing of the low flow season for the reference dataset. For visualisation purposes, some stations were removed especially in Germany and the UK*

2.4 Conclusion

The study area was mainly defined by the availability of streamflow data across Europe, which was provided by the European Water Archive. The best compromise between a good spatial coverage and a long time series is a dataset of 612 stations with a common time period from 1962-90. Ranging across several different climatic zones and diverse environments, the catchments of this dataset cover a great part of Spain, northern, central, and eastern Europe. To study the meteorological causes for drought in these regions, synoptic meteorological parameters for Europe will be used, as unlike for streamflow, no precipitation and temperature records are available at a daily resolution for this whole study area. However, classified circulation patterns, the North Atlantic Oscillation Index, and the mean sea level pressure, which are all available for the same period (1962-90) are well suited to describe the meteorological situation.

General synoptic meteorological situations, which are governed by extratropical northern mid-latitude westerlies, generate different weather features across such a large region as Europe. The diverse physical geography and geology adds further modification to the surface climatology in such a way as to create many different streamflow regimes. Most of the streamflow regimes show a typical annual variation with the maxima and minima depending on the rainfall and snowfall distribution and hydrological storage. A regional analysis of the timing of the low flow season holds important information for the analysis of drought.

3 Streamflow Drought and Streamflow Deficiency

3.1 Concepts of drought

Drought is commonly considered a natural hazard associated with temporary, unpleasant impacts on life and nature. Depending on the societal standards, the physical drought phenomenon, which is a result of natural climate variability, is perceived differently. Consequently, the definition of drought is difficult. In fact, the majority of drought literature regrets the lack of an objective definition of drought and the confusion about numerous different concepts are said to be an obstacle for efficient drought research (e.g. Yevjevich, 1967, Dracup et al., 1980, Wilhite & Glanz, 1985). According to Wilhite & Glanz (1985), drought definitions can be conceptual (encyclopedia type) or operational. The latter define the precise characteristics of a drought using a variable from the discipline of interest, for instance precipitation in meteorology, streamflow in hydrology or soil moisture in agriculture.

Beran & Rodier (1985) summarise that "*in any case it is evident that the notion of drought is relative, but its chief characteristic is a decrease of water availability in a particular period and over a particular area rather than a general decrease of water availability. It is thus this abnormal distribution which must be considered typical of droughts.*" Drought must therefore not be confused with aridity, which is a permanent feature of climate (NDMC, 2001) and not a temporary water deficiency. In order to determine the ’abnormal’ temporal and spatial distribution of the water availability, first the ’normal’ distribution has to be defined. The study presented follows this relative concept of drought.

As schematically illustrated in Figure 3.1, a drought event is caused by a certain meteorological situation, for instance a persisting anticyclone/high pressure system. Associated with the prevailing dry and warm weather, a meteorological drought with a rainfall deficit develops. The rainfall deficit and the high evapotranspiration reduce the soil water content, which might cause an agricultural drought if occurring during the growing season. Due to the precipitation deficit in the catchment, streamflow decreases until it is only fed by groundwater and finally the groundwater reservoirs will also deplete. Consequently, hydrological droughts lag the occurrence of atmospheric droughts and depending on the season and the crop also the

occurrence of agricultural drought. Water in hydrological storage systems such as surface and groundwater reservoirs is often used for multiple and competing purposes, e.g. flood control, irrigation, recreation, hydropower, navigation or wildlife habitat, further complicating the sequence and quantification of impacts (Wilhite, 2000). When the demand exceeds the supply, a socio-economic drought occurs. It is the rising demand on surface water resources (compare Chapter 1), which calls for a better prediction of the natural water supply and thus a better understanding and prediction of the characteristics of hydrological drought.

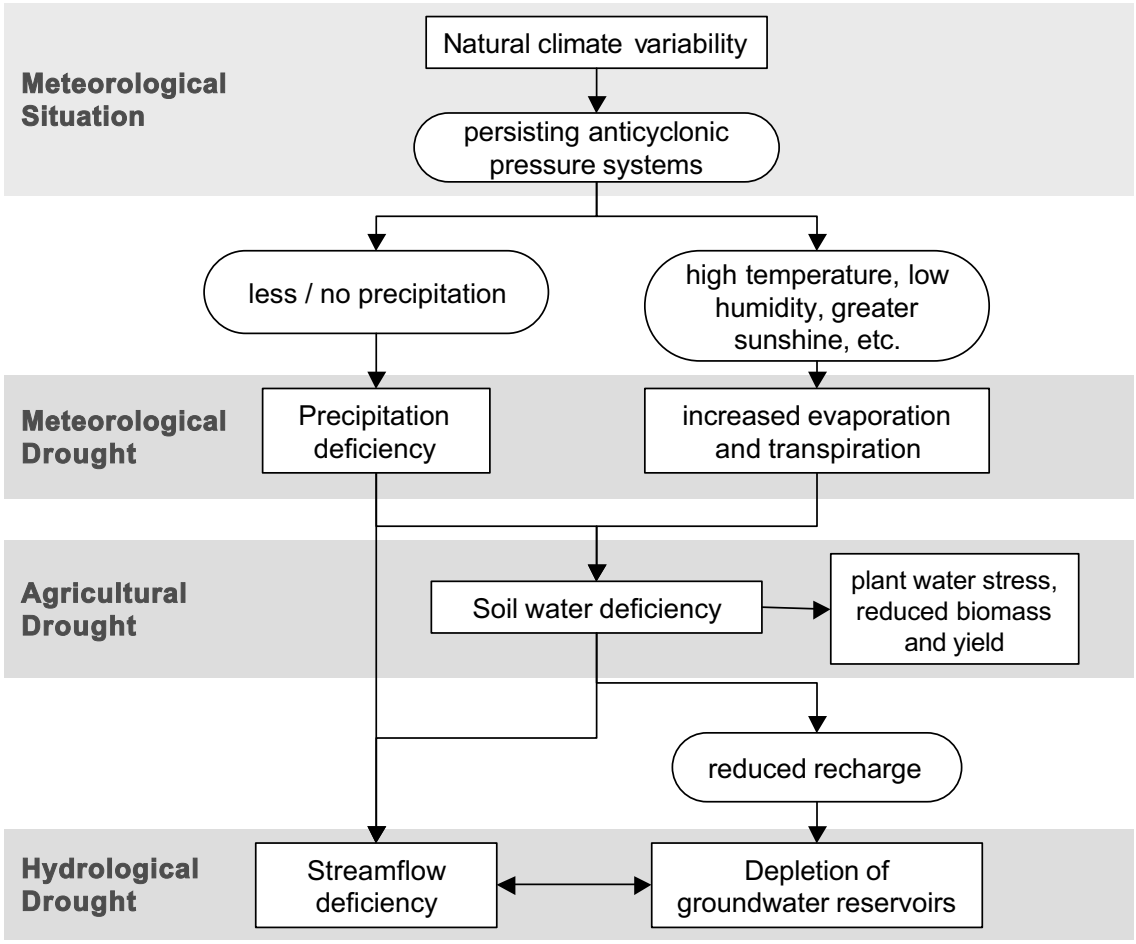

Fig. 3.1 *Propagation of drought through the hydrological cycle (modified after NDMC, 2001)*

Hydrological drought can be defined in many different ways. Tate and Gustard (2000) reviewed climatological, agro-meteorological, streamflow, groundwater, and operational drought definitions from a hydrological perspective. Water balance indices constructed from different hydrometeorological variables govern the climatological and agro-meteorological definitions while extreme values and runs below a threshold usually define drought in streamflow time series. Conceptual definitions for groundwater drought however are rare. Among the variables, which characterise groundwater drought (i.e. groundwater recharge, levels and

discharge), groundwater levels are the most sensitive parameter to base the definition on, as they characterize the present storage and can be measured directly with reasonable accuracy and frequency (van Lanen & Peters, 2000). Operational drought definitions can also be based on water supply and demand and then do not necessarily represent naturally induced events (Tate & Gustard, 2000).

The aim of this pan-European study is to investigate hydrological drought as a natural effect of an atmospheric drought signal. Streamflow data from rivers without considerable human influence are a readily available and well suited variable to study drought. Datasets on other hydrological parameters at the European scale are not available and national data are often obtained very differently. The quality of streamflow series also varies across the European countries. However, concepts relatively detecting drought in the streamflow time series are less sensitive to errors and varying accuracy than for instance water balance calculations. Finally, streamflow is visible for everybody and often directly used, which makes it an important indicator to study drought and water deficit periods.

3.2 Event definition

3.2.1 The threshold level method

Hydrological drought events derived from streamflow time series are most frequently defined by the threshold level concept: a drought event starts, when the flow falls below the threshold and ends either when the threshold is exceeded or when the water deficit volume below the threshold has been replenished. This concept was first applied in drought research, when Yevjevich (1967) adopted the statistical theory of runs for the analysis of time series. Parameters of the runs below the threshold (q_0), like the run-length (drought duration, d_i) and run-sum (deficit volume or severity, s_i) are now frequently used for a statistical characterisation of drought at a gauging station. To eliminate minor and mutually dependent droughts from the record of events, pooling procedures, like a smoothing of the original flow series or an inter-event criterion should be applied (Tallaksen et al., 1997). The parameters are often subjected to frequency analysis to obtain recurrence intervals of droughts of certain duration or severity, important information for hydrological design. Other studies model time series of run parameters as stochastic process (Sen, 1980). In the present study, the threshold level method is adopted to determine the historic drought events at European gauging stations. These events are the basis to study regional aspects of droughts using some of the drought parameters mentioned, but also individual events and daily time series of drought information.

The most important decision for drought definition is the choice of the threshold level. Basically, a threshold can be *constant* or *varying* over the year, depending on how one wants to define the ’abnormal’ situation (Chapter 3.1). If particular seasons are treated separately, a

different constant value can be chosen for instance to study summer and winter droughts (Figure 3.2a). If the 'normal' situation is considered to be a typical annual regime, the threshold should be varying at a monthly or daily resolution (Figure 3.2b/c). Such a varying threshold determines relative streamflow deficits during both, the high and low flow seasons. However, flow which is less then usual during a particular season but not absolutely low is commonly not considered a drought. Hence, events defined with the varying threshold level should be called streamflow deficiency or streamflow anomaly rather than streamflow drought. Details on the choice, derivation and application of the constant and varying threshold concepts for different ojectives in this study are given in Chapter 3.2.2 and Chapter 3.2.3.

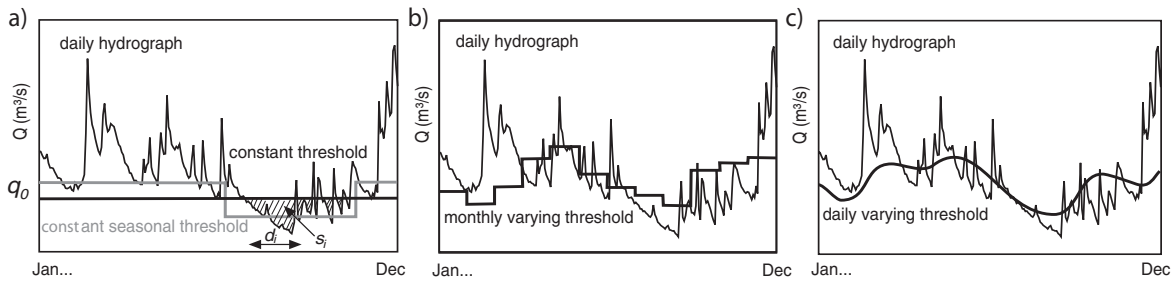

Fig. 3.2 *The threshold level method a) constant and seasonally constant threshold with indicated drought parameters d_i and s_i b) monthly varying threshold c) daily varying threshold*

A general decision to make is how to derive the actual threshold level value. This value can be a certain streamflow, e.g. necessary to fill a reservoir or to guarantee an ecological habitat in the river, or a certain water level required for navigation. It can also be derived as statistical value from the long-term hydrograph of the station. For a study which aims at comparing occurrence and characteristics of drought events across Europe, the threshold has to be chosen relative to the historic streamflow record at each site. Possible parameters include extremes of a certain period or season (low flow parameters), averages or a certain percentage of the average flow, or a percentile from the flow duration curve (fdc). Thresholds for drought definition are most commonly derived from a percentile of the flow duration curve, which is the complement of the cumulative distribution function of daily, weekly, monthly (or some other time interval of) streamflow (Vogel & Fennessey, 1994). The function can be determined by plotting the flow (Q in m³/s) versus the corresponding flow exceedance, a dimensionless index that expresses the proportion of time, p, that a specified daily flow is equalled or exceeded during the considered period (Gustard et al., 1992).

Finally, the time resolution to be used also depends on the purpose of the study and on the climatic region. If drought is defined as an abnormal situation, in the temperate humid zone with regimes of high within-year variability daily flow has to be used, as already short dry periods of less than a month are exceptional and might have undesirable effects. In regions with high inter-annual variability, droughts lasting for a year or several years, suggest the use of monthly or even annual averages for drought analysis. For the analysis covering both cli-

mates, and the majority of data from northern, central an eastern Europe, the daily resolution was chosen.

3.2.2 Streamflow drought - a constant threshold level approach

Method and drought parameters

The threshold level method with a constant or seasonally constant threshold level has been applied in many regional studies across Europe, mainly in the framework of the Northern European FRIEND Low Flow Group (e.g. Demuth & Heinrich, 1997, Tallaksen & Hisdal, 1997). Within the ARIDE project, the method was found most suited to study persistency and trends in historic drought series (Hisdal et al., 2001a, Chapter 4), as it determines the most severe summer drought events, which have been an issue in the latest climate change discussions.

If drought events are defined using streamflow data, two types of droughts can occur: droughts, which are caused by a lack of precipitation and high evaporation losses and so-called "winter droughts", which are due to precipitation being stored as snow or rivers being covered with ice. These two drought types have different implications for water resources management. The trend analyses in Chapter 4 excludes "winter droughts" as these are drought types not experienced in the whole of Europe. As European river flow regimes vary significantly, with regions with winter or summer low flow seasons and large transition zones (Chapter 2.3.4), three different season categories were defined.

- *All year:* no season was applied to the stations without influence of frost and snow in Spain, Britain, southern Scandinavia and most of the non-mountainous, central European catchments.
- *April 15 to November 30:* a long summer season was applied to the mountainous areas in Central Europe, coastal Norway and most of the eastern European catchments.
- *June 15 to October 31:* a short summer season was applied to the high alpine catchments and most of Norway and Sweden.

Based on the first and last month of the year with a mean monthly temperature above 0°C (CRU, 2001), monthly streamflow regimes (Chapter 2.3.4), the timing of maximum, median and minimum values of streamflow during the year, and other available information, all 612 catchments were classified into the three season categories. Chapter 3.3 discusses details and consequences of this classification.

The threshold level value for each station was then determined from the seasonal flow duration curve of the common time period 1962-1990. According to the recommendations in Hisdal & Tallaksen (2000), the Q70, the flow equalled or exceeded for p = 70% of the time, was chosen as threshold level for the trend analysis in Chapter 4. Some comparative analyses discussed in the following section and in Chapter 3.3 additinally used Q90 as threshold level.

Based on the comparison and description of three different pooling procedures by Tallaksen et al. (1997), the streamflow time series were smoothed with a 10-day moving average prior to the drought event definition. From the drought parameters duration d_i and severity s_i, the following annual parameters were derived (Hisdal et al., 2001a):

- AMD, annual maximum duration (days)
- ACD, annual cumulated duration of all drought events (days)
- AMV, annual maximum deficit volume standardised by seasonal mean flow (days)
- ACV, annual cumulated deficit volume standardised by seasonal mean flow (days)
- ND, number of drought events per year (-)

Influence of time period

The representativity of the threshold derived from the reference period Period 1 (1962-90) was assessed by analysing the dependency of the threshold level values Q70 and Q90 from the chosen period. Figure 3.3 compares the percentiles derived from Period 1 with the percentiles derived from the period of record, which varies for the stations. The variability is very high with the percentiles deviating up to 50% above or below the value of Period 1. However, there is no tendency for a trend with increasing length of the period.

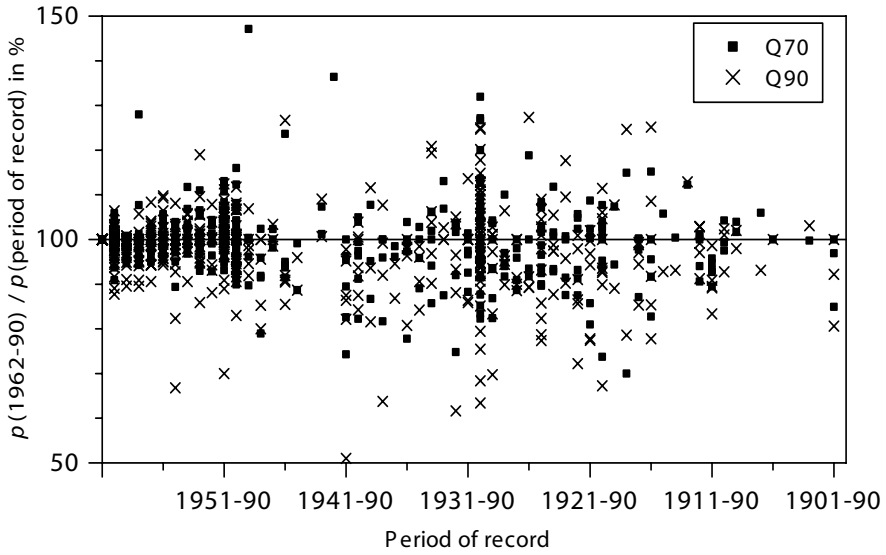

Fig. 3.3 *Variability of fdc percentiles (p) with the period of record*

To investigate the influence of the threshold level on the drought parameters, annual maximum drought duration series (AMD) were calculated for all records covering the long period 1931-90 and are compared with the AMD calculated for the two sub periods 1931-60 and 1961-90. Figure 3.4 shows the results for three stations in Germany. Due to a higher threshold level of Q70 in the sub-period 1961-90 in the Wesnitz (407005), the drought durations derived from this period are considerably higher compared to the durations calculated with

the threshold from the entire period. The Enz (161885) shows the opposite behaviour. For the Radolfzeller Ach (1620026) the length of the period has no effect on the result. The differences in the volumes calculated from the three different periods are considerable for all the stations as they are even more sensitive to a small change of the threshold level.

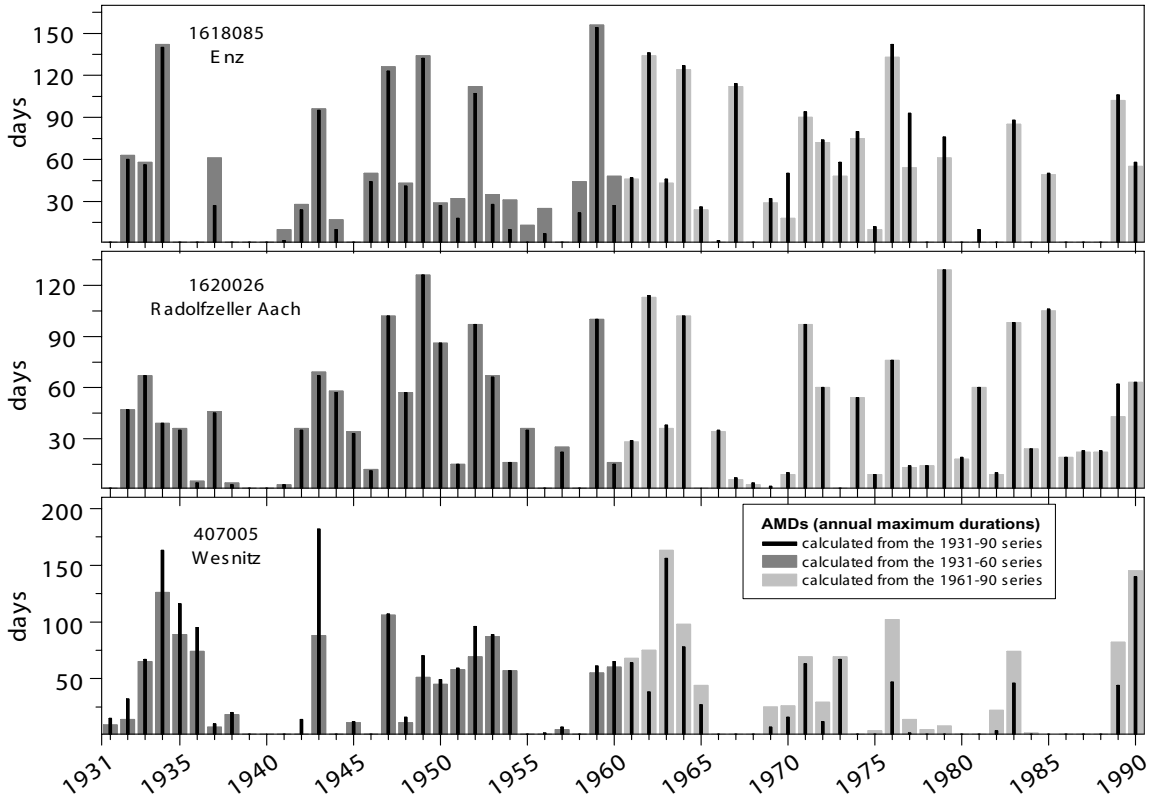

Fig. 3.4 *Influence of the selected period on the drought parameters*

Theses results led to the decision for further analysis to determine the threshold from the reference period and use the same threshold value when analysing drought for other periods. Thus Q70, the flow which is equalled or exceeded for 70% of the time in Period 1 (1962-90) is used to define drought events across Europe.

3.2.3 Streamflow deficiency - a daily varying threshold level approach

Method

Another event definition considers periods of streamflow deficiency defined as a departure or anomaly from the 'normal' annual low-flow cycle (varying threshold). There are several reasons, why such a relative approach was adopted in this study.

- Besides a wintry snow season, there might be other reasons for regular seasonal fluctuations in the annual streamflow regime to which nature and water resources management

have adjusted over decades. It is not the regular (and expected) summer low flow period, which causes problems, but any deviation from that normal range.

- The method can be applied across Europe's great variety of hydrologic, geographic and climatic regions without predefining specific seasons to be analysed. The resulting streamflow deficiency periods are independent from regional climatic characteristics such as snow storage in winter, because they are derived as departures from the typical regime. Hence they can be attributed mainly to an actual rainfall deficit situation.
- Deviations during the high flow season might also be important for the drought development. If groundwater recharge during the wet season is lower than usual, a groundwater drought is likely to develop during the following dry season. This missing recharge is also detectable in the lower than usual streamflow during the recharge season, caused by the same lack of rain triggered by prevailing unusual atmospheric circulation patterns.
- For the correlation of drought with preceding atmospheric circulation, continuous daily time series of a streamflow deficiency signal are required.

However, periods with relatively low flow either during the high flow season or for instance due to a delayed onset of the spring flood in high mountain or nordic regions is commonly not considered a drought. The low flow during the high flow season might result in a drought later, but there might not necessarily be any water deficit consequences at this moment. In the case of the delayed spring flood on the other hand, an end to the anomaly situation can be expected. Therefore, the events defined with the varying threshold are called *streamflow deficiency.* A streamflow deficiency during the low flow season corresponds to a severe drought.

The varying threshold level method determines periods below an annual threshold cycle, which consists of a specified exceedance probability, p, of daily flow duration curves. Since daily discharge values are used in the study, the varying threshold should also have a daily resolution. Normally, fdcs are based on calendar units (year, month, day) (Figure 3.5a). For a short time period like Period 1 (1962-90), a daily fdc would be constructed of 29 values only. To increase the sample size, a daily flow duration curve was obtained from a moving window sample also including the streamflow values of the preceding and following days (Figure 3.5b). This procedure allows the construction of a smooth fdc for each day of the year.

The method is illustrated using data from for the Brugga catchment in Germany. As an example, daily flow duration curves derived from the 29-year common time series and a 21-day moving window, are shown in Figure 3.6a. The resulting annual percentile cycles, possible varying threshold levels, are plotted in Figure 3.6b. The catchment has a high seasonality with higher flows in spring due to snowmelt in the high altitudes of the Black Forest mountains and a low flow period in late summer. During the high flow season, streamflow exhibits a high variability. Figure 3.6c shows the periods below the varying threshold levels Q70, Q80 and Q90 by displaying the daily deficiency indicators *DI(t)* with

$$DI(t)\mathrm{Z}\begin{cases}1 & if \quad Q(t) \le threshold\\ 0 & if \quad Q(t) > threshold\end{cases} \qquad \textbf{(3.1)}$$

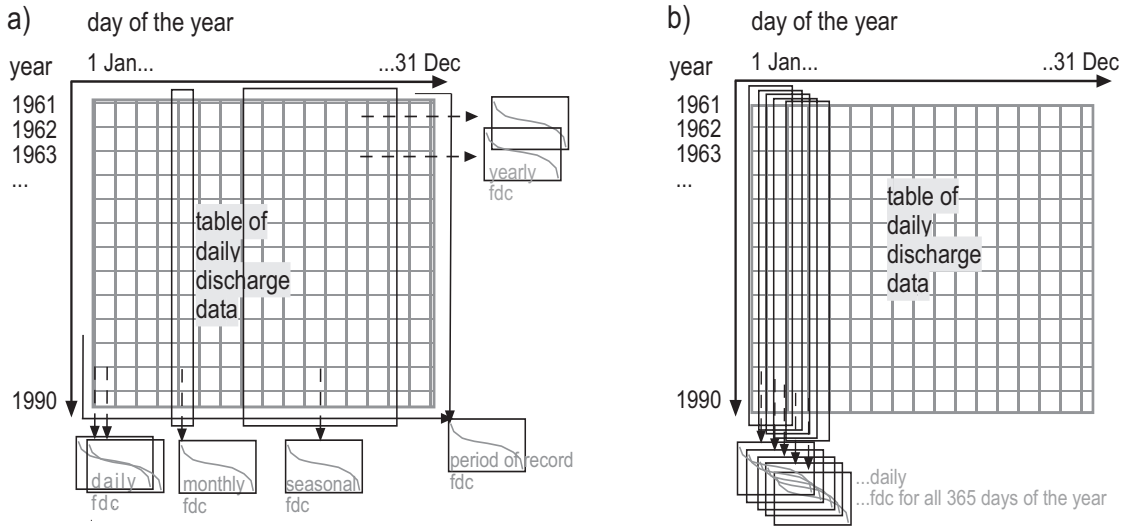

Fig. 3.5 *Flow duration curves a) based on calender units b) for each day of the year based on a moving time window*

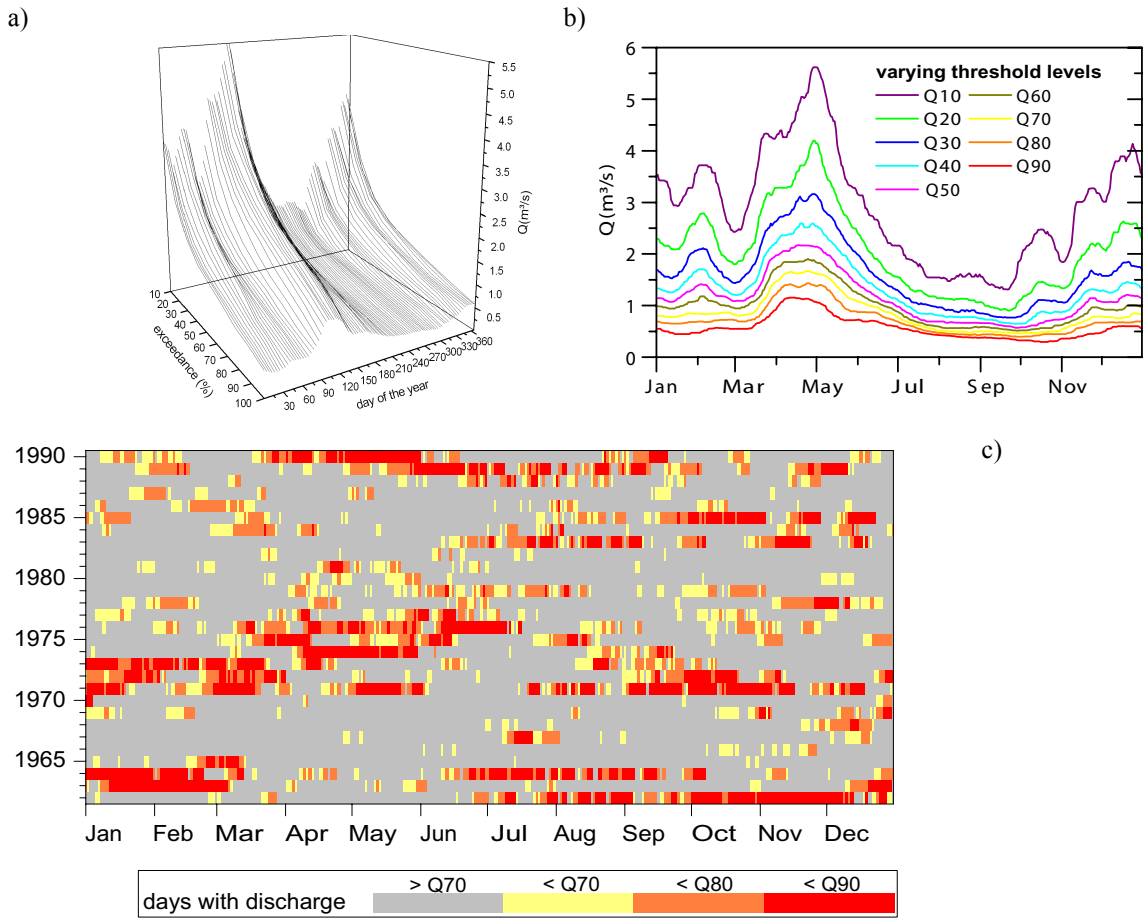

Fig. 3.6 *The varying threshold level approach applied to the Brugga river, Germany a) daily flow duration curves from a 21-day moving window b) the resulting annual exceedance cycles c) streamflow deficiency periods below the varying threshold levels Q70, Q80 and Q90*

coded in different colours. By definition, the resulting periods below the varying threshold occur during all times of the year. A dry spell in spring might indicate a delayed snowmelt, or a winter with less snow than usual and thus no recharge to the groundwater reservoirs. The latter situation may cause a summer water deficit to develop earlier than usual. Examples of spring anomalies can clearly be seen in Figure 3.6c (e.g. 1973-76, 1990).

Sensitivity of the method to window size and time period

The influence of the size of the moving window was evaluated to find out the shortest possible window to maintain the typical singularities in the annual cycle, while assuring a sample large enough to determine the discharge percentiles for each day and smooth enough to allow longer deficiency events to develop. With increasing window size, peaks in the varying threshold levels get lower and broader and minima get higher and broader. Typical fluctuations are smoothed. Window sizes between 1 day and 31 days for the sensitivity test were chosen subjectively on the assumption that a typical seasonal pattern would recur within the range of the same days to weeks of the year. To find the minimum required sample size, the number of streamflow deficiency days was calculated applying the varying Q90, Q80 and Q70 derived with window sizes from 1 to 31 days. These calculations were carried out for the 54 series covering Period 3 (Chapter 2.2.1) and for the two sub-periods 1930-61 and 1962-93 to assess the influence of the time period as well.

The sensitivity to the window size is assessed by the *DI*-excess, which is the sum of the resulting streamflow deficiency days *DI* in relation to the theoretical number of *DI* (10% of all days of Period 3 for threshold Q90, 20% for Q80, etc.). Most of the 54 series exhibit a similar pattern: the *DI*-excess varies considerably for small window sizes and starts to level off around the 10-day window. The median of the *DI*-excess of all the series for different window sizes is illustrated in Figure 3.7. Generally, the calculated number of streamflow deficiency days approaches the theoretical number with increasing sample size. The sample for construction of the daily fdcs can be increased either by a longer time period or by a larger window size. For Q90, some sample sizes are indicated as numbers in Figure 3.7a. Here, the variability of the *DI*-excess decreases for sample sizes larger than ca. 300 days for the 32-year sub-periods (1930-61 and 1962-93). This corresponds to a time window of ca. 9 to 10-days. For the long period (1930-95) or for the threshold levels Q80 and Q70 (Figure 3.7b/c), smaller window sizes are sufficient. For larger window sizes, differences are small. Plotting of the occurrence of the deficiency indicators for some examples showed, that there is hardly any effect. For the varying threshold method, it can thus be recommended to have a sample size of at least 300 days for the estimation of each daily percentile. The upper limit depends on the degree of variability one wants to keep in the yearly threshold cycle.

Finally, the exceedance percentiles for each day of the year were calculated from an 11-day moving window covering all years of the 29-year Period 1 (1962-90) to get a sample size of 319 values for the daily fdcs. Hence, the fdc for January 6th is constructed from all discharge

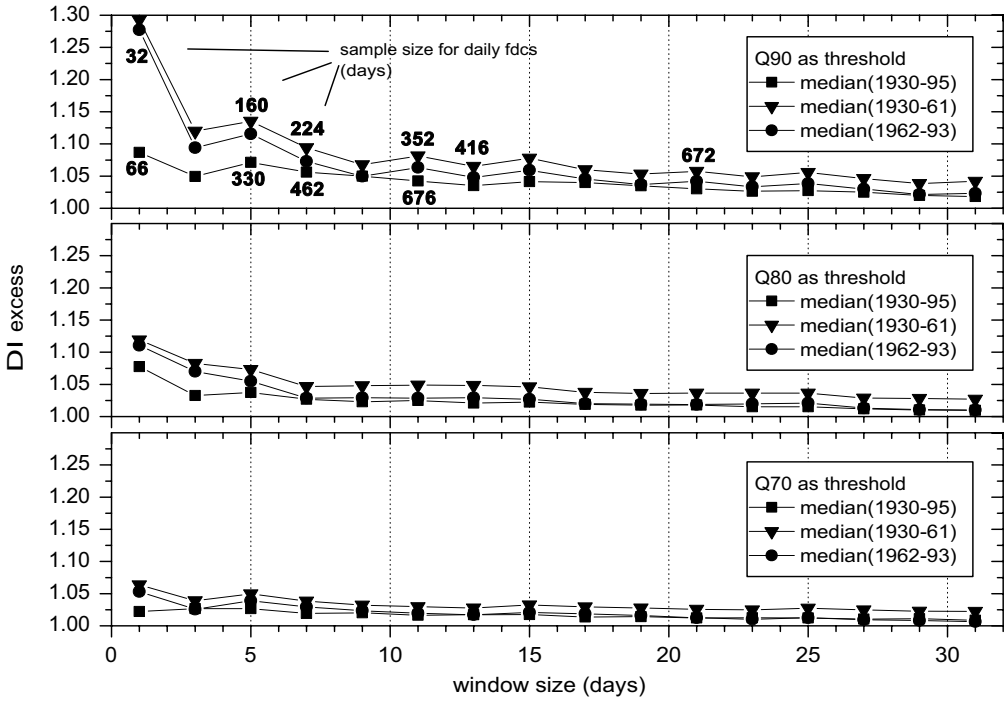

Fig. 3.7 *Influence of the size of the moving window, the period and the threshold level on the number of days with streamflow deficiency.*

values between January 1st and January 11th during the period 1962-1990, etc.. The 90% exceedance levels of these daily fdcs were chosen as the threshold level. The streamflow at each day of the time series from 1962-90 is then compared to the Q90 of the respective day of the year and coded into streamflow deficiency indicators (*DI*). This varying threshold level method was applied for the studies of time-space characteristics of events, the regional analysis, and the investigation of atmospheric circulation influencing streamflow deficiency (Chapter 5 to Chapter 8).

3.3 Comparison of streamflow drought and deficiency

For the dataset of Period 1 (1962-90), *streamflow drought* was determined with the seasonally constant threshold level method and *streamflow deficiency* with the varying threshold level method. Thus, daily time series of drought indicators and deficiency indicators for the constant and varying threshold levels Q90, Q80 and Q70 were determined. Figure 3.8 shows examples of the drought and deficency series for three stations, which belong to three different season categories.The examples illustrate the different type of events identified with the two threshold level methods. Some aspects of the relation of the two methods and the interpretation of the analysis of drought and deficiency are highlighted.

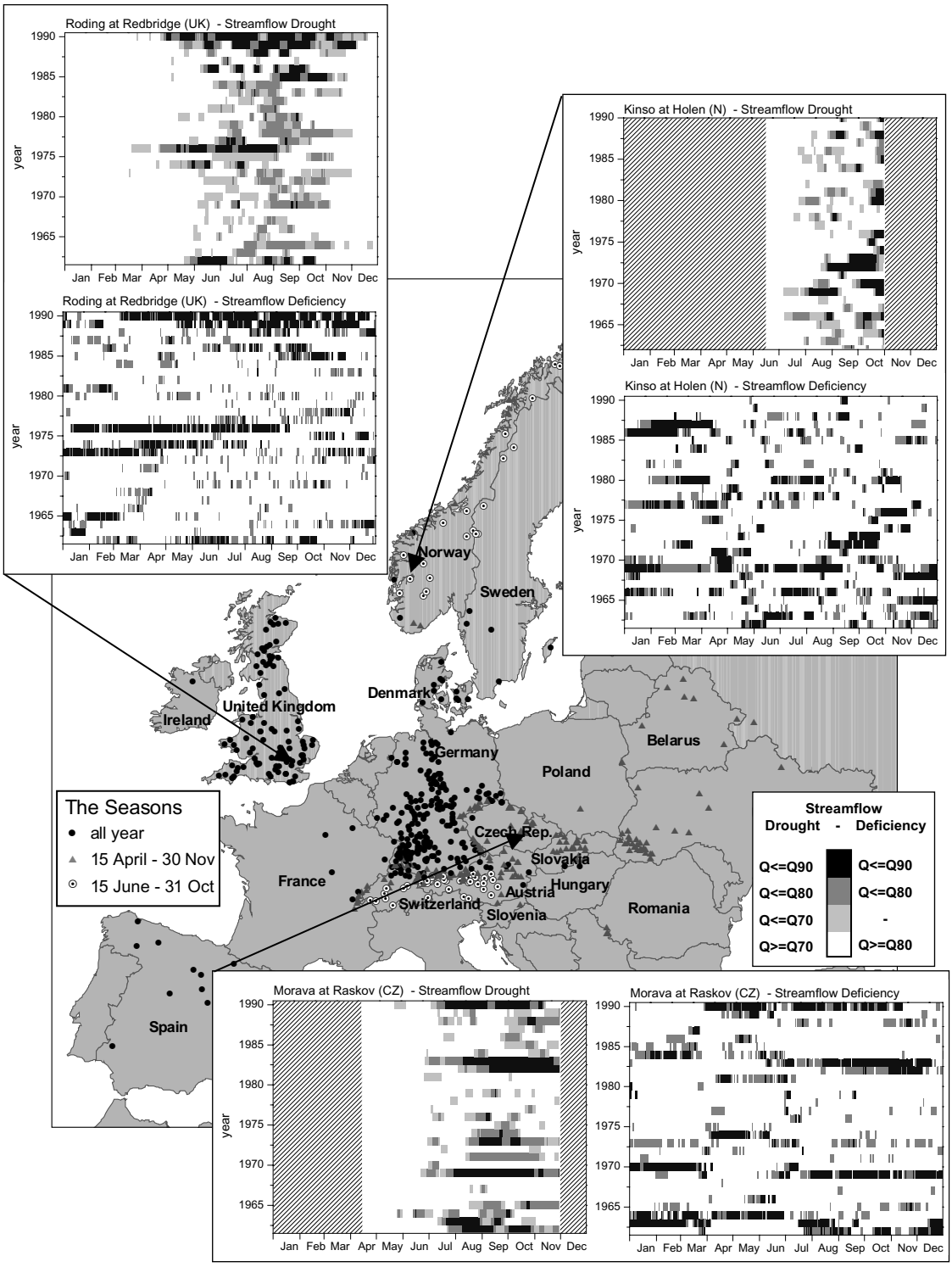

Fig. 3.8 *Drought and streamflow deficiency indicators for three selected stations in Europe.*

The river Roding in southeastern UK has an atlantic regime without influence of snow. Therefore, no season was considered for drought analysis (*all year*). The drought indicators show that low flows generally occur in summer time. The longest and severest drought events

occurred in 1962, 1974, 1976, 1985 and the summers of 1989 and 1990. The streamflow deficiency series generally shows the same severe years. The summer drought in 1976 was preceded by unusually low streamflow during autumn 1975 and spring 1976. Similarly, an extremely dry autumn and winter, which is normally the recharge season, precede the 1989 summer drought. However, there have also been dry winters without consequences in the following summers.

The river Kinso in Norway was classified into the short summer season (*June 15 - October 31*), as it has a mountain regime strongly influenced by winter freezing and snowmelt in spring. The most severe summer drought events occurred in 1966, 1969, 1970, 1972 and 1973 and then again in the early and late eighties. In particular the summer droughts in 1966 and 1969 followed streamflow deficiencies during the preceding winters and springs. Within this region, these winters might have been extremely cold with ice covered rivers. Since streamflow was also lower than usual the following spring and summer, the water equivalent or the amount of snow during winter might have been less than usual. Additional meteorological data would be necessary to prove such hypotheses.

The river Morava in the Czech Republic was classified into the long summer season (*April 15 - Nov 30*) for drought analysis, as its regime has a snowmelt maximum in March/April and a low flow season in late summer. The river tends to develop long dry spells. Severe droughts occurred in the summers of 1962 and 1963, in 1969, 1982, and 1983, when the drought lasted into the winter, and in summer 1990. The streamflow deficiencies also depict these events. However, they also point out some long relatively dry periods in spring and early summer (1964, 1974, 1981, 1989 and 1990), a season which is particularly important for the agriculture in the region.

3.4 Conclusion

Drought definitions found in the literature cover numerous different methods and variables. For a study across Europe, concepts which define drought as a relative departure of the normal situation have to be applied. Two different types of events were therefore defined from the European streamflow dataset: *streamflow drought*, defined by a seasonally constant threshold level method and *streamflow deficiency*, defined by a varying threshold level method. Streamflow drought was defined by a seasonal Q70 as threshold level. Minor and mutually dependent droughts were pooled by a smoothing of the streamflow series with a 10-day moving average. The derived drought parameters, i.e. drought duration and severity, are suited to analyse whether droughts in Europe have become more frequent or severe (Hisdal et al., 2001a; Chapter 4). Streamflow deficiency events were defined as periods when the streamflow is below a varying threshold describing a typically expected annual cycle of low flows. The threshold was derived from the Q90 values of daily flow duration curves. In the

European dataset, the variability of the annual cycles for the high percentiles ranges from highly fluctuating to almost constant. Without predefining seasons, this relative approach to defining deficiency periods allows the application to and the comparison across Europe's great variety of hydrologic, geographic and climatic regions. The resulting deficiency periods are independent from seasonal regional climatic characteristics such as snow storage in winter. Hence, they can be attributed mainly to the actual meteorological situation and are therefore suited for the link to atmospheric circulation (Chapter 7). Comparing the time series of drought and deficiency periods gives a first insight into the causes and seasonal development of summer drought periods, which are a crucial hazard across Europe.

4 Time Series Analysis

4.1 Introduction

While discussing suitable datasets and methods, the previous chapters have set the basis for a regional drought analysis across Europe. The choice of the time period and the datasets was mainly based on data availability, a good spatial coverage of stations and the use of most recent data. In this context, the influence of the variability of natural time series on the methods for drought event definition and consequently on the drought analysis have already been discussed. Now, after having derived the time of droughts and streamflow deficiencies from the original streamflow series, important and interesting features can be studied. A clustering of wet and dry years and the tendency of some records to develop very long dry spells, noticed in the example plots of the drought/deficiency indicator series (Chapter 3.3), call for the investigation of the persistency of drought. Furthermore, the dataset of drought parameters gives the unique opportunity to study changes in the historic series in a regional context. The question, whether *'droughts in Europe have become more frequent or severe?'* was assessed by a trend analysis on the drought parameters from the four different time periods (Chapter 2.2.1) and documented in Hisdal et al. (2001a), a summary of which is given in Chapter 4.3.

4.2 Persistency

4.2.1 The persistency phenomenon

Most hydrological time series exhibit persistency, as the underlying processes depend on many different feedback mechanisms. Droughts in particular are slowly developing phenomena and once initiated, they tend to persist. In fact, if they did not persist, their impact on man's activity would be minimal (Beran and Rodier, 1985). Different time scales of persistency can be distinguished for droughts and streamflow deficiency, the most important being within-year and inter-annual persistency. In Europe, most precipitation and streamflow regimes have a typical seasonal variation. Within-year persistency of droughts is then a result

of the natural storage processes in the hydrological cycle: in the dry season, the surface and soil reservoirs of the catchment are already drained and finally streamflow is merely fed by groundwater. The aquifers will not be recharged until the next rainy season and as a result, a drought might prevail during the dry season, if rainfall is low. In addition, there are evidences of considerable inertia and feedback mechanisms in the atmospheric phase, blocking tendencies being the most frequently mentioned phenomenon in context with temperate zone droughts (Beran and Rodier, 1985). As a result, depending on catchment properties and rainfall seasonality of the region, within-year droughts might strongly depend on previous events. There are also indications of inter-annual persistency of droughts, resulting from slowly reacting large aquifer systems and long-term climatic fluctuations. Such fluctuations influence sea surface temperatures, which in turn affect the persistence and recurrence of certain atmospheric circulation patterns that might be relevant for drought. Hydrological droughts and seasonal streamflow deficiencies can consequently be expected to be persistent at various time scales due to the aforementioned influencing factors.

4.2.2 Non-randomness in annual drought parameters

Most statistical methods often applied to drought parameter series require independency of the events in the series, as they assume randomness of the sample. Besides the better understanding of drought processes, a persistency analysis consequently has a general practical relevance in drought planning. Time series of drought events are usually highly skewed with many small events and a few large (compare Chapter 3.3). A parametric test for detection of persistency based on the normal distribution is therefore not recommended. Instead, a widely used non-parametric test for randomness recommended by the World Meteorological Organization (WMO, 1988) was chosen:

Runs are defined as a set of consecutive observations above and below the median of the sample. If the data are randomly distributed, the expectation E and the variance Var of the number of runs are

$$E(n_r) = 1 + \frac{n}{2} \tag{4.1}$$

$$Var(n_r) = \frac{n(n-2)}{4(n-1)} \tag{4.2}$$

where n is the number of data in the series and n_r is the number of runs. The approximately normally distributed test statistic T is calculated as

$$T = \frac{nr - E(n_r)}{\sqrt{Var(n_r)}} \tag{4.3}$$

If a series oscillates strongly, the number of runs is large. If the variable remains persistently above or below the median, the number of runs is small. In both extreme cases, the series is significantly non-random, but for drought, only non-randomness resulting from few runs can be related to persistency. In the considered series, the test only detected significant non-randomness if the number of runs was small. Thus, a clustering of wet and dry years, which means that droughts are persistent at the inter-annual scale, can be detected applying the run test to series of annual drought parameters. The results of the run test using a 5% significance level for the annual maximum drought durations (AMD) of the pan-European dataset covering Period 1 (1962-90) are shown in Figure 4.1.

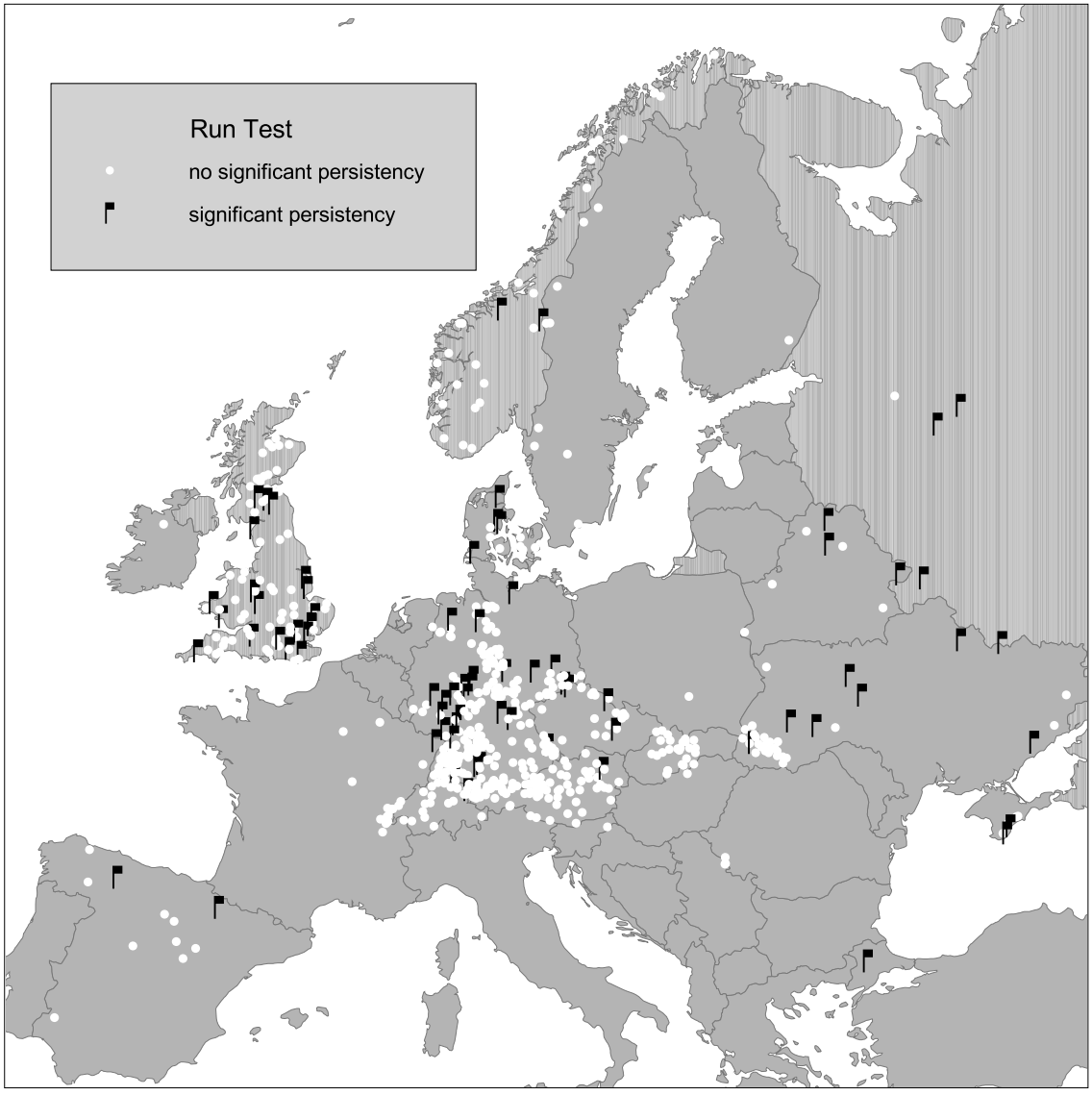

Fig. 4.1 *Non-Randomness in the series of the annual maximum durations (1962-90)*

Inter-annual persistency seems to dominate in the easternmost regions of Europe, Denmark and specific parts of western Germany. In the UK the picture is completely mixed with a slight tendency towards more non-randomness in the south east. A few more stations show non-randomness for the annual maximum deficit volumes (Hisdal et al., 2001b). All these regions are characterized by plains and sedimentary rocks, where streamflow is groundwater dominated, and therefore has a longer memory. Hardly any significant non-randomness is found for the mountainous regions in France, the Alps and Norway. The long series (Period 3, 1930-1995) reveal some stations with non-randomness in southern and eastern Germany (not shown). Few stations show persistency in both time periods. However, the dataset of the long series is very small, which makes it difficult to draw a general conclusion about persistency depending on the period.

4.2.3 Persistency in streamflow deficiency series

Within-year persistency, the tendency of a river to experience persistent extreme dry spells, can be studied using the streamflow deficiency indicator series, as they are continuous series of daily values for 29 years. The absolute number of runs above and below the varying threshold indicates whether the streamflow deficiency periods tend to be short and frequent or last long and thus are rare. Therefore the number of runs can be used to compare the within-year persistency of streamflow deficit of the streamflow records across Europe (Figure 4.2).

Between 200 and 500 runs were determined for most of the stations. The numbers vary strongly in space, but a pattern of small to large regions with similar persistency exists. The stations with the lowest number of runs were found in Spain, Norway and Sweden, eastern Europe and some stations in southern Britain. There are many stations with less than 300 runs in southwestern Britain, in central Germany and in the Czech Republic. The number of runs reflects the different behaviour already discussed in Chapter 3.3: with 183 runs in 1962-1990, the Morava at Raskov is a river which tends to persistent dry spells. The Norwegian river Kinso at Holen takes a medium position with 380 runs.

Rivers with many short (interrupted) dry spells are found in northern and also in southeastern UK, in northern Germany and France, in southern Germany, along the Alps and in Ukraine. Consequently the persistency seems not directly related to regime type or low flow season. Redbridge at the river Roding discussed in Chapter 3.3 is a river with many runs (503) above and below the varying Q90. However, Figure 3.8 in Chapter 3.3 shows that the dry spells are still concentrated on a few selected years, but are often shortly interrupted. Despite the water deficit in the natural catchment reservoir, the frequent rainfall typical for the UK then raises the hydrograph above the threshold, but after the rain has stopped, the streamflow quickly recedes back to low level. This example reveals a problem of the aggregation of deficiency days. If parameters like duration and severity are the scope of the study, a pooling method similar to the one used for drought event definition should be applied.

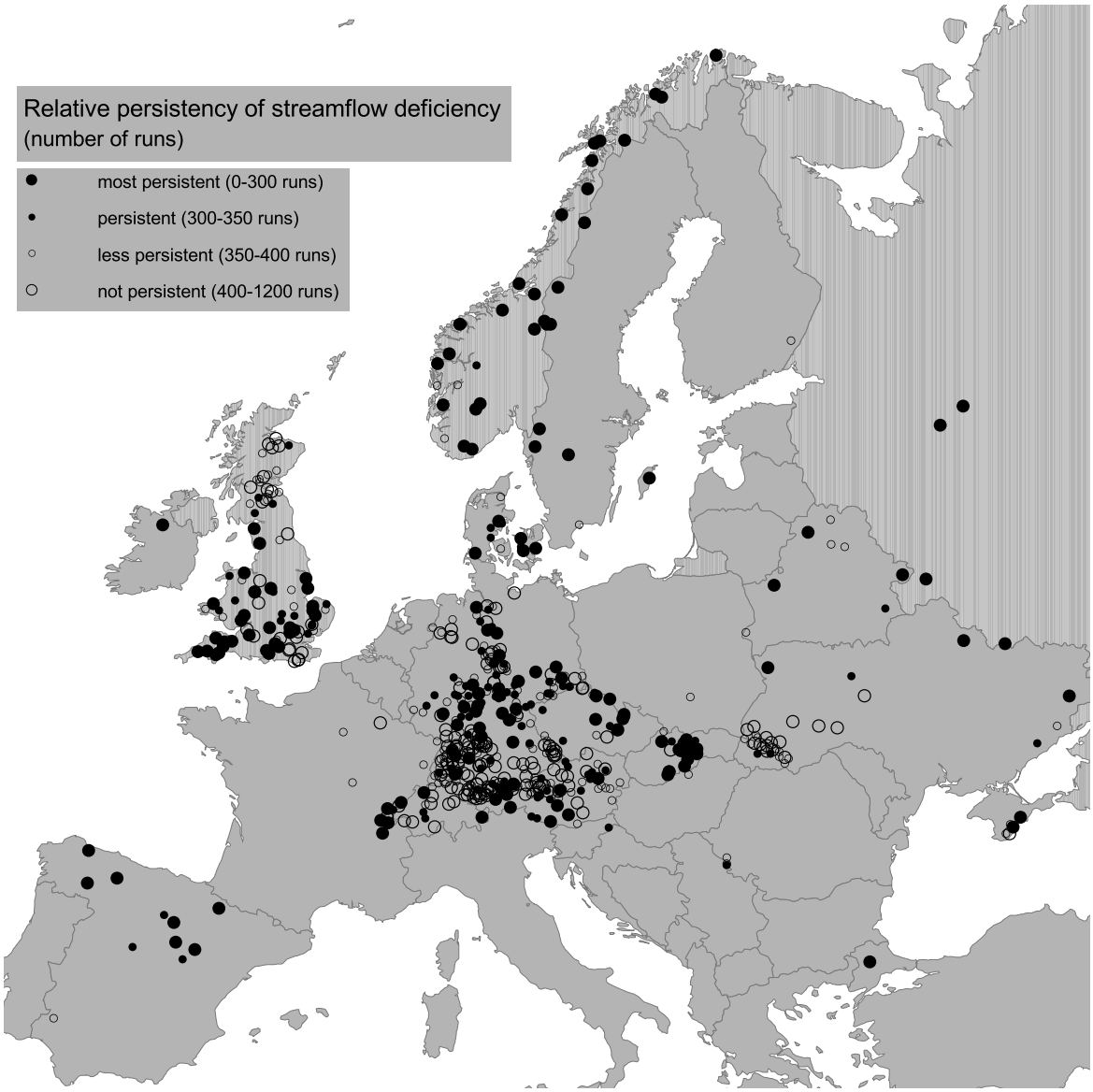

Fig. 4.2 *Persistency of streamflow deficiency periods across Europe*

4.3 Trends

4.3.1 Origin and analysis of trends in drought series

Trends in historic streamflow drought series might be caused by anthropogenic influences in the catchment, e.g. river regulation or irrigation. Another reason for trends is climatic change. In particular, a change in precipitation and evaporation would cause a change in hydrological drought. With the projected global temperature increase, scientists generally agree that the

global hydrological cycle will intensify and suggest that the extremes of droughts and floods will become more common (Watson et al., 1998). Media often reflect the view that recent severe drought events are a sign of human influenced climate change (e.g. Schmid, 1998). Many European river basins have experienced severe droughts in the late 80ies and during the 90ies (Arnell, 1994). It is also stated that in the last decades the drought situation in most of central and eastern Europe has worsened, because the frequency, duration and strength of the drought events have increased (DVWK, 1998). Finally, a trend found in a time series of the usual available length for streamflow might just be part of a natural fluctuation, which is difficult to find out due to the lack in the availability in longer series.

Due to the method for event definition, only drought determined with a constant threshold can be analysed for changes and related to the aforementioned causes. In the ARIDE project, a pan-European trend analysis of droughts tried to answer the question of whether streamflow droughts have become more frequent (in terms of the number of drought events each year) or severe (in terms of the maximum drought deficit volume and duration each year). Because of the skewed distribution of many drought parameters it was chosen to apply two widely used non-parametric trend tests: the Mann-Kendall test and a resampling test (Hisdal et al., 2001a).

The Mann-Kendall test is a rank based test for correlation of to variables, which in this case are time and drought series. For the drought parameter time series (y_t, $t = 1, \ldots, N$), according to Salas (1993), each value of the series yt', $t' = 1, \ldots, N\text{-}1$ is compared with all subsequent values series y_t, $t = t'+1, t'+2,\ldots, N$, and a new series z_k is generated by:

$$\begin{aligned} z_k &= 1 \quad if\ y_t > y_{t'} \\ z_k &= 0 \quad if\ y_t = y_{t'} \\ z_k &= -1 \quad if\ y_t < y_{t'} \end{aligned} \qquad \textbf{(4.4)}$$

in which $k = ((t'\text{-}1)(2N\text{-}t')/2)+(t\text{-}t')$. The Mann-Kendall statistic, S, is given by the sum of the z_k series:

$$S = \sum_{t'=1}^{N-1} \sum_{t=t'+1}^{N} z_k \qquad \textbf{(4.5)}$$

This statistic represents the number of positive differences minus the number of negative differences for all the differences considered. The test statistic, u_c, for $N > 40$ may be written as:

$$u_c = \frac{S - m}{\sqrt{Var(S)}} \qquad \textbf{(4.6)}$$

where $m = 1$ if $S < 0$ and $m = -1$ if $S > 0$. The variance, $Var(S)$, is calculated as:

$$Var(S) = \frac{1}{8}\left[N(N-1)(2N+5) - \sum_{i=1}^{n} e_i(e_i-1)(2e_i+5)\right] \quad (4.7)$$

where n is the number of tied groups, and e_i is the number of data in the i^{th} (tied) group. The statistic u_c is assumed to be zero if $S = 0$. The hypothesis of an upward or downward trend cannot be rejected at the a significance level if $|u_c| > u1\text{-}a/2$, where $u1\text{-}a/2$ is the 1-a/2 quantile of the standard normal distribution.

The resampling test (Good, 1994) is based on comparing the original test statistics to the test statistic calculated from many permutations of the original series. Again, consider the drought time series y_t, $t = 1,\ldots, N$. The hypothesis of no trend is to be tested against the alternative that there is a positive or negative trend. The test statistic, T, is calculated as:

$$T = \sum_{t=1}^{N} t\, y_t \quad (4.8)$$

Then $N!$ permutations of y_t are carried out and for every rearranged set, y_t^*, the value T^* is calculated as:

$$T^* = \sum_{t=1}^{N} t\, y^*_t \quad (4.9)$$

In the presence of a trend, the value of the test statistic, T, should be larger than 1-a/2 of the T^* values or smaller than 1-a/2 of the T^* values.

To reduce the number of permutations, the original data series were divided into six blocks and the test was carried out on the block averages. In this way 6! = 720 permutations and hence 720 values of T^* were calculated. A significant positive trend (drier conditions) or negative trend (wetter conditions) is indicated by the value T being larger (positive trend) or smaller (negative trend) than T^* in (1-a/2)*100% of the 720 cases.

Both tests were performed on all five drought parameters derived with a constant threshold of Q70 (Chapter 3.2.2), applying a two sided test with a five percent ($\alpha = 0.05$) level of significance. The results were assessed in three different ways: summary statistics on the significant trends, mapping of the spatial variability of the trends and plotting of test statistics for a long series based on successive 30-year periods.

4.3.2 Trends in European drought series

The percentages of stations with significant positive and negative trends were calculated. A five percent significance level implies that significant trends can be expected for five percent of the records, even if no trends are present in the dataset. However, the trend tests for all

drought parameters result in a higher percentage than five with the exact figure varying between 7% and 26% depending on the period, parameter and test (details in Hisdal et al., 2001a). For most stations, the test results for the parameters AMV, AMD, ACV, ACD are similar, the number of droughts shows contradicting results for some stations. For most periods, the number of negative significant trends pointing towards decreasing drought severity or fewer drought events exceeds the number of positive significant trends.

Although the majority of stations do not exhibit significant trends, clear regional patterns in trends were found. Figure 4.3 shows the trend statistics found for the Mann-Kendall test on AMV for the period 1962-90. The stations exhibiting significant trends in this period tend to cluster and the surrounding stations often show a Mann-Kendall statistic pointing in the same direction. The most apparent European regions, where drought severity increased during the

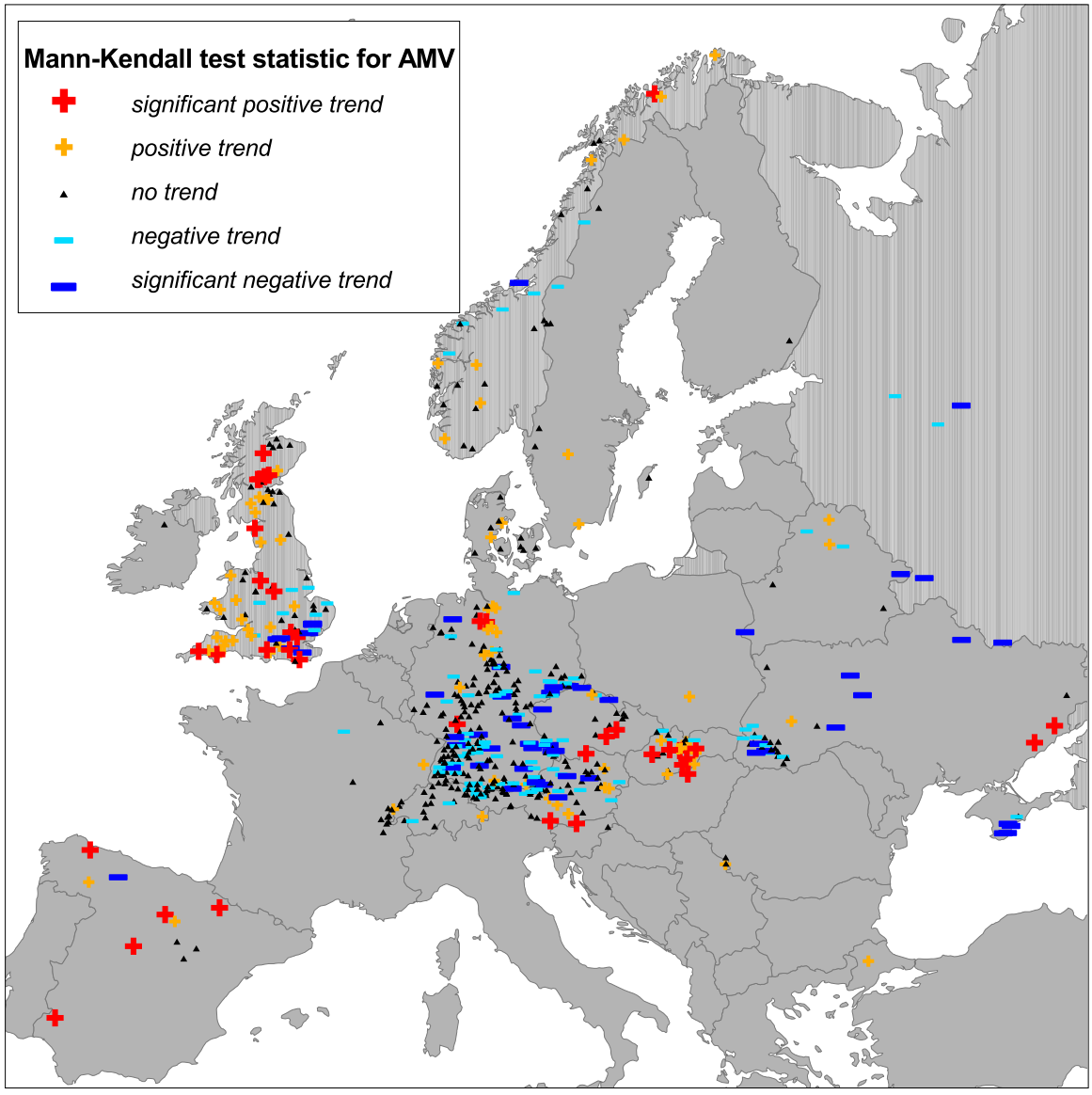

Fig. 4.3 *Results of the Mann-Kendall trend test (1962-90) for AMV*

period 1962-90, are Spain, southern and western Britain, the Czech Republic and Slovakia. Coherent regions with trends towards less severe droughts are found in areas in the southern part of Germany extending into Austria, in eastern Europe (i.e. Belarus and Ukraine) and to some extent the western coast of Norway.

The frequency of droughts, in terms of the annual number of drought events (ND), shows a different pattern (Hisdal et al., 2001a). The stations in the Czech Republic and Slovakia, a region with more severe droughts, also show a trend towards more droughts. Most of the UK, however, tends towards fewer drought events per year combined with more severe drought events. This might be explained through the physical characteristics of the catchments, the natural storage capacity being the most important. There is also a region with tends towards more events per year in an area stretching along the south of Germany and southwestward into France. In eastern Europe, the aforementioned trends towards less severe droughts coincide with trends towards fewer events per year.

Changing the period analysed also changes the trend patterns in some regions. The dependency of the trend on the period analysed can be illustrated by calculating the trends in successive periods using very long time series. Figure 4.4 shows the AMV series for the example of the river Vils from Germany together with the calculated Mann-Kendall test and Resampling test statistics for consecutive 30-year periods, starting with 1911-40, then 1912-41, etc. The statistics illustrate that trends might change from significant positive in the beginning of the period to significant negative at the end. This is a result of the calculated trends being very sensitive to the magnitude of the droughts in the beginning and end of the series.

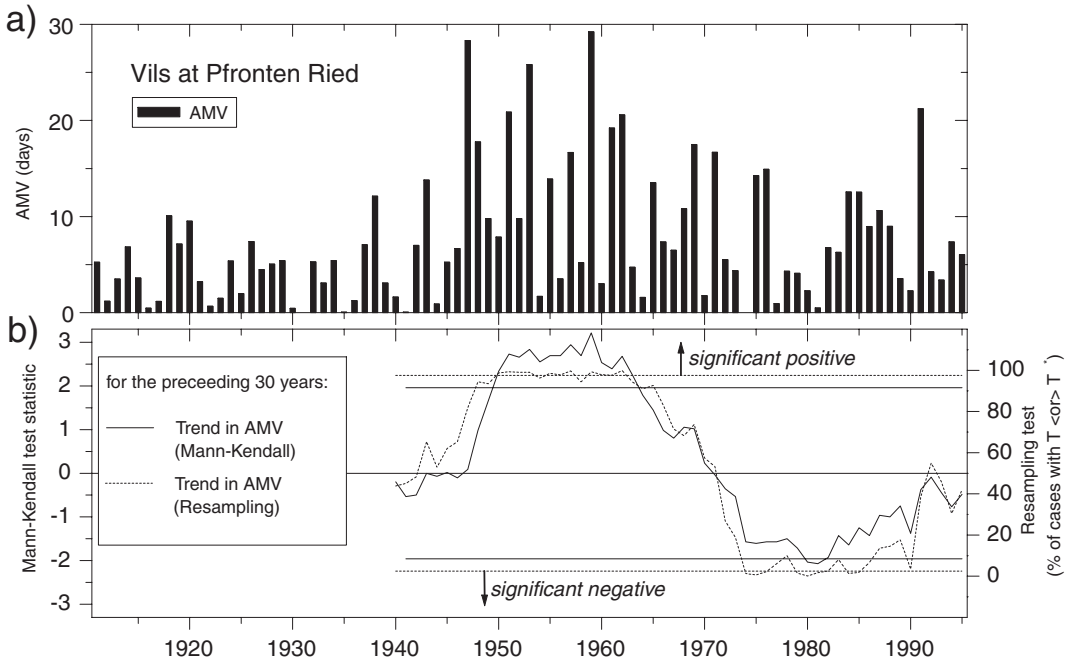

Fig. 4.4 *a) The series of annual maximum deficit volume (AMV) for Vils in Germany and b) the trend test statistics calculated for consecutive 30-year periods*

4.4 Conclusion

The persistency test carried out on the pan-European data set showed that with some exceptions, droughts in rivers from mountainous regions in Europe exhibit less persistency than rivers in lowland areas. This regional pattern suggests inter-annual persistency for catchments where streamflow is fed by large groundwater reservoirs. As information on the catchment characteristics is not available, this hypothesis cannot be analysed further in this study. The overall number of runs of streamflow deficiency as determined with a varying Q90 as threshold level, gives an indication of the within-year persistency of streamflow deficits in a catchment. Relative seasonal streamflow deficiency periods are also found to be persistent in regions with strong seasonal regimes, such as Norway and Spain. This might indicate the influence of the lack of snow or rain in winter on spring or summer, but might also reflect geological characteristics such as poor storage capacities. Nevertheless, inter-annual and within-year persistency are present in the series and thus demonstrate the importance to consider the history of the meteorology and hydrology as antecedent conditions for the analysis of drought development and causes.

The pan-European trend analysis revealed that despite several reports on recent droughts in Europe, there is no clear indication that streamflow drought conditions in Europe have generally become more severe or frequent in the time periods studied. However, for the common periods, clear regional patterns were found. Although for Europe as a whole trends towards decreasing drought severity were calculated, in regions like Spain, southern UK and the Czech and Slovak Republics, drought severity has actually increased in 1962-1990. These regional trends can to a large extent be linked to changes in precipitation patterns found in several regional studies and to indirect artificial influences in the catchments. Hisdal et al. (2001a) in detail discuss evident causes for changed drought severity and frequency.

Time series characteristics like persistency and trend are strongly influenced by the records selected for analysis and by the drought parameters studied. The importance of the temporal aspect when testing for trends was clearly illustrated. What is seen as an increased frequency or severity based on a 'short' period of observations, might turn out to be a part of a long term fluctuation and cannot be seen as evidence of human-induced climate change nor be used as a basis for drought prediction into the future.

5 Analysis of Major European Streamflow Deficiency Events

5.1 Introduction

Most reviews of European drought events rely on information from different publications (e.g. Bradford, 2000). Being based on different methods, the properties of the drought events are then difficult to compare. Yet, due to the lack of pan-European datasets of hydrological variables with long records and an adequate method to be applied across Europe, a review based on homogeneous data has been difficult. Álvarez & Estrela (2000) have analysed droughts in terms of precipitation anomalies since the beginning of the century. The large-scale dry spells across Europe found in their study partly confirm other drought records. However, whether a precipitation deficit actually causes a hydrological drought, strongly depends on the meteorological history, the season and the basin characteristics. Arnell (1994) and Shorthouse & Arnell (1997) found that large parts of Europe show similar patterns of streamflow extremes over time and that the Nordic countries show a different pattern of variation over time than the rest of Central and Western Europe. Within the ARIDE project, a versatile drought visualisation atlas *ElektrA* was developed by CEH Wallingford (Zaidman et al., 2000). The software enables creation and display of animated sequences of maps, on which the historic daily streamflow conditions are shown as colour-coded grid based exceedance values. Odziomek (2000) demonstrated the benefit of such animated sequences for public information on drought and some examples are displayed in the visualisation section on the ARIDE project homepage (www.uni-freiburg.de/hydrology/forsch/aride/). Hence, the European Water Archive and the application of the varying threshold level method provide a great opportunity to study the dynamics of major European streamflow deficiencies in time and space.

In this study, the streamflow deficiency indicator series derived from the application of the varying threshold concept (Chapter 3.2.3) were used to explore the major large-scale European dry spells during the reference period 1962-1990. Similarly to the daily published streamflow conditions map of the USA (USGS, 2001), a new PV-Wave application was designed to visualise the whole period or any desired sub-period as animated map sequences. In addition to the hydrological situation, the daily maps also show the contoured mean sea

level pressure (MSLP) data over Europe and the North Atlantic. This new computer application allows to observe how historic streamflow drought events initiate, spread across Europe, and contract or break off in relation to the meteorologic situation.

5.2 Dynamic visualisation of synoptic meteorology and streamflow deficiency

For 602 European catchments from the streamflow dataset covering Period 1 (1962-90), the daily streamflow deficiency indicator series (*DI)* were derived by applying the varying threshold level approach with a varying Q90 as threshold. Since the station density varies considerably across Europe, the plot of the number of stations affected by streamflow deficiency on each day during the period (Figure 5.1a), can still give a rough indication of the occurrence of the largest drought events in Europe. However, droughts which have occurred only in small regions with a low station coverage may be overseen. They will be discussed later in a regional investigation. Figure 5.1a shows a clustering of the dry years during four periods: long dry spells occurred in 1962 to 1965, several large events occurred in the first half of the seventies with the most severe drought in 1976 (Figure 5.1b), a single large and short dry period occurred in 1983, before a major European drought of considerable duration occurred in 1989/90. The highest percentage of the whole period was reached in July 1976 with ca. 75% of all gauging stations simultaneously experiencing streamflow deficiency lower than Q90. Considering a streamflow lower than their varying Q70, on 7 July 1976, the percentage of the stations simultaneously experiencing even increased to 90% (not shown). Very high values were further found for February/March 1963 and spring 1974.

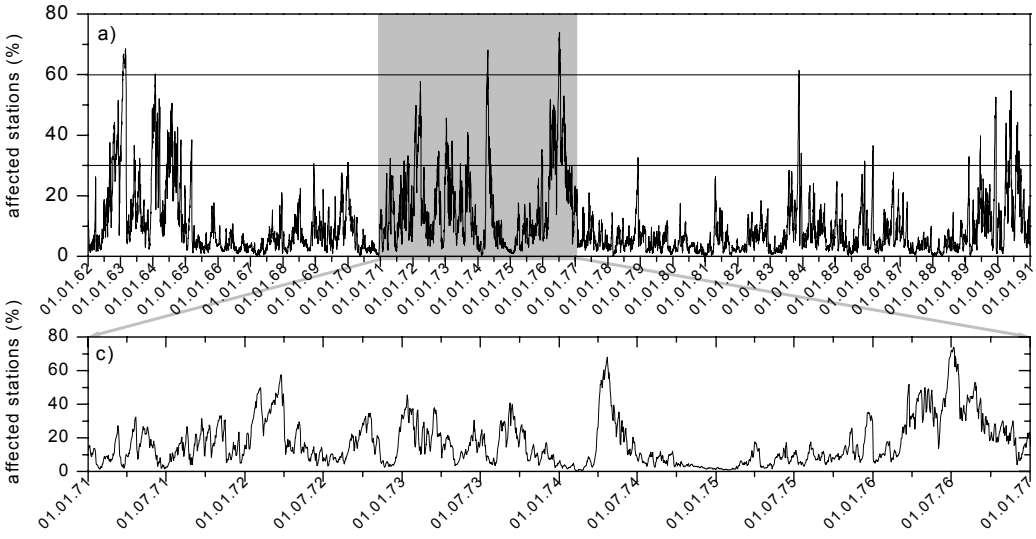

Fig. 5.1 *Daily fraction of stations affected by streamflow deficiency < varying Q90*

The daily sum of simultaneously affected European stations enables the identification of the large events and their durations, but does not indicate where in Europe these dry spells actually occurred. Therefore, the spatial development and extent was visualised on maps, where the stations with discharge equal or below varying Q90 (*DI*=1) are marked in red. Figure 5.2 shows the peak day of the 1976 drought, adding more information by including stations with the streamflow below Q80 in orange and Q70 in yellow. The simultaneous visualisation of the atmospheric mean sea level pressure (MSLP) distribution with indicated high and low pressure centres over Europe allows a visual analysis of the synoptic meteorologic situation which caused the streamflow anomaly. Instead of the MSLP, the pressure at the 500 hPa or 750 hPa level is also available to be visualised in the PV Wave application. However, most users of such a visualisation system will be more familiar with MSLP, which is widely known from weather forecasts, whereas the interpretation of upper troposphere pressure requires special meteorological expertise. The snapshot of 7 July 1976 in Figure 5.2 shows that most of central and western Europe experienced the most severe streamflow deficits. Southern Scandinavia also had lower streamflow levels than usual. The MSLP distribution shows an unusual situation of high MSLP with very low differences across Europe, a situation classified as CP-type *North Iceland high, anticyclonic* (HNa, Chapter 2.2.2, Table 2.1).

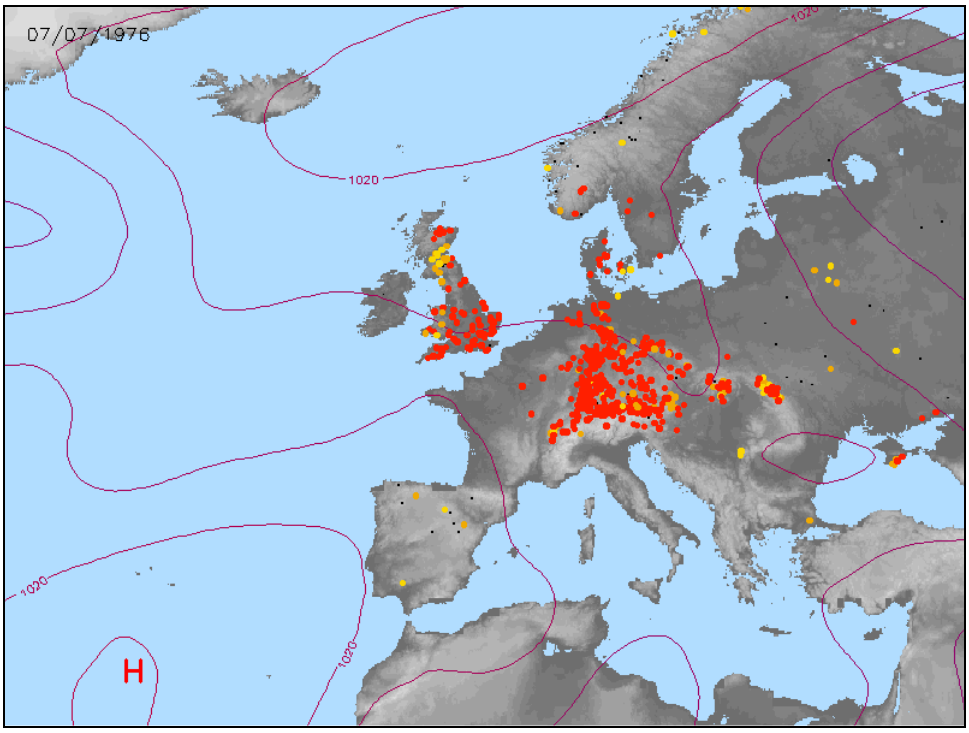

Fig. 5.2 *Maximum extent of the 1976 drought (colour code for stations: red < Q90 < orange < Q80 < yellow < Q70). CP-type HNa (North Iceland high, anticyclonic)*

5.3 Spatial and temporal dynamics of major events

Animated map sequences of mean sea level pressure and streamflow deficiency before and during the major events identified in the previous section were visually analysed. The main features of the dynamics and extent of these events and their associated synoptic meteorology are summarised in the following paragraphs. Nevertheless, it should be stressed, that the full capability of the animations for the analysis in time and space can only be exploited by viewing the sequences electronically. Here, only a few figures of daily snapshots can be shown to illustrate particular situations and to give an idea of the type of information that can be seen in the entire computer animations. The indication of the CP-types (Chapter 2.2.2, Table 2.1) adds further information to the visualisation application and facilitates the interpretation of the meteorologic situation.

Events 1962 to 1964

During the period from late summer 1962 to the end of 1964, three large dry spells, with more than 50% of the stations affected, occurred. During autumn 1962, stable blocking high pressure systems persisted from western over central to eastern Europe, a synoptic meteorological situation described by the CP-type BM (*central European high pressure ridge*, Chapter 2.2.2). In October, streamflow levels from the western Alps to the Carpathian Mountains had dropped below their varying Q90 threshold level (Figure 5.3a). The extraordinary meteorological situation continued to persist and caused a spreading of the dry spells further northwest and east into central Europe (Figure 5.3b). Streamflow levels during the winter 1962/63 were not only below their seasonal low flow as determined with the varying threshold, but also low in absolute terms, as a comparison with the original hydrographs showed.

a) 3.10.1962, CP-type: BM

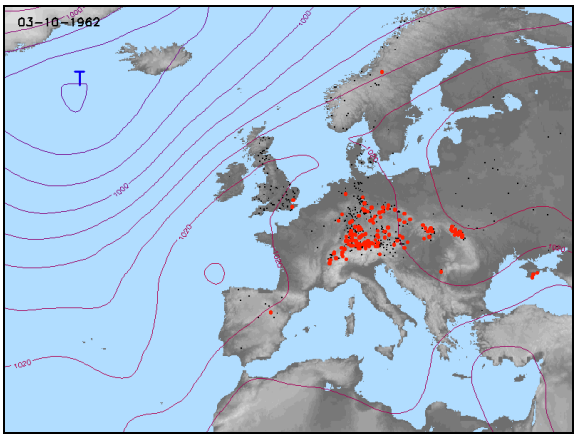

b) 27.2.1963, CP-type: HM

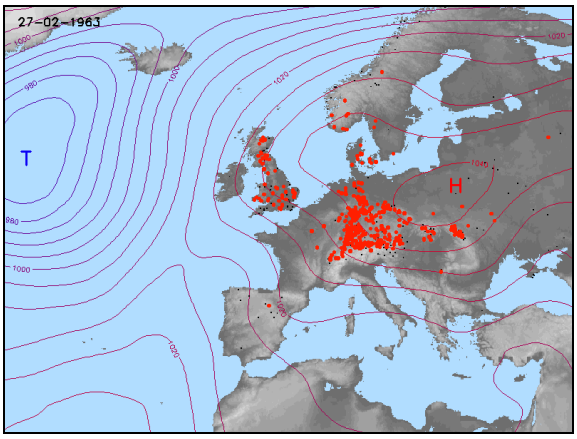

Fig. 5.3 *Daily snapshots from the streamflow deficiency period 1962-1964*

The dry period was abruptly ended by rain of frontal cyclones moving into Europe from the Atlantic in the beginning of March 1963. Although not below the threshold, late spring streamflows were somewhat lower than normal in the Nordic countries and eastern Europe. Summer was rather dry from Germany to Eastern Europe. Later in the year, the affected region contracted to Germany and Austria.

The following winter (1963/64) was again exceptionally dry. Initiated in central Europe, the affected region spread across the UK as well as eastwards when a high pressure ridge from Britain to eastern Europe persisted for several weeks in January. The extent of this winter drought was not as far north as the year before (Figure 5.3b). Norway and Denmark were not affected. However, the event extended farther west. Although spring was rather wet, in 1964 a strong summer drought developed across central and Eastern Europe, and flow was lower than normal in many British rivers.

Both described winter periods were characterised by very unusual meteorologic situations with almost a complete absence of zonal circulation patterns, which are in general quite frequent during wintertime. Therefore, central Europe was influenced by high pressure and dry and cold air masses from the east. In some regions, the associated lack of winter rainfall supported the development of droughts in the following summer.

Events 1972 to 1976

In the seventies, four major periods above the 30% line were identified from Figure 5.1: winter/spring and autumn in 1972 and 1973 respectively, April 1974, and spring through summer of 1976.

February and March in 1972 experienced quite contrasting situations. In February, a strong high pressure cell with its centre over Russia brought dry air masses from the southeast into central Europe (CP-type SEa) causing low streamflows in eastern and central Europe, while an extreme low pressure centre resided just west of the British Isles (Figure 5.4a). In March, the inverse situation with low pressure over eastern Europe and high pressure over central Europe and Britain shifted the region affected by streamflow deficiency farther west into France and the UK. The October-event in 1972 occurred after a September governed by anticyclonic conditions. It affected mainly the west coasts of the UK and southern Scandinavia, as well as the south of Germany, Switzerland and Austria. Central Germany was not affected (Figure 5.4b).Without additional information, the situation is difficult to be attributed to certain long- or short-term meteorological causes.

February and March of the following year, 1973, were again characterised by streamflow deficits. This time, a high pressure ridge stretched east-west across Europe and caused low flows in central Europe, then as in 1972 shifted more to the British Isles in March. The following late-summer drought in August affected mainly central Europe and occurred after a period of several weeks of uninterrupted high pressure over central and particularly over northern Europe (HNa, HNa and HNFa).

a) 2.2.1972, CP-type: SEa

b) 16.10.1972, CP-type: HB

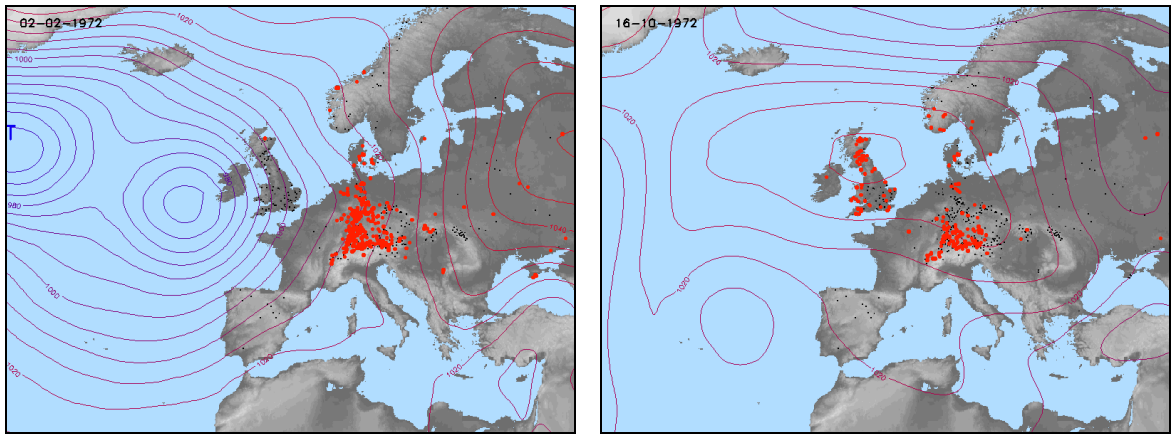

Fig. 5.4 *Daily snapshots from the streamflow deficiency period 1972*

An exceptional month was April 1974. On March 21, only 3% of the stations showed a low streamflow, but under the influence of high pressure systems in the Baltic region (HFa, HNFa) the streamflow deficiency quickly spread north, east and west affecting more and more stations, until 54% of all stations had receded below the threshold by 9 April. The circulation pattern changed to a British high (HB) and affected Europe's mid latitudes between 45° N and almost 60° N from the UK to Russia. The peak of the event occurred only a month after the unusual situation had started: on the 22 April 1974, 67% showed a streamflow deficiency. Only Spain and Norway were not affected. Rainfall, soilwater, and streamflow deficit during April are important for agriculture, as this is the beginning of the growing season for many central and southern European regions.

After a moderate to dry year in 1975, the 1976 drought took more than half a year to develop to the full extent. Zaidman & Rees (2000) in detail analysed the development. In 1976, streamflow deficits were first noticed in southeastern UK, then France and Western Germany during spring. The simultaneous pressure visualisation and the circulation patterns revealed unusual meteorological situations: from February to spring, strong high pressure dominated over the European continent blocking a (quite strong) low pressure centre to persist close to Iceland. Only rare cyclones affected Northern Europe. From the beginning of June to the largest extent of the drought on 7 July, the drought affected area spread farther east and north within one month. Even the alpine region was affected (Figure 5.2). The entire clipping for visualisation showed hardly any pressure difference (1020 hPa everywhere) across Europe during this time, which was classified as the rare CP-type HNa. Drought conditions started to recover in Britain and France, when zonal circulation was reinforced in the end of July and the beginning of August. However, delaying the recovery, another period of prevailing high pressure returned to persist during the second part of August. When the centre was located farther east over northern continental Europe, the drought also moved into Scandinavia. By the end of August, drought conditions finally ceased from west to east, when a low pressure trough moved into Europe from the Atlantic.

Event 1983

During the period from July to December 1983, some regions across Europe were experiencing strong streamflow deficiencies. In late July, a belt between 10° E and 15° E extending north-south from Sweden to Slovenia was affected after two months of prevailing high pressure over the north eastern part of Europe (Figure 5.5a). The entire autumn was governed by high pressure and anticyclonic synoptic meteorological conditions (CP-types HM, BM, SWa) across most of Europe, causing low flow conditions to exacerbate. At the end of November, the western part of the UK and central to eastern Europe up to about 30° E were affected (60% of all stations, Figure 5.5b). .

a) 26.7.1983, CP-type: TRW

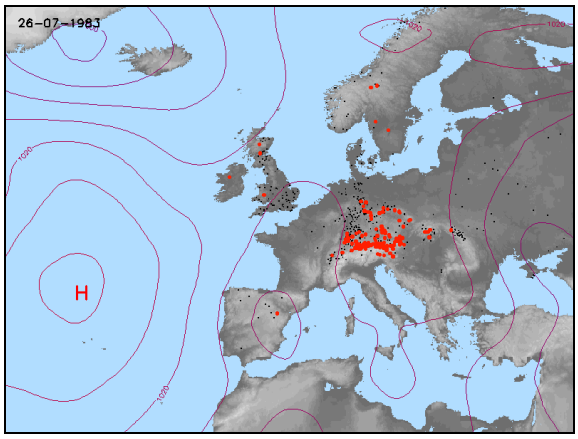

b) 22.11.1983, CP-type: NWa

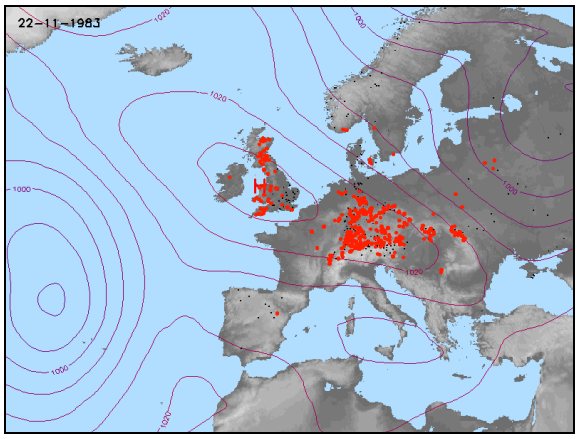

Fig. 5.5 *Daily snapshots from the streamflow deficiency period 1983*

Events 1989 to 1990

In February 1989, southwestern and western Europe (Spain, France, UK) were already very dry (Figure 5.6a) following an exceptionally long period of 30 days of anticyclonic and high pressure conditions (CP-types Wa, HM). A few months later, the same region and also Denmark and the Northern part of Germany were affected by summer droughts (Figure 5.6b). December 1989 showed a peak with slightly over 50% of stations affected by streamflow deficiencies (Figure 5.6c).

The 1989/1990 winter was characterised by anticyclonic meteorological conditions with southern airflow (mainly CP-types Wa and SWa). Consequently, the high river flows usually expected in Central and western Europe over the winter season failed to occur, and there was little replenishment of reservoir or groundwater storage. For Spain, the situation was even worse, as it was the second dry winter season. Although there was some precipitation in the UK and central Europe during February 1990, this did little to redress the situation there, and when high pressure returned in March 1990, drought conditions spread rapidly across Europe (Figure 5.6d). The situations shown in Figure 5.6e/f illustrate the drought conditions that actually continued for most of the summer, when persistent periods of up to 20 consecutive

a) 10.2.1989, CP-type: Wa

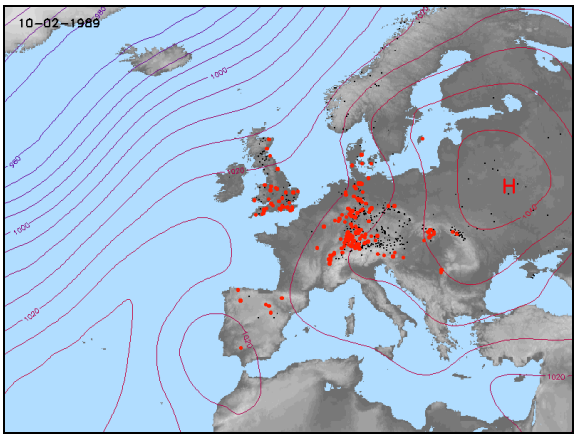

b) 19.6.1989, CP-type: NEa

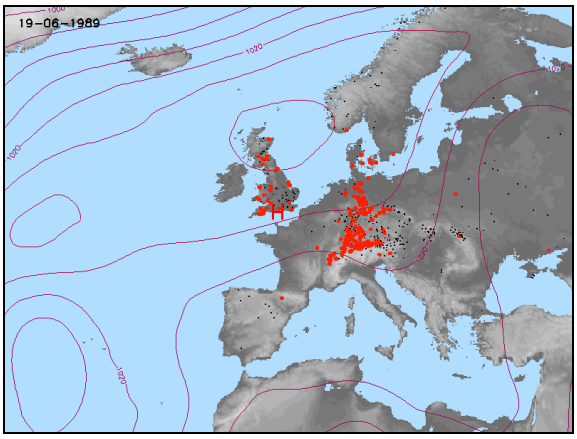

c) 8.12.1989, CP-type: HB

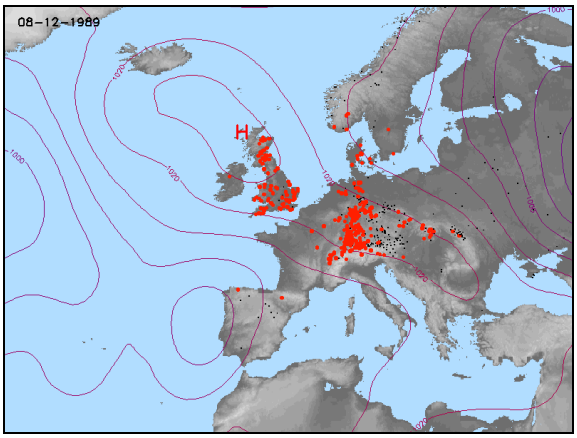

d) 5.4.1990, CP-type: TRW

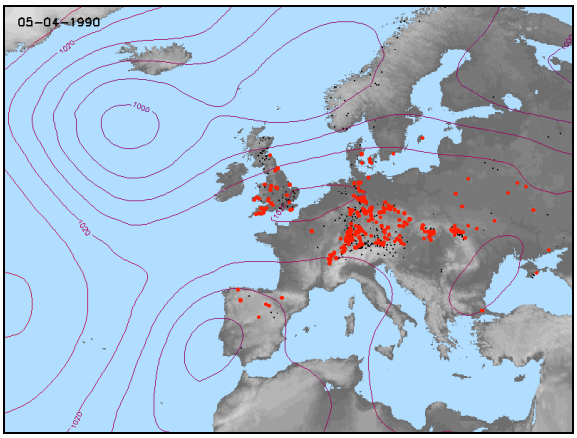

e) 30.5.1990, CP-type: HB

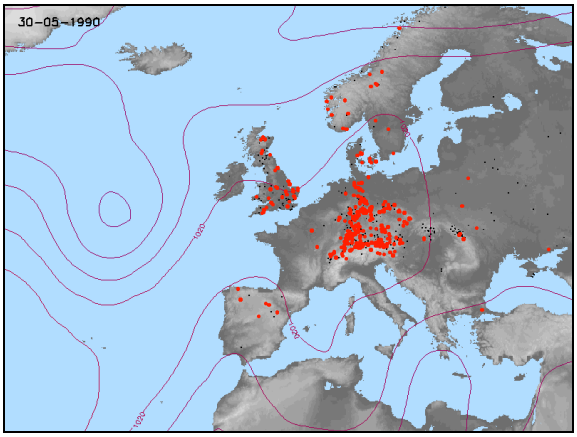

f) 11.8.1990, CP-type: BM

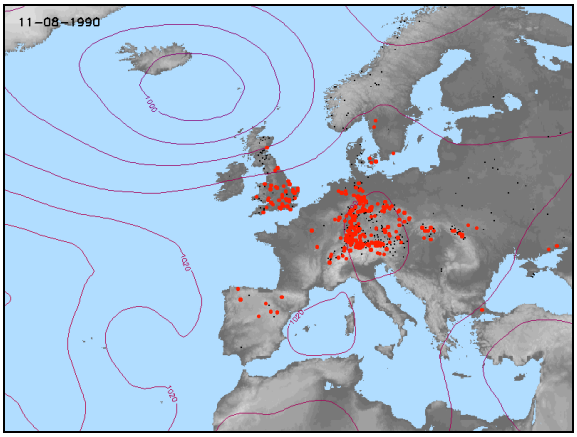

Fig. 5.6 *Daily snapshots from the streamflow deficiency period 1989-90*

days of either British High (HB) or central ridges (BM) were only shortly interrupted by a few days of zonal conditions (Wz, NWz or SWz). The streamflow deficiencies never completely recovered.

5.4 Summary and discussion of causes and characteristics of the major events

The detailed description of the dynamics of the major European streamflow deficiency periods covered events in different seasons and different regions. Duration, extent, and other characteristics varied considerably, but also repeating patterns and meteorological situations were observed. Table 5.1 summarises the properties of the meteorological and hydrological conditions before and during the events together with literature references on these droughts.

As shown in Table 5.1, most of the events identified are also documented in other drought reviews. This finding underlines that the streamflow deficiencies defined by the varying threshold reproduce severe drought events across Europe. Only in the case of winter events, further information is necessary in cold regions, where storage of precipitation as snow and frozen rivers influence the streamflow regime.

A comparison of the details on drought dynamics with some of the references, however, remains difficult, as they are based on different parameters, like annual precipitation deficit in Álvarez and Estrela (2000) or even on different documented studies (Bradford, 2000). The dynamics of streamflow deficiencies of the two longest and largest events 1976 and 1989/90 were discussed in detail by Zaidman & Rees (2000). They argue that both droughts commonly started in winter and had spread from western to central and eastern Europe. The analysis in this study shows that other patterns of spreading also occurred. For instance, most discussed winter deficiencies initiated in central or eastern Europe and later spread westward (e.g. 1963, 1964, 1972), but also the event in summer 1983. The event in April 1974 developed more or less everywhere at the same time. Some periods showed heavy fluctuations with the affected areas extending and contracting into different directions within a short time (e.g. 1973, 1990).

This variability in the dynamics of drought events across Europe shows that generalisations about initiation points and spreading directions are very difficult to make. They are also critical due to the low data availability and thus the lack of information in southern and eastern Europe. Nevertheless, the visualisation of the events illustrated a strong regional character of the streamflow deficiencies. Large regions were often simultaneously affected. Examples of such homogeneous regions are southeastern UK, Denmark together with southern Sweden, the Czech and Slovak Republics, the Alps, etc.

Finally some seasonal aspects of the events can be discussed. Drought events in summer or autumn often occurred after winter periods with extreme streamflow deficiencies like in 1964, 1972/73, and 1989/90. Zaidman, et al. (2000) found that groundwater fed catchments in chalk geology regions of southeastern UK and northwestern France appear to be prone to this behaviour if groundwater recharge winter is lower than normal. However, not all winter deficiencies are followed by a summer drought, and not all summer droughts are preceded by lower than usual winter streamflows. Concerning the synoptic meteorology, winter deficien-

Table 5.1 *Event characteristics*

Dry Period	Year Season	Duration	Spatial extent and dynamics	Meteorology Most frequent CPs	Reference to event in B, A/E, Z/R, O/C*
1962-64	1962 autumn	Sep-Nov	Alps, Carpathians, then eastwards spread	Sa, HB, BM	Z/R: 1963 and 1964 western/central Europe
	1962/63 winter	Jan-Feb	central	no zonal circul., high MSLP in central and northern Europe: air from east and north	
	1963/64 winter	Dec-Mar	central+western Europe UK+Scand west coast		
	1964 summer	Jun-Sep	central+eastern Europe	high pressure: HM, BM, HNa, HNFz	
1972-76	1972 winter	Jan-Mar	central, to eastern, then central to west Europe	all CPs with southern airflow	B: USSR A/E: central Europe Z/R: 1972 western/ central Europe
	autumn	Sep-Oct	western Europe, southern Scandinavia, Switzerland+Austria	anticyclonic cond. in Sept. NEa, HB	
	1973 winter/ spring	Dec-Apr	central Europe, eastern UK, then entire UK and Germany+Denmark	persistent BM, frequent CPs with northern airflow	A/E: eastern Mediterranean (1973-75)
	autumn	Aug-Oct	central Europe, Denmark, southeast UK	HNa and HNFa	
	1974 spring	Mar-Apr	entire Europe between 45° N and 60° N	HFa, HNFa, then HB	
	1976	Mar-Sept	UK, western and southwestern Europe, then spread to central, and in late summer to northern and eastern Europe	frequent anticyclonic conditions (SEa, Sa, HFa, HB, etc.) June-Aug: low pressure difference across Europe (HNa)	O/C: UK, Belgium B: all Europe, varying time and intensity Z/R: three stages: UK - western and central Europe - northwestern Europe
1983	1983 summer autumn	July-Dec	Sweden to central and eastern Europe, later western UK	high pressure and anticyclonic condition (HM, BM, SWa)	O/C: Bulgaria, Romania A/E: eastern Europe Z: mentioned
1989-90	1989 winter	Feb	southern and western Europe	one month of Wa and HM	B: most of Europe 1988-92 A/E: eastern Mediterranean, France, UK, 1989/90
	1989 summer	May-Jul	France, Switzerland, Northern Germany and Denmark, western UK	BM particularly persistent in May, frequent NEa	
	1989 late	Nov/Dec	western Europe	British high HB	
	1990 all year	Apr-May	southern Europe, then southwest UK, central and eastern Europe	Wa in March, then long periods of BM with short interruptions of Wz	Z/R: southern UK and western Europe, later Scotland/Norway
		Aug-Sept	western, central and northern Europe		

* B: Bradford (2000), A/E: Álvarez & Estrela (2000), Z/R: Zaidman & Rees (2000), O/C: OFDA/CRED (2001)

cies in this study were often associated either with blocking high pressure systems over Europe and reduced zonal circulation (in particular in 1963, 1964, 1972) or zonal circulation of long periods of anticyclonic conditions like in 1998 and 1990. The winter season before the 1976 drought showed mixed atmospheric conditions. Rare meridional circulation patterns like SEa, Sa, NEa and later in the year HNa were particularly frequent and persistent. Most of the severe summer droughts across Europe were associated with high pressure systems across central Europe. Generally, drought associated synoptic meteorology is characterised by high MSLP, but the circulation pattern types vary not only with the season but also for all individual discussed events.

5.5 Conclusion

A new computer application to create animated sequences of maps of mean sea level pressure and streamflow deficiency conditions across Europe was introduced. This simultaneous visualisation of synoptic meteorology and surface hydrology for the first time allows the visual investigation of the synoptic meteorological causes for the dynamics of streamflow deficiency and drought events. Large events were identified from the available European streamflow deficiency series dataset for Period 1 (1962-90) and analysed in detail.

Generally, the streamflow conditions strongly follow the changes in large-scale atmospheric circulation over Europe and the North Atlantic. The detailed analysis and description of the most important events of winter deficiencies in the early sixties, winter and summer events in the early seventies, the 1976 drought, a short but strong event in 1983 and the drought years 1989 and 1990 revealed interesting new information. Using the visualisation technique, the meteorological causes and dynamics of single events can be very well characterised. For several events, similarities in the development and dynamics were detected. The streamflow deficiencies consistently show strong regional patterns and depending on the season, those regional events seem to be caused by certain persistent and recurrent synoptic circulation situations. For instance, summer droughts during long high pressure periods quite often followed relatively dry winters with reduced zonal circulation.

Yet, there is also a high variability in the dynamics of the events and many different circulation patterns can have the same hydrological effect. Consequently, the visualisation is a good tool to analyse specific events and to demonstrate the regional character and the dependency of streamflow deficiency on synoptic meteorology. Although the deduction of general recurring patterns and links are difficult to obtain with this method.

6 Regional Patterns of Streamflow Deficiency

6.1 Introduction

The analysis of the dynamics and extent of large-scale drought events across Europe in the previous chapter underpins that droughts are phenomena always affecting a large region. However, the analysis also demonstrated, that each event has its special characteristics concerning spatial extent and dynamics. Visual analysis alone is not sufficient to delineate regions in Europe typically affected by streamflow deficiencies at the same time. A statistical classification can find such regions and thus allows investigation of drought-causing processes effective at the regional scale. Within the ARIDE project some studies delineated regions in Europe according to different parameters (Demuth & Stahl, 2001). Briffa et al. (1994) defined nine regions of coherent summer moisture variability by rotated principal components of the Palmer drought serverity indices (PDSI). The present study aims at classifying the response of surface hydrology to meteorological dry periods.

There are many different ways to determine homogeneous hydrological regions at the continental scale. The method which is to be chosen strongly depends on the objective of the study and the available data. Also using FRIEND data, several studies have regionalised low flow related streamflow parameters based on catchment characteristics across Europe. Demuth (1993) regionalised low flow characteristics in western Europe and Gustard & Irving (1993) classified the low flow response of soils across Europe. Rees et al. (1997) regionalised water availability based on low flows. Arnell et al. (1993) presented maps of typical low flow regime characteristics, which were discussed in Chapter 2.3.4. Yet, fewer studies have considered the regional character of the variable timing and the spatially simultaneous behaviour of low flows and droughts in rivers at the pan-European scale. Arnell (1994) and Shorthouse & Arnell (1997) found regional patterns of monthly streamflow anomalies in the positive and negative direction.

In the present study, the aim is to exclusively analyse the regional structure of water deficit periods and therefore, the streamflow data series were reduced to this information before being subjected to classification. As high flow anomalies tend to be more variable in time and

space than low flow anomalies, they could dominate the time series characteristics of the entire anomaly series, especially if a daily resolution is used. Cluster analysis provides a suitable objective statistical classification method to find groups of catchments experiencing simultaneous streamflow deficiencies without directly defining regional events or series. Being an analytical method, it leaves some freedom to choose a final region delimitation from the result. An aggregation of the regional streamflow deficiency information can then be particularly designed for analysis at the regional scale.

6.2 Methods

6.2.1 Regional classification by cluster analysis

The goal of a cluster analysis is to group the variables of a data matrix in a way that the characteristics of the variables within the group are optimally homogeneous, but the characteristics of the variables between the groups are optimally contrasting. Therefore, the first and most important step is to define a measure for the similarity or dissimilarity (*distance*) between the characteristics of two variables. Depending on the scaling of the variables being quantitative, binary, or count data, various similarity and distance measures are available. Among the most common measures are Euclidean Distance, Pearson Correlation, Chi², etc. The choice for a similarity or distance measure strongly depends on the purpose of the classification. In the next step, the chosen distance measure is calculated for each pair of variables to obtain a distance matrix. Searching this distance matrix, *hierarchical clustering* procedures identify relatively homogeneous groups of variables using an algorithm which starts with each variable in a separate cluster and combines clusters until only one is left (agglomeration). Since hierarchical cluster analysis is an exploratory method, results should be treated as tentative until they are confirmed with an independent method (Norius, 1995).

The objective for the application of cluster analysis to the historic streamflow deficiency time-series of the EWA stations in this study was to investigate the regional patterns of simultaneous occurrence of streamflow deficiencies across Europe. Hence, the variables to be grouped were the gauging stations *G* from the EWA. Those variables contain the daily streamflow deficiency indicator series data of $DI = 0$ for flow above the threshold and $DI = 1$ for flow below the threshold over the common time period 1962-90. *Binary Euclidean distance, D,* was used as distance measure and hence calculated for all pairs of variables. The distance for the pair of stations G1 and G2 is then calculated from the frequency table:

***G*1** / ***G*2**	***DI* = 0**	***DI* = 1**
***DI* = 0**	a	b
***DI* = 1**	c	d

$$D(G1 \mid G2) = \sqrt{b + c} \qquad (6.1)$$

where *b* represents the number of cases present the first variable and absent on the second, and c represents the opposite situation. In this study *b+c* corresponds to the number of days during 1962-90, when the *DI* of two considered stations was different. The commonly used *Ward-Method*, which minimises the distances within a cluster, was then applied for the hierarchical clustering. This method produces small, clearly separated clusters of hyperspheric shape (Norius, 1995).

The decision for a certain number of clusters that represent 'homogeneous' groups is not fixed and strongly depends on the objective of the study. Since there is a lack of a consistent definition of *'cluster'* and its structure and content, it is difficult to define hypothesis tests (Aldenderfer & Blashfield, 1984). In this study two criteria were used to determine the optimum number of clusters in terms of the least possible number with the highest possible homogeneity.

- A jump in the plot of the distances between the clusters at each step of agglomeration (agglomeration schedule)
- Cluster homogeneity based on the frequency distribution of the resulting Regional Streamflow Deficiency Index values *RDI* (see next section)

6.2.2 The regional streamflow deficiency index

For representation of the aggregated streamflow deficiency, a cluster based (regional) index *RDI* is calculated (Stahl & Demuth, 1999). The daily deficiency indicators *DI(t)* of all the individual stations *G* in a cluster *C* are summed and normalised by the number of stations *n* in the cluster.

$$RDI_C(t) = \frac{1}{n} \sum_{G=1}^{n} DI_G(t) \qquad \textbf{(6.2)}$$

Hence, the *RDI* represents the daily fraction of catchments in a cluster affected by streamflow deficiency. Taking into account the spatial severity of streamflow deficiency, the time series of this index can then be used for regional analyses. Furthermore, the distribution of the *RDI* values of a cluster is a measure of homogeneity of the group of catchments forming a cluster. By definition, an optimum simultaneous behaviour of the cluster members would be denoted by an *RDI* value distribution of 90% (threshold percentile *p*) of zero and 10% of one. The area between this optimum and the cumulative distribution *F(x)* of the real *RDI* values of a cluster can be used to measure the cluster's homogeneity. Figure 6.1 illustrates the homogeneity of this *RDIarea* parameter, which is calculated as:

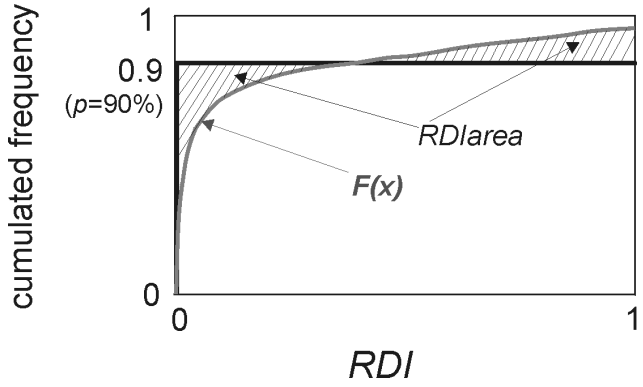

$$RDIarea_c = \int_0^1 |F(x) - p| \qquad (6.3)$$

Fig. 6.1 *Schematic derivation of RDIarea*

6.3 Results

6.3.1 Spatial classification

Optimum cluster solution

The decision for the optimum cluster solution was based on the aforementioned group-homogeneity criteria: the agglomeration schedule and *RDIarea*. Figure 6.2a shows the agglomeration schedule and the mean *RDIarea* for the last 30 stages of the hierarchical clustering process. The agglomeration schedule, in terms of the increase in mean cluster distance from one clustering step to the next, exhibits a change in slope from the 18-cluster solution to the 17-cluster solution. The change in *RDIarea* suggests a considerable loss of homogeneity after 22 clusters. Therefore, the range of solutions between the 18-cluster solution and the 22 cluster-solution was closer investigated. Figure 6.2b shows that in the 22-cluster solution two clusters exist, which consist of only two members. Those two groups lower the mean *RDIarea* value. In the 20-cluster solution there is still one cluster with only two members. As there is not much difference in the mean *RDIarea* between the 17-cluster solution and the 19-cluster solution, the 19-cluster solution was finally chosen for further analysis due to its more consistent geographical distribution.

Spatial distribution

The analysis was carried out on streamflow deficiency data without including any geographic information. Therefore, the resulting clusters do not necessarily have to correspond to geographic regions. Nevertheless, the classification results in 19 spatially coherent clusters. Figure 6.3 shows the geographical distribution of the clusters. The UK is divided into an eastern, a northern, and a southwestern part. The Norwegian stations form a cluster excluding the

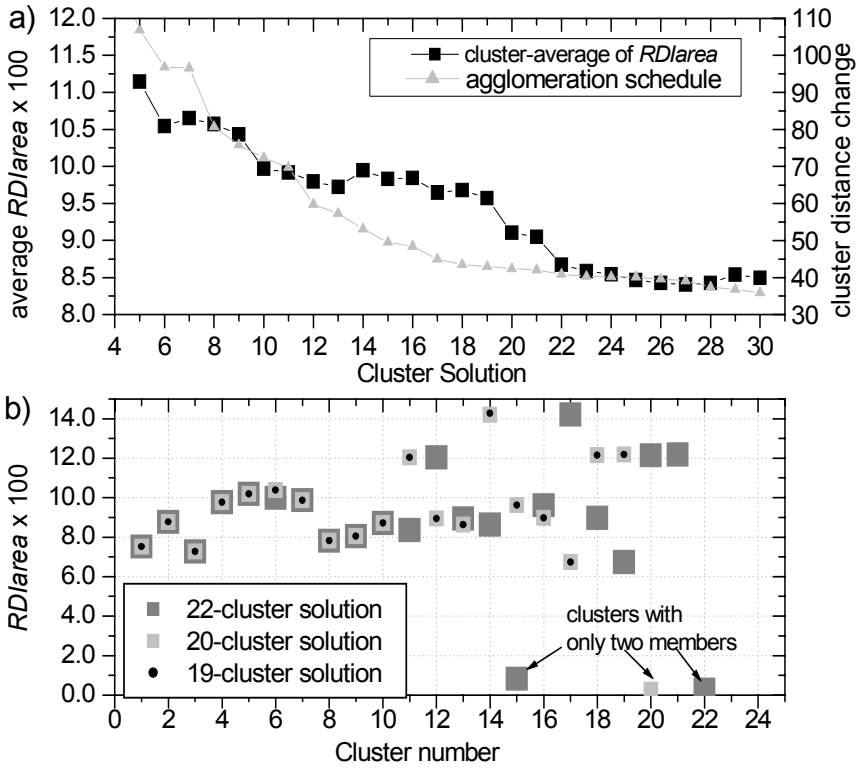

Fig. 6.2 *Finding the optimum cluster solution a) Group homogeneity criteria during the clustering process b) RDI parameter of individual clusters for selected solutions*

southeastern part, which belongs to the cluster covering Denmark and southern Sweden. The Spanish stations appear as one separate cluster as do the most eastern stations (mainly Russia, Belarus, Ukraine). The remaining classification in central Europe is strongly governed by topographical features such as the Alps, the Pre-Alps, the Carpathian Mountain ranges and plains like northern Germany.

The spatial result of such an analysis depends on the dataset and the time-series used. In order to test this dependency, a subset of stations with a reduced but spatially more homogeneous station density across Europe, as well as a randomly chosen subset of days from the time-series, were also subjected to cluster analysis and the spatial classification of the different solutions from five to 30 clusters was sighted (not shown). At different stages in the clustering process, both experiments determined regions similar to the ones in Figure 6.3, which allows the conclusion that the defined regions can be accepted as homogeneous relative to other groups. Regions with similar summer variablity of the PDSI found by Briffa et al. (1994) further support the regionalisation with some general similarities. Using principal component analysis, they found a region in northwestern Europe which corresponds to clusters C2, C3, C4 and C8, C9, C10 covering the UK, southern Scandinavia and northern Germany. The Spanish cluster roughly corresponds to the northwestern mediterranean region in Briffa et al. (1994), who further distinguished the Danube basin, and devided eastern Europe in a northern and southern (Volga basin) part.

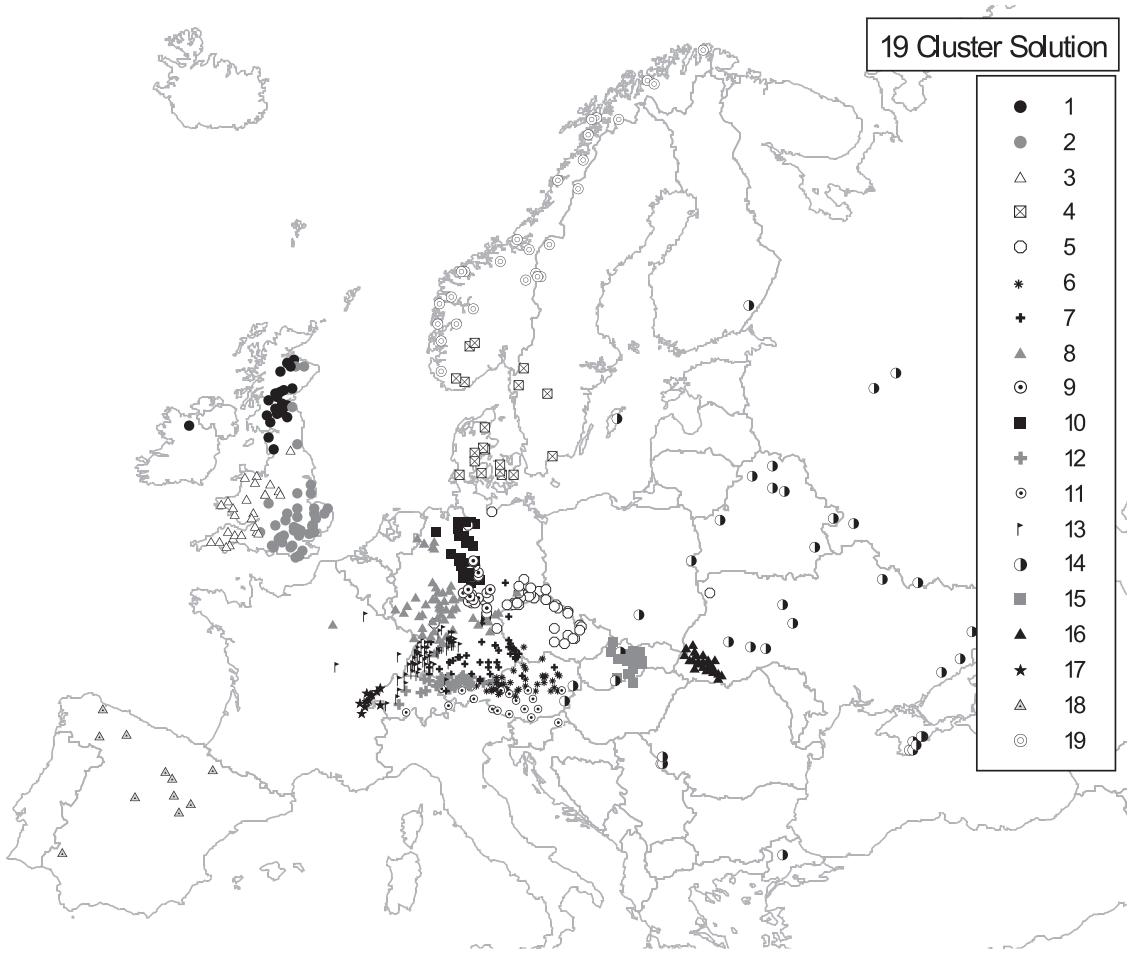

Fig. 6.3 *Spatial distribution of the 19 Cluster solution*

Cluster homogeneity

The cumulative frequency distribution of the *RDI* values for each cluster illustrates the different homogeneity of the clusters (Figure 6.4). In fact, most of the distributions are very similar. The more homogeneous clusters exhibit about 40% to 60% of the time with no deficiency simultaneously in all stations. During 90% of the time, the *RDI* is lower than about 0.3 to 0.4 for most clusters. The least homogeneous clusters are C19, C14 and C18. They show more days with low *RDI* values, and especially C14 and C19 don't reach very high values, which means that the stations do not often experience streamflow deficiencies at the same time.

6.3.2 Discussion of regional drought characteristics

The 19 defined regions are spatially coherent, but vary in their characteristics. Table 6.1 summarises geographic locations, numbers of stations, and the *RDIarea* homogeneity parameters of the clusters. Most clusters contain between 20 and 50 members. Values below 10 for the *RIDarea x 100* can be considered quite homogeneous. With a value of 14.28, the eastern

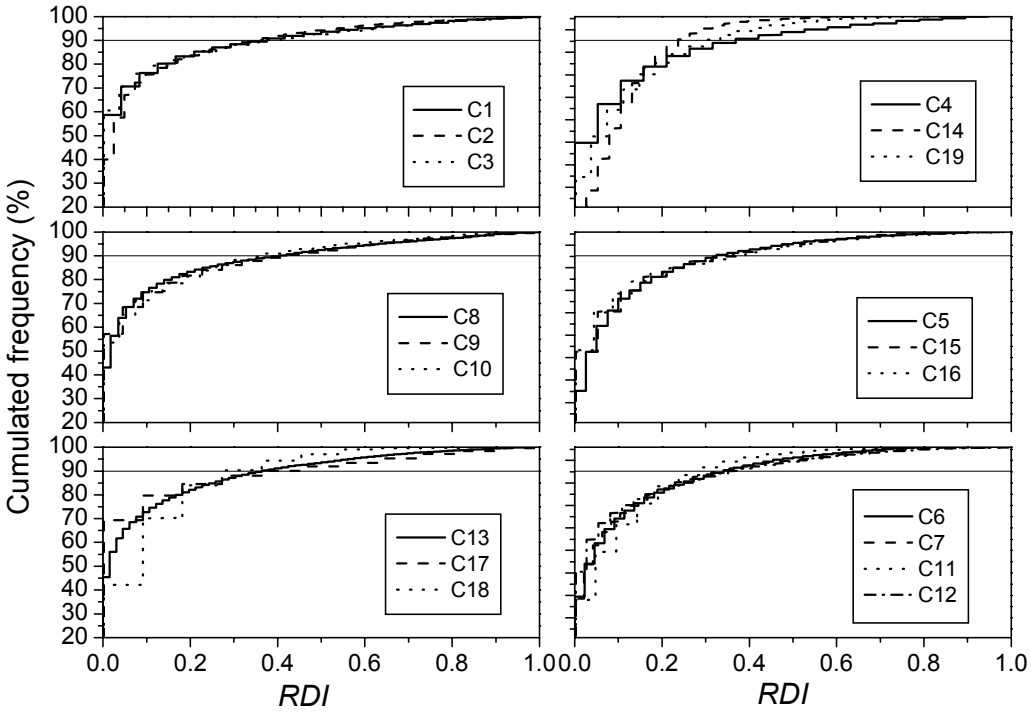

Fig. 6.4 *RDI distribution for the 19 Clusters*

European cluster C14 is the least homogeneous region. Like the Spanish and the Norwegian Clusters (C18, C19), which are also less homogeneous, it covers a large geographical region. However, these three regions were defined at early stages in the clustering algorithm, which indicates that their series are contrasting relative to the remaining stations. They experienced streamflow deficiency at distinctly different times than other regions across Europe.

The *RDI* time series from 1962 to 1990, plotted as colour maps, provide the best illustration of the cluster characteristics (Figure 6.5). Red colours indicate higher *RDI* values, while orange and yellow colours indicate lower *RDI* values. For better regional comparison, the cluster series are arranged according to their geographic location. Hence, not only can the varying cluster homogeneity be investigated, but also the regional differences and similarities.

The *RDI* time series of cluster C1, northern Great Britain, is characterised by either low or high *RDI* values, meaning that either there is no station in this cluster which shows a streamflow deficiency, or most of the stations are affected at the same time. The events are homogeneous with rather short durations, which confirms the low persistency found earlier for the individual stations in this region (Chapter 4). The *RDI* of the less homogeneous Norwegian cluster C19 reaches values above 0.5 (half of the stations affected) less often, but exhibits long periods of low *RDI* values. At first sight, the two most northern regions in Europe do not exhibit streamflow deficiencies during similar periods, but there are some periods when northern Great Britain summer deficits precede dry autumn periods in Norway (e.g. 1976, 1980, 1984). This lag-time corresponds to the frequent eastward shift of summer drought

Table 6.1 *Cluster description and characteristics*

No.	geographic location*	no. of stations	*RDIarea x 100*
C1	northern Great Britain	24	7.53
C2	southeastern UK	41	8.77
C3	southwestern UK	27	7.26
C4	southern Scandinavia	19	9.76
C5	Czech Rep. and eastern Germany	40	10.18
C6	northern Austria	44	10.37
C7	southeastern Germany	48	9.87
C8	western Germany	57	7.82
C9	central Germany	22	8.05
C10	northern Germany	27	8.72
C11	southern Austria and Switzerland	21	12.04
C12	high Alps, Switzerland, Germany, Austria	37	8.93
C13	southwestern Germany	66	8.63
C14	eastern Europe	38	14.28
C15	Slovakia	19	9.61
C16	Carpathian Mountains, Ukraine	23	8.97
C17	south Jura, France	11	6.74
C18	Spain	11	12.14
C19	western and northern Norway	27	12.18

* For sake of convenience, the location relates to the region with the majority of stations.

detected by the visualisation analysis. Besides these direct meteorological causes, the Norwegian rivers have snow dominated streamflow regimes (Chapter 2.3.4). In Norway, the natural reservoirs in the catchments are filled up by snowmelt during spring, compared to northern Great Britain, where recharge occurs mainly in winter. If both regions are influenced by the same dry weather period in summer, Norway may have a delayed response in the streamflow.

In Norway, the highest values during summer times were reached in 1968, 1969, and 1980. Autumn deficits can be noted in 1974, 1976, 1981, and 1982. This *RDI* value distribution probably results from the cluster covering a large, hydrologically diverse area, but also originates in the catchments' individual behaviours such as a high temporal variability in summer and long regular low flows in winter due to snow and frost.

The clusters, which cover the southwestern (C3) and southeastern (C2) part of the UK, experienced the same major events. The most severe streamflow deficiencies, with up to all stations affected, occurred in the winters of 1962-1964, during the well-known drought year 1976, in 1984 and in 1989/90 (compare Chapter 5). In the southwestern cluster, the streamflow deficiencies are not as long and persistent as in the southeastern cluster. This observation can be attributed to the exposure to the Atlantic and westerly winds with the associated

precipitation distribution and frequency (Chapter 2.3.2), but also to the hydrogeology dampening the hydrological response (Zaidman & Rees, 2000).

In southern Scandinavia (C4) the major European streamflow deficiencies affected most stations at the same time. Some inhomogeneity results from different start and end dates of those events, which when looked at as a regional event, can be described as the slow development of and recovery of streamflow deficiency. Geographically, the region is very flat and the hydrogeology is mainly governed by large aquifers in unconsolidated glacial and fluvial sediments with high storage capacities. These conditions can explain the slow streamflow deficiency response becoming particularly severe in extended periods with a lack of rainfall and recharge as in the beginning of the seventies.

The eastern European cluster (C14) is very inhomogeneous due to the large region covered. Unfortunately, data availability does not allow a further regional division. Eastern Europe also experienced the dry period in the beginning of the sixties with long summer droughts after extreme winters. Further homogeneous streamflow deficiencies occurred during spring and summer 1972, a period with severe consequences (Table 5.1), spring 1974, and in autumn 1975.

All the German clusters (C7, C8, C9, C10, C13) again reflect the three major European dry periods (Chapter 5.4), although the 1989/90 drought was often interrupted in western Germany (C8) and was not very pronounced in southeastern Germany (C7); a pattern already observed in the visualisation (Figure 5.6f). Homogeneity is quite good for the small northern (C10), central (C9), and western German (C8) clusters. They tend to develop long dry spells. The more southern (C13) and southeastern clusters (C5, C7) and are slightly less homogeneous. They also cover a more diverse region with several different mountain ranges and geological characteristics, which can explain some local variations in the general streamflow variability. The *RDI* pattern of Cluster C17, a small cluster describing stations in the southern Jura mountains in Switzerland and France, is quite similar to Cluster C13 (southwestern Germany) concerning the general periods of the major streamflow deficiency events. However, the exact timing of the very homogeneous events is different.

The two clusters, covering most of the alpine and prealpine regions (C12 and C6), experienced different streamflow deficiency periods compared to the clusters north of the Alps. The three major European drought periods are still visible, but both clusters developed regionally homogeneous dry spells, which, particularly during summer, are much shorter and more frequent than the events in the previously discussed clusters. Stable seasonal streamflow regimes governed by spring snowmelt in this high altitude region can explain these characteristics.

The cluster in Slovakia (C15) also shows more dry periods at slightly different times. Early summer droughts occurred in the sixties and seventies, but generally the eighties were characterised by many periods with streamflow deficiency in autumn and winter. The trend analysis in Chapter 4.3 revealed significant trends towards increased drought severity and fre-

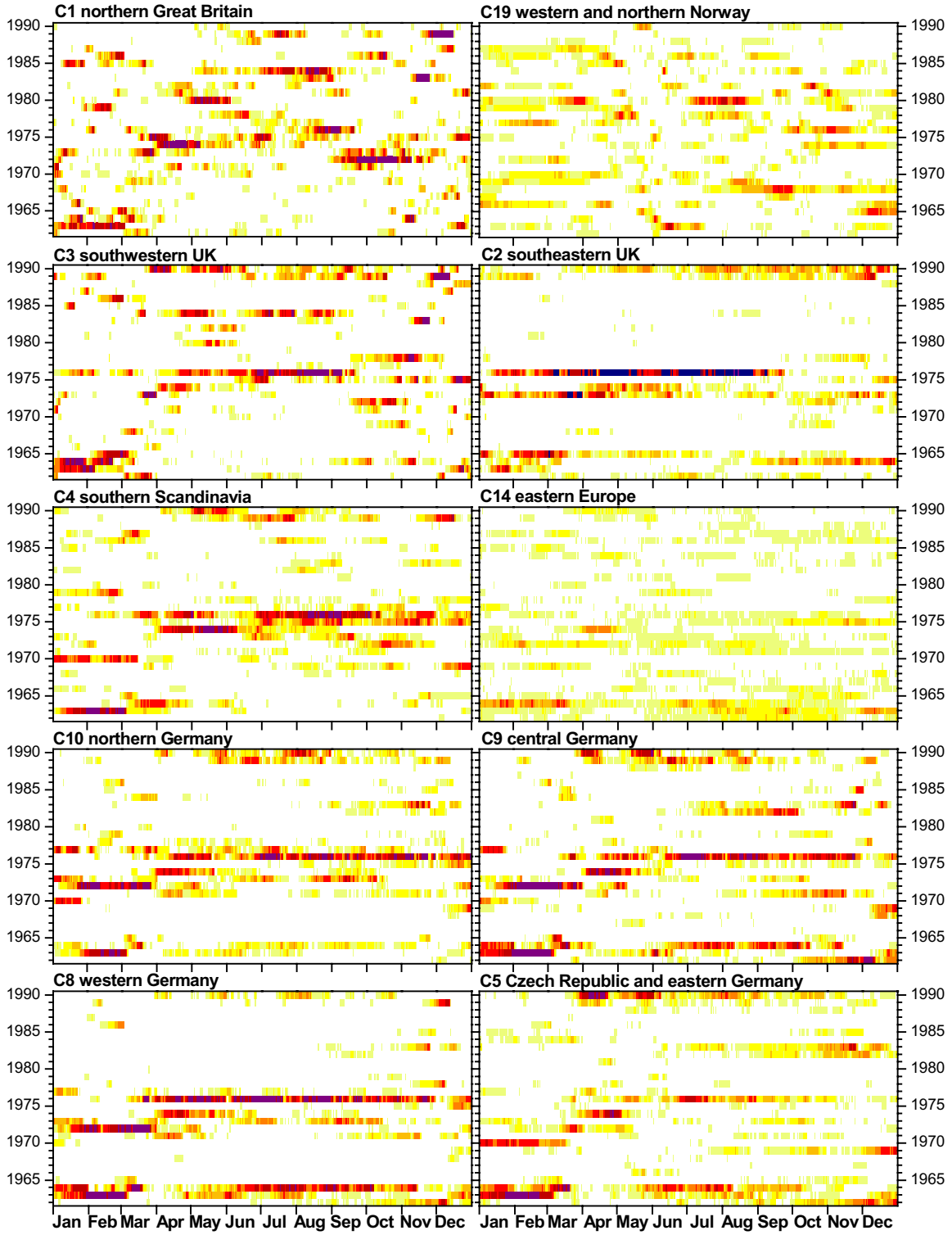

Fig. 6.5 *The RDI time series for the 19 clusters across Europe, arranged according to their geographic location*

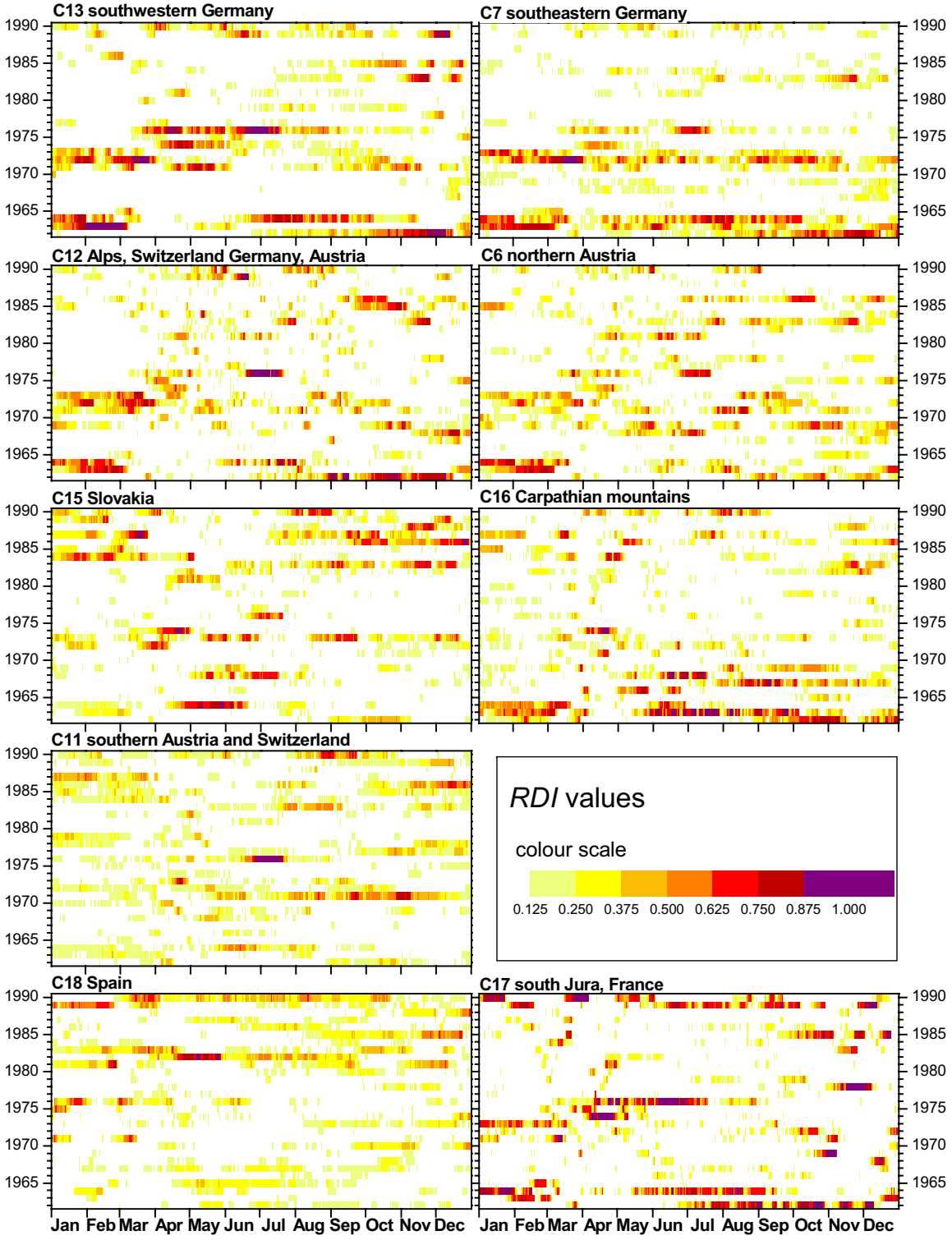

Fig. 6.5 *The RDI time series for the 19 clusters across Europe, arranged according to their geographic location. (continued)*

quency for this region. Also, a lack of rainfall and considerable water shortages have been reported in the country (Hisdal et al., 2001a). The cluster covering the Carpathian Mountains in Ukraine (C16) again shows a different pattern with drier conditions in the beginning of the period. The cluster is quite homogeneous, but there are some periods with low *RDI* values. The analysis of the low flow regimes of the stations already showed some stations with different characteristics within this area.

Cluster C11, which covers a long stretch along the southern rim of the Alps is not very homogeneous either. It shows some dry periods similar to clusters C12 and C6 to the north, but also some completely different dry periods, for instance in winter and spring of 1984 to 1986. As they are located south of the Alps' main divide, it is most likely that the stations belonging to this cluster are often affected by different weather conditions.

In Spain (C18), the eighties were considerably drier than the two decades before (compare Chapter 4.3). Long dry spells occurred in 1981 to 1983, in 1985 and in 1989 to 1990. The cluster is not very homogeneous as it covers the whole country. For an analysis at this scale, it is not possible to divide it into further groups, due to the lack of more long-term data series.

This detailed description of the *RDI* series revealed regions which are characterised by long persistent regional dry spells, as for example C2, C4, C8, C9, C10. These clusters comprise of southeastern UK, southern Scandinavia and northern Germany, which is a relatively flat area dominated by rivers with a high contribution of groundwater to streamflow. It is most likely that the behaviour extends into Eastern Europe, but is difficult to prove due to the lack of sufficient homogeneity of cluster C14. Other clusters have lower tendency to develop persistent regional streamflow deficiencies, for example clusters C1, C6, C12, C15, C16. These clusters represent mountainous regions (e.g. Alps). Here, even short rainfall events can end a dry spell, because of different catchment characteristics compared to the previously discussed regions: a faster runoff generation due to low natural storage systems in hard rock aquifers and steep catchment slopes, and/or the exposure to frequent weather changes (cluster C1, northern Great Britain). For instance, for the 1976 drought, a difference can be noted for the two British clusters (C2 and C3). The dry spell in the western cluster (C3), which is more exposed to moisture from the Atlantic and consists of faster reacting catchments, is interrupted in spring. The event is also discussed in the visualisation section in Chapter 5.3.

6.4 Conclusion

Although purely statistical, the classification by cluster analysis produced 19 regions, which are spatially coherent. This result confirms the strong regional character of low streamflows observed in the previous chapters. Many stations which showed simultaneous streamflow deficiencies in the trend analysis (Chapter 4) or in the dynamic visualisation (Chapter 5) were classified into the same cluster. The finally presented classification provides a relative delin-

eation of regions based on the whole period 1962-1990, therefore focusing on the average simultaneousness over a long period. Particular events, however, may certainly affect only parts of a cluster. The presented regional classification is well suited to carry out more detailed investigations on drought at the regional scale, but the varying homogeneity and the limitation due to the varying station density across Europe should be kept in mind in the interpretation of further cluster-based analysis (Chapter 7, Chapter 8).

For the 19 delineated regions, an adequate representation of streamflow deficiency at this regional scale had to be developed. The regional streamflow deficiency index series, *RDI,* for each cluster proved to be capable of reproducing the main features of the dynamics of particular streamflow deficiency and drought events. Some regional trends and persistency features detected in the time series analysis on drought parameters of the individual stations discussed in Chapter 4 are also still contained in the regional series. Due to the aggregation of the individual station information, the development within the considered region, as well as the relation between the regions, can be described with these index series. The *RDI* series include the spatial dimension in the definition of severe dry periods. Originally based on the varying threshold level approach, such periods are filtered by typical or expected regional and seasonal climatic characteristics such as snow storage in winter. Hence, they can be attributed mainly to a recent weather situation, which is a prerequisite for an analysis of the direct relationship between synoptic meteorology and the regional hydrological parameter.

7 Atmospheric Circulation and Regional Streamflow Deficiency

7.1 Introduction

As shown in the previous chapters, streamflow deficiency is a regional phenomenon depending on certain meteorological situations, which, by their persistence, cause a water deficit to develop and propagate through the hydrological cycle. The streamflow deficit then spreads across a region. Due to various factors delaying the hydrological response to an atmospheric dry signal, drought causing processes are difficult to be represented in a model. Nevertheless, a major task for hydrologists is to develop models as tools to analyse the large-scale to regional-scale causes and processes for the occurrence and space-time characteristics of streamflow deficiency and drought. Moreover, a reliable regional drought forecasting and the investigation and prediction of climate change impacts on regional drought occurrence also depends on the availability of appropriate models.

At the pan-European scale, little is known about the large-scale atmospheric processes causing drought and drought forecasts are not carried out operationally. Unlike floods, which are a hazard emerging quickly within the range of hours to a few days, droughts generally take longer to develop. Respectively longer is the required lead time for forecasting, which would allow preventive actions. Across Europe, the forecast requirements vary with the climatic region, because of the different perception of drought as discussed in Chapter 3. One limiting criterion concerning the input to a forecasting model is that mid-range and seasonal weather forecasts are still difficult to make and highly uncertain. Rainfall-runoff models work properly only if they are calibrated to appointed catchments with good data availability. However, a water shortage only causes problems when it spreads and finally extends across a large region. Coupled continental or global climate models manage the simulation of seasonal or annual averages, but are not designed to predict timing and duration of extreme surface hydrological events (e.g. Ropelewski & Folland, 2000). Research on suitable methods for mid-range to long-range drought forecasting currently concentrates on lagged teleconnections of precipitation or streamflow with circulation indices such as the El Nino Southern Oscillation Index (ENSO) or the North Atlantic Oscillation Index (NAOI) or with circulation patterns (CPs). An advantage of using such indices or circulation patterns is that they are

based on reliable air pressure data for which long time series are available. A detailed review on studies linking hydroclimatological parameters to atmospheric circulation in this regard is given in Chapter 7.2.

For Europe, some studies have considered the link of atmospheric circulation and drought at a regional or national scale. However, a pan-European study investigating and comparing the relationship across the continent has not yet been carried out. The simultaneous visualisation of mean sea level pressure (MSLP) and at-site streamflow deficiency conditions across Europe in Chapter 5 showed a strong response of streamflow conditions to changes in the large-scale atmospheric circulation patterns over Europe and the North Atlantic. This response suggests to study the link between CP types and regional streamflow deficiency in more detail. First, the frequencies of 30 CP types during drought events were investigated. Based on the results, the CP types are grouped, and a model is established to further analyse and describe the link between CP occurrence and regional streamflow deficiency.

7.2 Linking synoptic meteorology to hydrological variables - a review

As the available literature on teleconnections of hydroclimatological variables is numerous, the following review concentrates on studies either linking circulation indices or circulation patterns to drought, streamflow conditions, and extreme hydrological events. Generally, there are studies statistically *analysing* the relationship and studies *modelling* the relationship. Statistical analyses of the link aim at identifying the causing atmospheric processes, at explaning trends or at describing typical event characteristics. Furthermore, they can precede a modelling study to explore and pre-select the appropriate predictors and a suitable link approach for the modelling. Circulation indices are usually used to investigate regional-scale seasonal or annual meteorological and hydrological averages, while circulation patterns focus on higher, often daily, time resolution (Chapter 2.2.2). Circulation patterns can either be identified based on their relationship to surface climatological variables or they can be classified a priori, only based on atmospheric data.

Analysis

Redmont & Koch (1991) carried out a study relating the Pacific North America Index (PNA) to precipitation, temperature and annual streamflow. They determined significant correlations between winter atmospheric circulation and summer streamflow anomalies. Close relationships between streamflow anomalies in the United States and Australia and the preceding ENSO signal were described by Dracup & Kahya (1994) and Piechota & Dracup (1996). Chiew et al. (1998) concluded that the lag-relationship of streamflow to the circulation index

was strong, but the serial correlation of streamflow was even stronger, and therefore both must be combined to obtain an adequate forecast of streamflow.

Several investigations in Europe used the North Atlantic Oscillation Index (NAOI). Dry winter time conditions in southern Europe have widely been attributed to high phases of winter NAOI (e.g. Hurrel & van Loon, 1997). Due to a larger pressure difference between the Icelandic Low and the Azores High, surface westerlies in high index winters are stronger than in low index winters. With the storm tracks being shifted further north, wetter and warmer conditions than usual prevail in northern Europe while rainfall is low in southern Europe. Shorthouse & Arnell (1997) confirmed this influence by showing a link between the NAOI and average monthly runoff across Europe.

In the framework of the ARIDE project, the correlation of the NAOI to different European drought series was investigated, and details are reported in Stahl et al. (2001). In this study, one of the parameters correlated to NAOI were the monthly averages of the Regional Streamflow Deficiency Index (*RDI)* series for the 19 European clusters (Chapter 6.3.2). Low correlations were found for the whole time series applying different lags and averaging periods. The northern Britain cluster (C1) shows the highest correlation ($r = 0.32$). Streamflow deficiency in Spain is generally associated with high NAOI values (NAOI >1) and streamflow deficit in the UK, northern and central Europe are associated with low NAOI (NAOI < -1). Seasonal correlations were much higher: For the winter season, the *RDI* of most regions shows a significant negative correlation with NAOI. Only the Spanish series is correlated significantly positive, meaning high NAOI values were related to streamflow deficiency. For the summer season, weak negative correlations were only found for northern Europe. The results are in line with correlation patterns found in other studies (e.g. Shorthouse and Arnell, 1997). The influence of NAPOI related atmospheric circulation on the European hydrology is generally strongest in winter and weaker in summer, but for specific regions, a relationship between the NAOI and streamflow deficiency in spring and autumn could also be detected. The results strongly vary with the analysed season and averaging interval.

Several studies have identified or analysed circulation patterns responsible for drought periods in particular European regions. Adler et al. (1999) used canonical correlation to identify atmospheric situations leading to droughty periods in Romania. Dry conditions were attributed to lower than normal southwesterly mediterranean circulation in winter. Maheras (2000) analysed synoptic situations responsible for drought in the Mediterranean basin. He used principle component analysis of MSLP data during anomalously dry months. Pre-classified circulation patterns such as the 'European Grosswetterlagen' (Chapter 2.2.2) have also been used to study dry periods. Cappel (1975) found that anomalously dry months show 2-12 days more high pressure CPs and less western CPs than usual. Stahl & Demuth (1999) found positive frequency anomalies of several high pressure CP types during drought in southern Germany.

Modelling

Most research dealing with the coupling of atmospheric and hydrologic systems has focused on the downscaling of large-scale GCM output to regional scale hydrology. Generally, there are two approaches: dynamical downscaling, which uses physically-based hydrological models at the subgrid scale nested into a GCM, and empirical downscaling, which uses a direct link function to describe the relationship between synoptic meteorological situations and hydro-climatic parameters. Comparisons of dynamical and empirical downscaling methods show similar predictive skills (e.g. Murphy, 2000). Circulation patterns classified from air pressure data have proved great value in establishing a direct link with hydrologic parameters. The empirical link function can be statistically based, a conditioned stochastic process, a deterministic black box model, derived by logic or fuzzy logic rules, neural networks, etc. In this review only empirical downsaling is considered, as methods commonly used for this approach provide possible applications for this study.

Following the 'weather generator principle', Bardossy & Plate (1992) presented a stochastic rainfall model conditioned on daily CPs. Extended by a spatial covariance function, the daily local probability and the spatial amount of precipitation could be simulated. A similar approach was adopted by Wilby (1993) and Wilby et al. (1994) for coupling Lamb's Weather Types with a conceptual rainfall-runoff model and a hydrochemical model in an experimental basin in the UK. The results indicate that the frequencies of floods and droughts depend upon the synoptic scenario. Periods of prolonged anticyclonic activity experienced the lowest flows (Wilby et al., 1994). Although these studies concentrated on particular catchments, they demonstrate the close link of CPs to the hydrological response.

Several studies have addressed the direct relationship of surface hydrological extremes to circulation patterns at the regional scale. Duckstein et al. (1993) linked daily CP occurrences to partial duration series of floods in Arizona, USA. Groups of flood-producing CPs could be determined and their seasonally varying contribution was analysed. The monthly Bhalme-Mooley Drought Index (BMDI) has been modelled as a CP-conditioned first-order autoregressive stochastic process (Bogardi, 1994). Other studies did not assume a stochastic process: Using fuzzy rules, Pesti (1996) presented an alternative link method to predict regional monthly Palmer Drought Severity Indices (PDSI). The drought index was predicted on the basis of preceding frequencies and the centres of gravity for each Circulation Pattern. Also based on fuzzy rules, Pongracz et al. (1999) combined the influence of Circulation Patterns and the Southern Oscillation Index for drought modelling in Nebraska, USA.

Within the framework of the ARIDE project, a logistic regression model was derived for each of the 19 clusters across Europe (Chapter 6). Details of the analysis are presented in Stahl & Demuth (2001). The regression model predicted periods with $RDI > 0.3$ using CP-group occurrences and their frequencies for a 30-day lag and a 150-day lag as predictor variables. The percentage of the correctly classified days ranged from 88% to 95%. If only the event days were considered, the best result was obtained for western Germany (cluster C8) and

southwestern UK (C3) with about 60% of the event days (*RDI* > 0.3) classified correctly. Due to the high number of predictor variables, the partial contribution was difficult to assess, but separate models for the two lags indicated the different sensitivity of a cluster to either the short-term CP frequencies (30-day lag) or to the long-term lag. This sensitivity could partly explained with the promptness of the hydrological response typical for the geological and climatological characteristics in the region. However, a drawback of the logistic regression method is the additional introduction of a spatial threshold to define the events from *RDI*. The prediction can only consider days above or below this threshold, but not the spatial spreading originally described by *RDI*.

7.3 Analysis of circulation pattern frequencies

7.3.1 Method

Although the simultaneous visualisation of MSLP and regional streamflow deficit in Chapter 5 has shed some light on the atmospheric processes responsible for extreme dry periods in different regions across Europe, it did not allow to quantify the relationship. The *RDI* as a regional measure for the occurrence and dynamics of dry periods gives the opportunity to analytically investigate the related circulation patterns. With the *RDI* for 19 European regions calculated for 1962-90 and the daily circulation patterns available for the same period, a detailed analysis of the occurrence frequencies was possible.

To obtain CP *frequency anomalies* related to streamflow deficiency, the relative frequency of each CP type for the whole period 1962-90 was subtracted from the relative frequency of the same CP type during *severe* regional streamflow deficiency periods. *Severe* periods were defined as periods above the *RDI*, which was exceeded for 90% of the time during the whole period. For most clusters, this corresponds to periods with *RDI* > ca. 0.3. For all 30 CP types, anomalies were derived for:

- the whole year
  - → simultaneous frequencies
  - → lagged frequencies (during a moving time window of 10 days to 150 days preceding the *RDI*)
- four seasons
  - → spring (March - May)
  - → summer (June - Aug)
  - → autumn (September - November)
  - → winter (December - February)

A *positive anomaly* for a CP means that the CP occurs more frequent than usual and is thus associated with dry meteorologic conditions causing *streamflow deficiency.* A *negative anomaly* respectively indicates wet conditions.

7.3.2 Results

The CP frequency anomalies during severe dry periods for the whole year range between +7% and -6% with some exceptions showing even higher values (Figure 7.1). Again, the six graphs in Figure 7.1 are arranged according to the clusters' geographic location as in previous illustrations. Due to the method, the anomaly values also give an impression of the generally different occurrence frequencies of the 30 CPs. The two most frequent CPs, West cyclonic (Wz) and central European high (HM) (Table 2.1), also show the largest negative and positive anomalies for most clusters. For instance, for the German clusters C8 and C9, the relative occurrence frequency of HM is about 7% higher during severe streamflow deficiency periods than during the whole period, which can be considered a strong influence of HM on streamflow deficiency. Clear exceptions from the general pattern of positively and negatively associated CPs across Europe are the Norwegian cluster (C19), for which HM and the ridge across Europe (BM) do not favour streamflow deficiency and Spain (C18) for which Wz actually does favour streamflow deficiency.

For most of central Europe and the UK, the central European high-pressure CPs (HM, BM) and the CPs describing high pressure centres over Britain and the North Atlantic (HB, HNa, HNz) are associated with dry periods. For the eastern clusters (right column), the CPs with high pressure over Fennoscandia (HFa, HNFa) and with a southeastern flow direction (SEa, SEz) are also positively associated with streamflow deficiencies. Negatively associated with dry periods are most west CP types and the low pressure types (TB, TRW, TRM, TM). Only eastern Europe (C14) is not influenced by the trough over western Europe (TRW) and shows a positive anomaly.

Lagged CP frequency anomalies show the same positive and negative deviations found as the simultaneous CP occurrence. However, for most clusters the anomaly signal strongly decreases with increasing lag time. The 30-days preceding anomalies of HM in clusters C13 and C17 dropped to about 3% (compared to almost 8% for simultaneous frequencies). Only a few exceptions show a stronger signal for the 30-day lag. One is for instance the anomaly for BM in Cluster C17, which increases from 1.5% to 4%.

Calculated independently for the four seasons, frequency anomalies are even stronger and more specific (Figure A.1 to Figure A.4, Annex). In spring, the major CP responsible for streamflow deficiency across Europe is the British High (HB). In summer, the ridge across Europe (BM) shows the most positive anomaly, except for Norway and northern Britain, for which the same CP shows a negative anomaly. The same synoptic situation was already discussed in the visulisation study (Chapter 5.3), and the daily visualisation snapshot for 11 Aug

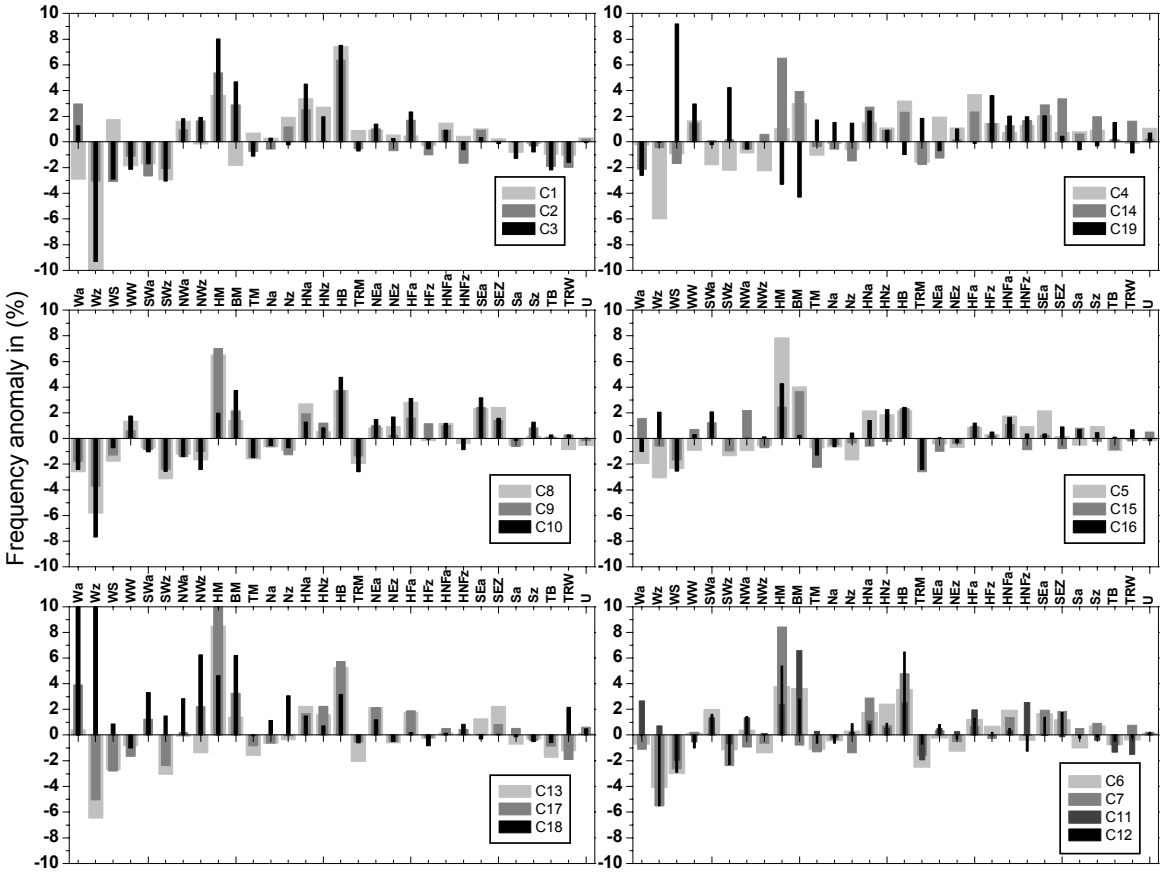

Fig. 7.1 *CP frequency anomalies during severe regional streamflow deficiency periods*

1990 in Figure 5.6f illustrates the hydrological response to this particular CP with dry streamflow conditions across Europe except for northern Europe. In autumn, again the British High (HB), but also the central Europe High (HM), show positive frequency anomalies in many clusters. The absolute autumn anomaly values, however, differ more between the clusters than for other seasons. Examples for spring and autumn events caused by a British High (HB) were also discussed in the visualisation study with snapshot illustrations for 16 Oct 1973, 8 Dec 1989 and 30 May 1990 (Chapter 5.3). A few clusters further show a positive association of *RDI* with anticyclonic western CPs (Wa and NWa and SWa) in autumn. In winter, except for Norway (C19), the central European High (HM) is the CP which is most widely associated with streamflow deficiencies. In central Europe, the anomalies exceed +10% (e.g. for C5, C7, C8, C13, C17). Such a wintry HM situation is also illustrated in the visualisation study (Chapter 5.3, Figure 5.3b). The northern high pressure CPs (HNa, HNz, and HB) are also associated with winter streamflow deficiencies across Europe. Contrasting to the other seasons, in winter the southern CPs (SEa and SEz) are also positively related to *RDI* in many clusters.

During all seasons, the Spanish cluster (C18) shows a positive association of the western CPs, (Wz and Wa) with streamflow deficiency. The anomalies are most pronounced in summer

and autumn. Most other clusters show negative anomalies for Wz in all seasons. They are largest in winter and smallest during summer, when anomalies in northern and eastern Europe, particularly C4, C14 and C16 even turn positive. Another seasonal contrast is found for the high pressure ridge (BM), which shows large positive anomalies in most clusters in summer, but negative anomalies for many central European clusters in winter.

The frequency analysis demonstrates a strong direct link between the synoptic situation and dry conditions in surface hydrology. However, due to the different effect of some CPs, a seasonal consideration is important and has to be taken into account in a modelling study.

7.4 Modelling the link between circulation pattern occurrence and regional streamflow deficiency

7.4.1 Modelling approach

The frequency anomalies during periods of severe regional streamflow deficiency shown in the previous section underpin the strong relationship between CP occurrence and *RDI*. Therefore, the development and test of a model to simulate occurrence and spread of the regional streamflow deficiency *RDI(t)* within a predefined response region (cluster) by the CP occurrence is a promising approach. Due to different CPs exhibiting the same effect on the regional spread of streamflow deficiency and the rare occurrence of several CPs with relative frequencies lower than 2%, the 30 CPs were classified into nine groups of drought association.

The grouping was based on the seasonal anomalies found for each cluster, as the relationship between CP and *RDI* is not necessarily the same in all seasons. Hence, a new daily time series reduced to the occurrence of nine CP-groups was derived according to Table 7.1 describing the atmospheric circulation patterns for the model input. Detailed seasonal classification tables containing the group number assigned to each of the 30 CPs for the 19 clusters are included in Table A.1 to Table A.4 (Annex).

Table 7.1 *CP-group classification*

CP-group name	Frequency anomaly
CPg1	> 10%
CPg2	5% to 10%
CPg3	2% to 5%
CPg4	0.5% to 2%
CPg5	-0.5% to 0.5%
CPg6	-2% to -0.5%
CPg7	-5% to -2%
CPg8	-10% to -5%
CPg9	< -10%

To account for the persistency in the regional streamflow deficiency series, the underlying idea for the model is the basic recursive process, that the regional streamflow deficiency state on day *t* depends on the state of the previous day *t-1*, which is modified according to the

occurrence of a CP-group Z_i. This modification is described by a positive (increase) or negative (decrease) weight factor b_i. If Z=1 for the occurring CP-group and Z=0 for all other CP-groups on day t, a series of daily states $Y(t)$ describing the streamflow deficiency spread within the cluster can be estimated as:

$$Y(t) = Y(t-1) + \sum_{i=1}^{n} b_i Z_i(t) \qquad (7.1)$$

where n is the number of CP-groups.

Since the process to be simulated is the occurrence and spreading of streamflow deficiency across a defined region, $Y(t)$ is bound. When the entire region is already affected (all stations in the cluster), no further spread is possible if another 'dry' CP occurs. Similarly, if the entire region has recovered, a 'wet' CP can not cause more recovery. The values for this upper and lower boundary of $Y(t)$ were arbitrarily chosen as:

$$\begin{aligned} Y(t) &= 1 \quad if \quad Y(t) > 1 \\ Y(t) &= -1 \quad if \quad Y(t) < -1 \end{aligned} \qquad (7.2)$$

By definition of the *RDI*, which varies between 0 and 1, and by the choice of Q90 as varying threshold level, the mean of *RDI* for all clusters is 0.1. To obtain a simulated *RDI*, only the part describing the streamflow deficiency spread has to be selected from the $Y(t)$ series. This is achieved by finding the threshold y_0 so that the transformed series RDI_{sim} has a mean value equal to 0.1:

$$\begin{aligned} RDI_{sim} &= \frac{Y(t) - y_o}{1 - y_o} \quad if \quad Y(t) > y_0 \\ RDI_{sim} &= 0 \quad if \quad Y(t) < y_0 \end{aligned} \qquad (7.3)$$

Hence, y_0 defines the onset of the actual streamflow deficiency spreading RDI_{sim}, which is now described by values between 0 and 1.

The n weight factors b_i for the CP-groups were fitted to the observed *RDI* using a sequential uncertainty domain parameter fitting procedure (Abbaspour et al., 1997), which is a global search algorithm. For all parameter combinations the goodness-of-fit is calculated and the most probable parameter set is chosen. Therefore, the result of the fitting procedure is independent from the initial parameter values assumed. The goodness of fit was based on the Pearson product moment coefficient r. This correlation measure was chosen, as the aim of this model is to capture the main fluctuations and the major extreme events in the series. Other goodness of fit measures emphasise the differences between the simulated and observed values, which due to the many 0 values in the *RDI* series should not be given too much weight.

To guarantee an adequate model validation, the time series was split into a calibration and a validation period. The calibration period of 17 years and 5 months was chosen from the 1 Dec 1970 to 31 May 1987 to have common wet periods in all clusters in the beginning and in the end of this period. Thus, the starting value for *Y(t)* could be reliably set to *Y(t)* = -1. The remaining years from 1962 to 1970 and from June 1987 through 1990 were used for validation.

To illustrate the functioning of the model, Figure 7.2 shows an example of the model simulation for the events in the early seventies in cluster C10, northern Germany. *Y(t)* is the series predicted by the model. It runs between -1 and 1. The threshold y_0 for cluster C10 was determined to be close to zero (y_0 = -0.03). However, for other clusters it can differ considerably from zero depending on the response of the cluster to the CPs and on its homogeneity. The part of *Y(t)* above the threshold is the prediction RDI_{sim}. Only for this part, the goodness of fit is assessed. Nevertheless, the figure also contains the part below the threshold to illustrate the reaction and recovery behaviour of the cluster.

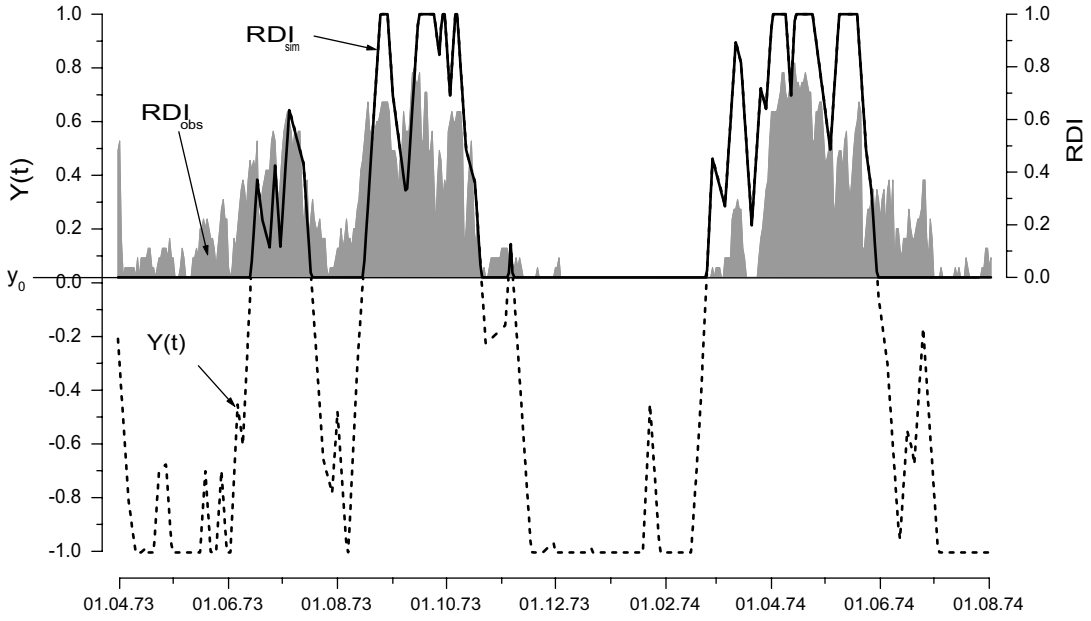

Fig. 7.2 *Example of the model predictions for cluster C10*

7.4.2 Simulation results

Goodness of fit

For all 19 clusters, the model was fitted to the *RDI* of the calibration period. In addition to the Pearson correlation coefficient r, which was used to calibrate the model, the index of agreement *a* (Willmott, 1981) was calculated to independently assess the results. Similar to *r*, this

index varies between 0 (no agreement) and 1 (full agreement) taking into account the differences in the observed and simulated values:

$$a = 1.0 - \frac{\sum_{i=1}^{N} (O_i - P_i)^2}{\sum_{i=1}^{N} (|P_i - \overline{O}| + |O_i - \overline{O}|)^2} \qquad (7.4)$$

where O are observed data and P are the model-simulated data. The overbar denotes the mean of the entire period of N time increments.

Table 7.2 gives an overview of the goodness-of-fit measures calculated for the original series of daily values for the calibration period, the validation period and the entire reference period (1962-90). Furthermore, the goodness-of-fit measures for seasonally aggreagated average values of the reference period were determined.

The close agreement of r and a for the two periods (Table 7.2), demonstrates that the model is able to predict the *RDI* for the validation period just as well as for the calibration period for many clusters. The best correlation ($r = 0.65$) and agreement ($a = 0.776$) for the entire reference period was obtained for cluster C7, southeastern Germany. Also very good agreements were obtained for clusters C1, C2, C3, C4 (UK and southern Scandinavia) and C8, C9, C10 and C13 (southwestern Germany). For a few clusters, the measures indicate difficulties to fit an appropriate model to the *RDI*. These comprise cluster C11, which spans east-west across the southern rim of the Alps, and C14, which includes all Eastern European stations, cover large regions and are both quite heterogeneous (Chapter 6.3.2). For clusters C5 and C6, eastern Germany, Czech Republic and northern Austria, mediocre model fits were found. This can be attributed to the regions including versatile environments in plains and mountains at different altitudes. The model for C16 (Carpathian Mountains of Ukraine) is quite poor, although the cluster is rather small and homogeneous. On the other hand the models for Norway (C19) and Spain (C18) indicate some predictive potential although they cover large diverse areas.

The comparison of the observed and simulated series aggregated to seasonal averages of *RDI* are very good with many correlation coefficients exceeding 0.7 and coefficients of agreement exceeding 0.8. (Table 7.2).

Parameters

The parameter sets for the 19 clusters are summarised in Table 7.3. A parameter set includes the weight factors for the n CP-groups, which are the calibrated parameters, and the threshold y_0, which is determined by the criterion that the mean of RDI_{sim} has to be equal to 0.1 (Equation 7.3). Due to the classification of the CP-groups (Table 7.1), for some clusters only $n = 8$

Table 7.2 *Goodness of fit for different periods*

Cluster	Correlation coefficient *r*			Index of agreement *a*			Seasonal *r*	*Seasonal a*
	calib.	valid.	1962-90	calib.	valid.	1962-90	1962-1990	1962-1990
1	0.604	0.610	0.594	0.774	0.759	0.769	0.706	0.840
2	0.675	0.558	0.629	0.802	0.711	0.768	0.774	0.869
3	0.506	0.611	0.551	0.705	0.768	0.732	0.702	0.837
4	0.609	0.532	0.581	0.767	0.713	0.750	0.723	0.844
5	0.436	0.539	0.507	0.630	0.717	0.693	0.662	0.803
6	0.457	0.397	0.428	0.628	0.591	0.611	0.607	0.737
7	0.621	0.676	0.650	0.753	0.796	0.776	0.881	0.921
8	0.647	0.503	0.588	0.803	0.700	0.764	0.744	0.857
9	0.585	0.601	0.592	0.758	0.763	0.763	0.758	0.867
10	0.613	0.500	0.570	0.769	0.671	0.738	0.749	0.861
11	0.391	0.209	0.318	0.570	0.407	0.509	0.464	0.604
12	0.428	0.536	0.483	0.645	0.714	0.683	0.655	0.801
13	0.581	0.587	0.580	0.745	0.736	0.740	0.751	0.858
14	0.434	0.495	0.461	0.506	0.597	0.551	0.664	0.691
15	0.437	0.402	0.421	0.634	0.593	0.617	0.541	0.709
16	0.331	0.292	0.306	0.552	0.549	0.557	0.490	0.698
17	0.473	0.515	0.498	0.671	0.712	0.695	0.730	0.849
18	0.399	0.559	0.467	0.581	0.642	0.616	0.694	0.752
19	0.471	0.560	0.509	0.643	0.685	0.663	0.715	0.779

or $n = 7$ CP-groups exist, because CPs with high anomalies did not occur. As the parameters for the CP-groups determine the increase or decrease of RDI_{sim} from the previous day, they are a direct measure of how strong the CPs in this group influence the development of a regional streamflow deficit. For most clusters the parameter values agree with the a priori grouping. Values for groups CPg1 to CPg4 are positive and values for groups CPg6 to CPg9 are negative. The indifferent group CPg5 is around zero in most of the clusters. Often increasing parameters are found from CPg4 to CPg1, causing a larger increase of *RDI*, when the CPs occur which were found to be stronger associated with drought. The negative parameters are mostly higher than the positive parameters, which indicates a generally faster drop and a slower rise of the *RDI*. The sum of all parameters is negative, indicating that the modelled series *Y(t)* often reaches the lower limit. For an assessment of the influence in detail, the relative frequency of the CP-groups in the period and the threshold have to be considered. The absolute threshold indicates how long a cluster needs to develop a regional deficiency event. For homogeneous clusters, a low threshold can be attributed to faster reacting hydrological conditions. This can be observed for Cluster C1 in northern Britain and also for the German

Table 7.3 *Parameter values*

Cluster	*n*	CPg1	CPg2	CPg3	CPg4	CPg5	CPg6	CPg7	CPg8	CPg9	y_0
1	8	-	0.138	0.076	0.038	-0.028	-0.169	-0.253	-0.100	-0.250	-0.829
2	8	0.101	0.101	0.014	0.051	0.000	-0.006	-0.175	-0.100	-	-0.191
3	8	-	0.140	0.076	0.054	-0.151	-0.022	-0.113	-0.259	-0.399	-0.230
4	7	-	0.101	0.076	0.096	-0.014	-0.075	-0.150	-0.106	-	-0.370
5	8	0.103	0.101	0.079	0.045	-0.050	-0.100	-0.100	-0.150	-	-0.647
6	7	-	0.126	0.101	0.032	0.080	-0.150	-0.100	-0.100	-	0.243
7	9	0.177	0.101	0.038	0.076	0.034	-0.038	-0.188	-0.175	-0.100	-0.299
8	7	-	0.101	0.043	0.050	0.001	-0.019	-0.150	-	-0.324	-0.796
9	7	-	0.101	0.062	0.005	0.057	-0.075	-0.150	-	-0.379	-0.469
10	8	-	0.138	0.101	0.006	-0.025	-0.050	-0.100	-0.100	-0.275	0.027
11	8	0.316	0.101	0.038	0.001	0.005	-0.075	-0.299	-0.101	-	0.210
12	7	-	0.146	0.088	0.055	0.001	-0.227	-0.224	-0.240	-	-0.488
13	7	-	0.127	0.052	0.052	0.000	-0.100	-0.100	-0.100	-	-0.056
14	8	0.101	0.025	0.151	0.057	0.000	-0.188	-0.075	-0.213	-	-0.254
15	6	-	0.176	0.093	0.061	-0.075	-0.150	-0.080	-	-	0.075
16	6	-	0.353	0.055	0.036	-0.152	-0.150	-0.286	-	-	-0.969
17	8	0.251	0.251	0.075	0.038	0.009	-0.299	-0.298	-0.250	-	-0.256
18	7	0.176	0.101	0.076	0.076	0.009	-0.134	-0.149	-	-	0.212
19	8	0.288	0.180	0.094	0.076	-0.047	-0.055	-0.150	-0.109	-	-0.572

Clusters C5 and C8, as well as for Norway, C19 and the Carpathian Mountains, C16. The higher hydrological variability and differences within those regions have been discussed in previous chapters. They never develop long and persistent dry spells. Larger thresholds can be found for homogeneous clusters characterised by more persistent dry spells (e.g. C2, C10).

7.4.3 Discussion of simulations and model performance

For a slowly developing and persistent phenomenon such as drought, an aggregation to seasonal values is a reasonable step to facilitate the evaluation and discussion of the results. Figure 7.3 shows the seasonal averages for the observed and simulated *RDI* for all clusters except for C6, C11, C14, and C16, which were excluded from further analysis due to their poor goodness of fit (Chapter 7.4.2).

Generally, the fluctuations of the occurrence of severe dry seasons are well simulated by the model, particularly if considering that the dry winters and summer droughts in the beginning of the period and the 1989/90 drought occurred during the validation period. No considerable

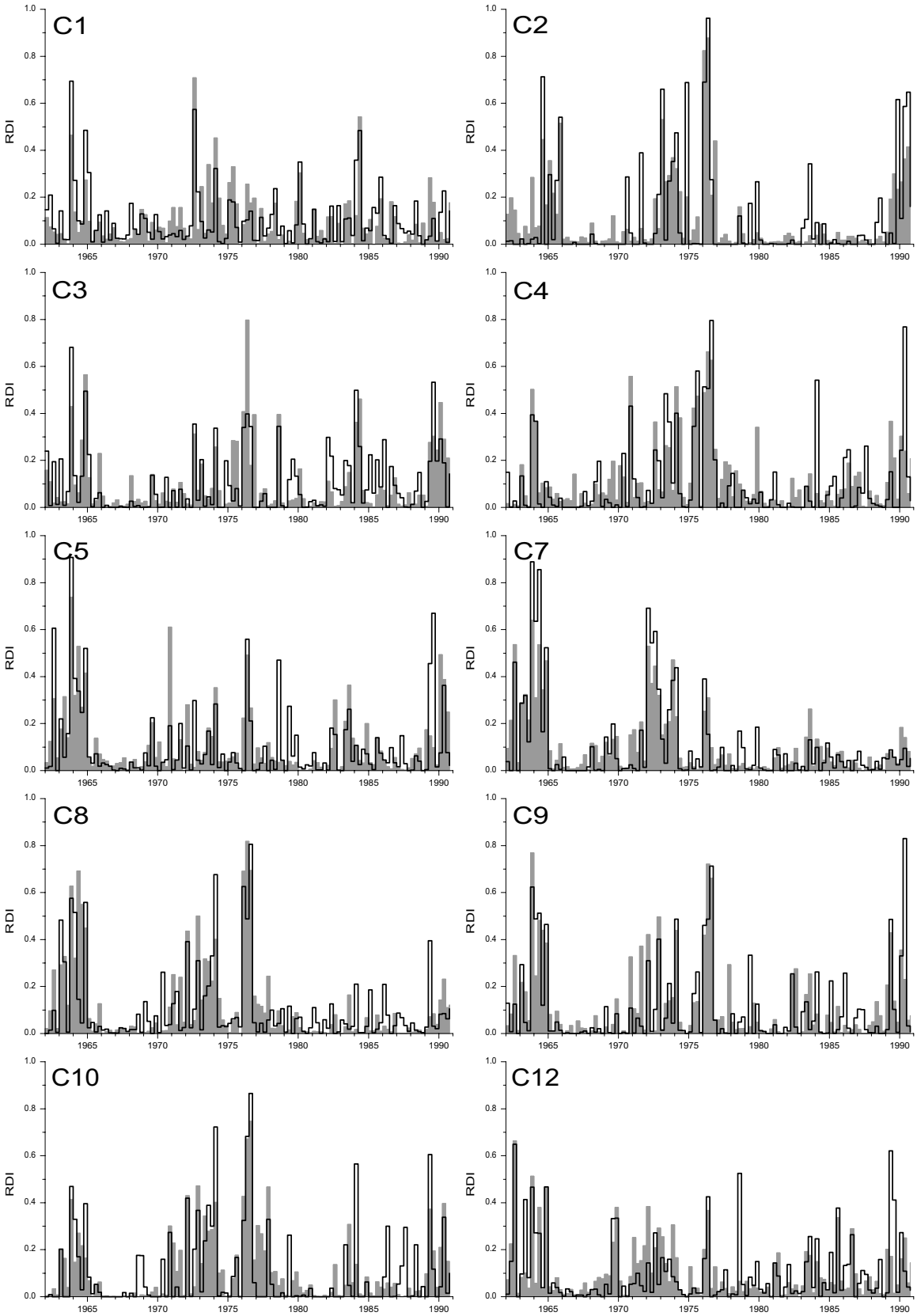

Fig. 7.3 *Seasonal averages of the observed and simulated RDI series across Europe*

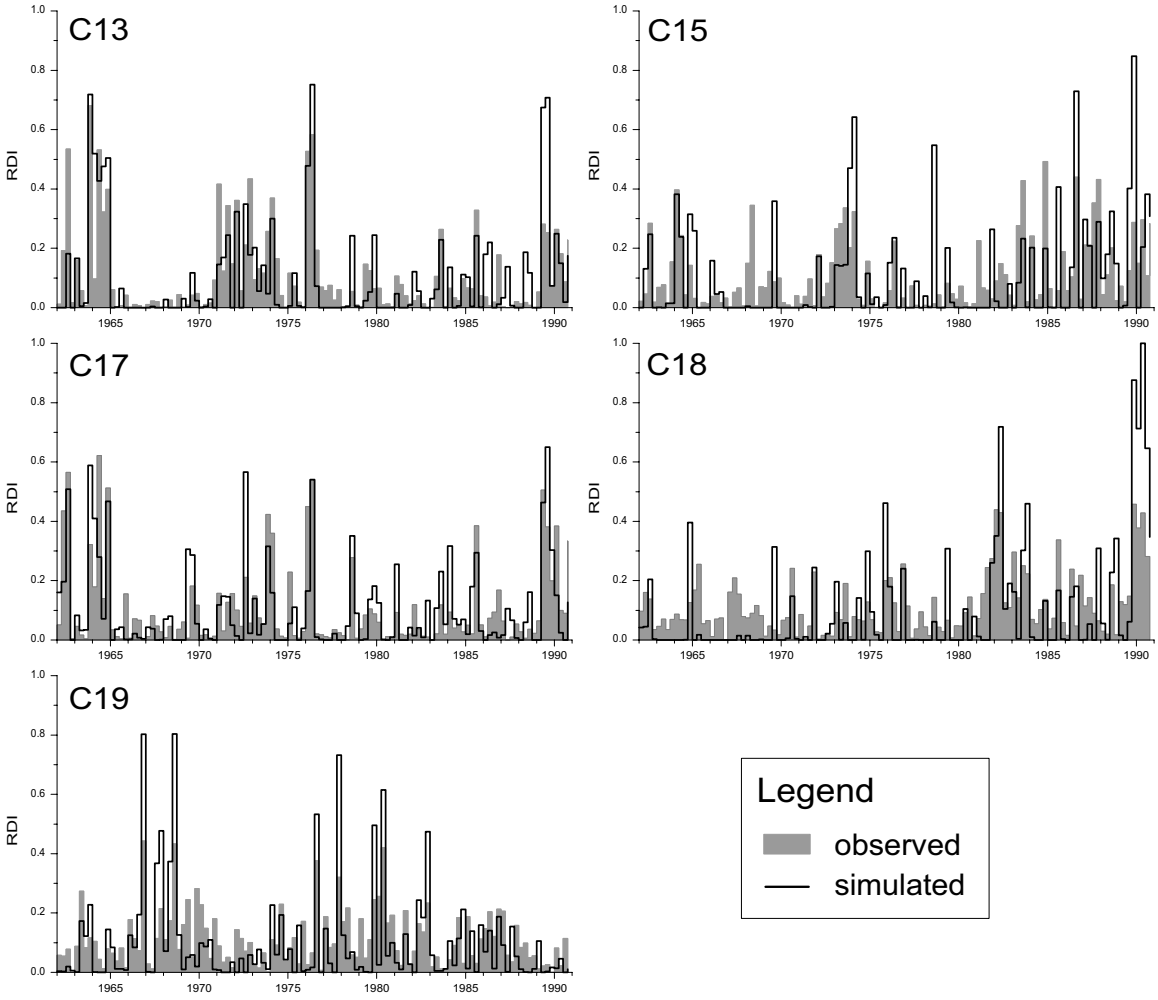

Fig. 7.3 *Seasonal averages of the observed and simulated RDI series across Europe (continued)*

differences emerge between the calibration period and the validation period. The 1976 drought is very well modelled for all affected clusters. Other events tend to be overestimated, especially in less homogeneous clusters as C18 and C19. These clusters rarely reached high *RDI* values. Generally, *RDI* series, which show less fluctuations but a more pronounced tendency towards long and severe dry periods, are better represented (e.b. C2, C7, C10). Despite the mediocre model fit, long term features like the trends towards drier conditions in the end of the period in Spain (C18) and Slovakia (C15) are well reproduced.

Some events in the early seventies were generally underestimated, whereas events in the eighties were overestimated. Some studies indicate a change in atmospheric circulation in the beginning of the eighties, which might be one reason for this change. Details on this topic are discussed in Chapter 8. The dry period in spring 1989 was also considerably overestimated in Germany (C5, C8, C9, C10, C13) and in the Alps (C12). The entire May was dominated by the circulation patterns BM and HFa, only interrupted by four days of Wz. For the German clusters, the CP types BM and HFa are in positive CP-groups with parameter values of

around 0.5. Summer and autumn were overestimated in C15 (Slovakia) and C18 (Spain). The summer was governed by CP-groups with high positive parameter values, thus the lower *RDI* in reality has to be attributed to the moderating influence of natural reservoirs from preceding wetter periods. Nevertheless, other sources have documented a severe drought in Spain in 1989. A similar situation can be noted for summer 1990, when the *RDI* is considerably overestimated in Clusters C2, C4 and C9.

7.5 Conclusion

The link of atmospheric circulation patterns to regional streamflow deficiency was studied at the European scale. An initial analysis of CP frequencies detected strong occurrence anomalies for certain CPs during severe events. These anomalies vary with the considered season and are very specific to the analysed European region with a clear decrease of the influence of zonal circulation and a decrease of the influence of meridional circulation from north to south and from west to east. As mentioned in many other studies (e.g. Briffa et al., 1994) most contrasting influences were detected for Norway and Spain. For western and central Europe atmospheric influences on streamflow deficiency show some similarities but also differences for certain CPs. Due to this variability, the cluster based information about CP frequency anomalies was used to classify the 30 CP types into nine CP-groups of different drought association. These CP-groups then provided the input for a model to predict *RDI*. The simple recursive modelling approach applied calculates the *RDI* based on the occurring CP-group and on the value of the previous day, thus accounting for persistency in the hydrological system.

The results showed that the CP-*RDI* link model is capable of simulating the major fluctuations for most clusters. Assessing the parameters, which describe the influence of each CP-group on the development of *RDI*, revealed a correct functional relationship. In this context it should be mentioned that other CP-group classifications (Baur, 1944, Gerstengarbe & Werner, 1999) were tested, but were found not to be able to predict the *RDI* series. These findings underpin the regional character of the atmospheric influence and the necessity of a region-oriented CP-grouping.

The best agreement of observed and predicted *RDI* series was found for temporally aggregated values; e.g. seasonal series of average *RDI* are well reproduced. In particular long and severe streamflow deficiency events can well be detected with this model. Consequently, the approach is well suited for drought analysis. Due to the chosen approach and the better performance at the seasonal time scale, real time forecasting might only be possible for homogeneous regions, and some additional work on the goodness-of-fit optimization will be necessary. The model could also benefit from additional predictors such as the NAOI or sea surface

temperatures. It will then be possible to assume a short-range scenario in terms of a probable CP sequence to predict the drought development within the following weeks.

However, the aim of the model in its present simple form was to prove the strong potential of empirical downscaling of regional drought parameters. The direct link between CP occurrence and *RDI* allows to analyse the effect of atmospheric circulation patterns across a large region, and thus the assessment of the regional impacts of changes in the atmospheric system.

8 Impact of Climate Change on Regional Streamflow Deficiency

8.1 Introduction

There is no doubt anymore that observed global climate change continues, in fact that it has been reinforced in the last two decades (Schönwiese, 2001). In this study, the term *climate change* is used according to IPCC (2001) 'referring to any change in climate over time whether due to natural variability or as a result of human activity'. A great degree of natural variability at different time-scales exists in the atmospheric circulation and surface hydroclimatological parameters, and often it is difficult to decide, whether changes found in historic series of climatic variables are part of a natural variability or indicate an actual change. Considering the decadal to century variability, which is caused by solar output, volcanic activity etc., the last five centuries (16th-19th) have been dominated by colder and more variable conditions, whereas the recovery occurring during the 20th century was probably enhanced by anthropogenic greenhouse gas warming (Jones, 1998). IPCC (2001) even points out that available observational changes in climate, particularly increases in temperature, have already affected a diverse set of physical and biological systems in many parts of the world. Increasing hydrological extremes as floods and droughts are one indication for this impact. However, it has to be born in mind, that compared to atmospheric variables (CPs since 1881), long hydrological data series are rare and often influenced by human activity, and conclusions about trends remain difficult (compare Chapter 4.3).

This chapter will evaluate how the relationship between CP frequencies and regional streamflow deficiency *RDI* determined in Chapter 7 can be used to assess the impact of climate change on drought in Europe. *Historic series*, as well as a *future scenario* were investigated for this assessment. To provide a basis for the interpretation of the reconstructed and predicted streamflow deficiency events in terms of climate change, Chapter 8.2 will first discuss the main mechanisms relevant to understand potential changes, and will summarise findings from European climate change studies concerning water shortage and drought. Using the known relationship to CP occurrence, regional streamflow deficiency events were reconstructed for the complete CP series from 1881 to 1998 and compared with documented historic events. Finally, changed circulation pattern occurrences and frequencies were assumed

to generate a scenario and assess its influence on the regional streamflow deficiency series. The main aim of these experiments was to explore the potential of the application of a CP-drought link model as presented in Chapter 7 for prediction of drought under changed climatic conditions.

8.2 Climate variability and hydrology in Europe

8.2.1 Influence of climate change on hydrological drought

Hydrology in a changing climate

Literature on climate change impact on hydrology is numerous. Most studies either assess historic series to detect changes or they predict changes based on the downscaling of GCM scenarios. These GCM scenarios assume increased greenhouse gas forcing during the next century, which will cause further global warming. In a warmer environment, the hydrological cycle intensifies, because higher temperatures generally lead to higher potential evaporation. As warming over land exceeds warming over the sea, evapotranspiration over land is likely to increase more (Rind, 2000). With the closed global water balance and the higher content of water vapour in a warmer atmosphere, precipitation will also increase. This general global mechanism is strongly modified by seasonal differences at a regional level.

In Europe, most rivers show a strong seasonal regime (Chapter 2.3.4). In summer, higher temperatures and higher evapotranspiration will decrease the natural reservoir of a catchment and thus the streamflow. Higher temperatures in winter will increase the amount of rain compared to snow, which will cause higher streamflows. For rainfed regimes, winter is the main recharge season, whereas for snowfed regimes, spring snowmelt recharges the soil and groundwater reservoirs. Consequently, winter temperature and rainfall changes can also have a strong influence on the hydrological summer conditions. For the hazard of summer low flows and droughts, it can be summarised, that higher temperatures in summer induce drier surface hydrological conditions. However depending on the precipitation changes, the type of regime and the storage characteristics in the catchment, the sensitivity of the surface hydrological response can vary strongly. Arnell (1992) showed that flows in catchments with large groundwater reservoirs can be maintained even during dry summers if winter rainfall increases. Seasonal variability is therefore important to assess the impact of climate changes on the complex hydrological system.

Observed changes

A major change in the atmospheric circulation over Europe has occurred since the 1980s, when the North Atlantic Oscillation Index has remained in an extremely high phase (Hurrell

& van Loon, 1997). In particular during winter time, enhanced North Atlantic Oscillation has influenced the climatic conditions in Europe. A northward shift in the storm tracks was associated with wetter-than-normal conditions over northern Europe and Scandinavia, while drier conditions than normal persisted over southern Europe and the Mediterranean.

Hydroclimatological changes over the 20th century observed across Europe are summarised in Watson (1998):

- Temperature rise has been most marked during the winter period
  - → 1°C per century in the British Isles or along the Baltic coastline
  - → 2°C per century in southwestern Europe (Iberian Peninsula, south and central France)
  - → 3°C per century in some places in the northern and central parts of European Russia
- Annual precipitation trends in this century were characterized essentially by
  - → increases ranging from 10% to close to 50% in the northern half of Europe (i.e., north of the Alps to northern Fennoscandia)
  - → decreases by as much as 20% in some areas of the region stretching from the Mediterranean through central Europe into European Russia and Ukraine

However, these changes did not occur continuously and large temporal fluctuations were found. Moreover, the values may have varied with the seasons. Some studies also reported a decrease of summer precipitation in western and central Europe (e.g. Schönwiese, 2001). Changes in surface hydrological variables have been difficult to assess. Therefore, systematic trends are rarely found, but it seems like the occurrence frequency and severity of extremes has increased (Schönwiese, 2001).

Future projections

GCM simulations, driven with increased anthropogenic greenhouse gas forcing, predict a further northeastward shift of the NAO's northern variability centre (Ulbrich & Christoph, 1999). Consequently, storm track activity over the eastern Atlantic and western Europe will also increase. Large scale models accordingly predict a continuation of the increased winter precipitation in the North. Arpe & Roeckner (1999) found an intensified extension of the Azores High into Europe, causing drier summer conditions in the next century. However, detailed quantitative statements about regional-scale climate change impacts on water resources are difficult as many regions include a wide range of hydroclimatic regions (Watson, 1998). Regional model results for precipitation are often uncertain and highly variable for different scenarios (IPCC, 2001). This variability is reflected in several modelling studies. Some examples are:

- Arnell & Reynard (1996) simulated changes of ±20% in annual runoff for 21 catchments in Great Britain with a tendency towards lower amounts of discharge, especially in sensitive areas and during the summer months.

- A modelling study by Weatherald & Manabe (1999) concluded that for southern European regions, CO_2 induced summer dryness won't be noticable until several decades into the 21st century.
- Murphy (2000) found great differences comparing temperature and precipitation predictions resulting from different downscaling methods.

Nevertheless, the expected effects on different regions of Europe can be classified according to the climatic gradients from north to south and from west to east (the maritime-to-continental gradient) (Watson, 1998). According to current and projected distributions of rainfall, there may be an increase in summer drought. Precipitation is expected to decrease in summer and increase in winter and spring. Such a change is likely to affect mainly areas that already are sensitive to drought: the southern and continental parts of Europe, especially the Mediterranean region. Additional consumption of water for irrigation may create additional depletion of water reservoirs and groundwater. These findings by IPCC summarised in Watson (1998) call for an intensive concentration on drought research.

8.2.2 Trends and changes in the CP series since 1881

Certainly the discussed hydroclimatological changes have also been observed in the atmospheric circulation patterns over Europe. The series of the daily CP-types used in this study, the German *Grosswetterlagen*, are available since 1881, and the recently revised series have been tested for homogeneity (Gerstengarbe & Werner, 1999). Various studies have assessed trends in the time series of the CP frequencies and changes in the persistency of the individual CP types. Bardossy & Caspary (1990) detected a change point in the eighties. They showed that since about 1973, frequencies of CPs of the major type 'west', particularly west cyclonic (Wz) have increased in winter, while CPs with north and east components have decreased, a combination, which they argue lead to the warm and snowless winters in Germany in the 1980s. Klaus (1993), found strong changes in frequency and especially in persistency of certain CP groups, which he explained by a change in the preferred location of troughs over Europe:

- increasing persistency and maximum duration of mixed circulation CPs (especially SWz, SWa, BM) since the mid-sixties
- increasing frequency and mean persistency (by 10 days) of zonal circulation during winter since the mid-sixties
- significant increasing trend of the CPs with southern airflow (60 to 120 days per year for the period 1881-1992)
- significant decreasing trend of the CPs with northern airflow (170 to 110 days per year for the period 1881-1992)

Gerstengarbe & Werner (1999) published the latest version of the catalogue of European Grosswetterlagen and in detail studied annual and seasonal frequencies, persistency and their

changes from 1881 to 1998 confirming the aforementioned changes. Werner et al. (2000) confirmed climatic changes by an analysis of the CP frequencies and residence times of the major type 'west'. An outlier test of the decadal behaviour of these variables identifies the period 1981-90 as the onset of climate change with a trend commencing in the beginning of the 1970s.

Although the exact time of the determined change varies for the different CPs and the different studies, there seems to be an agreement that changes occurred in the last three decades, and that they involve mainly the increased zonal circulation in winter and the generally increased persistency of CP sequences.

8.3 Reconstruction of regional streamflow deficiencies 1881-1998

8.3.1 Results of the reconstructed *RDI* series

With the daily CP types available since 1881, *RDI* series for the 19 European clusters can be reconstructed for the same historic period using the CP-*RDI* link model and the parameters b_i determined in Chapter 7. Figure 8.1 shows the results of the reconstructed historic series and the observed *RDI* for the reference period 1962-90. The series were aggregated to annual mean *RDI* values, and the clusters with a poor model fit were excluded from the analysis. For better regional comparison, the graphs for the clusters are arranged according to their geographic location (compare Figure 6.3). The fluctuations of the reconstructed *RDI* series confirm the properties discussed in Chapter 6.3.2. Some clusters tend to be affected by severe and persistent dry spells (e.g. southeastern UK (C2), northern Germany (C10)), whereas other regions fluctuate with a high frequency and a lower amplitude (e.g. northern Britain (C1), Alps (C12), Jura (C17), Norway (C19)). Additionally, general trends in the average *RDI*, historic periods particularly characterised by extreme events, and changes in the variability of *RDI* over time can be noted.

Decreasing levels of annual *RDI* values are found for northern Britain (C1), southwestern UK (C3), southeastern Germany (C7) and the Jura Mountains (C17). The increasing trends for Spain and Slovakia observed in the trend study of the reference period (Chapter 4.3, Hisdal et al., 2001a) are still a striking feature visual in the long period since 1881. Particularly in Spain, the 1990s was the driest decade of the period of record. In northern and western Germany (C10, C8), the major events during the reference period (early 1960s, 70s and late 80s), which were discussed in previous chapters, are also among the largest events if the whole period since 1881 is considered. Apparently, the northern German clusters (here comprising western Germany (C8), central Germany (C9), and northern Germany (C10)) and southern

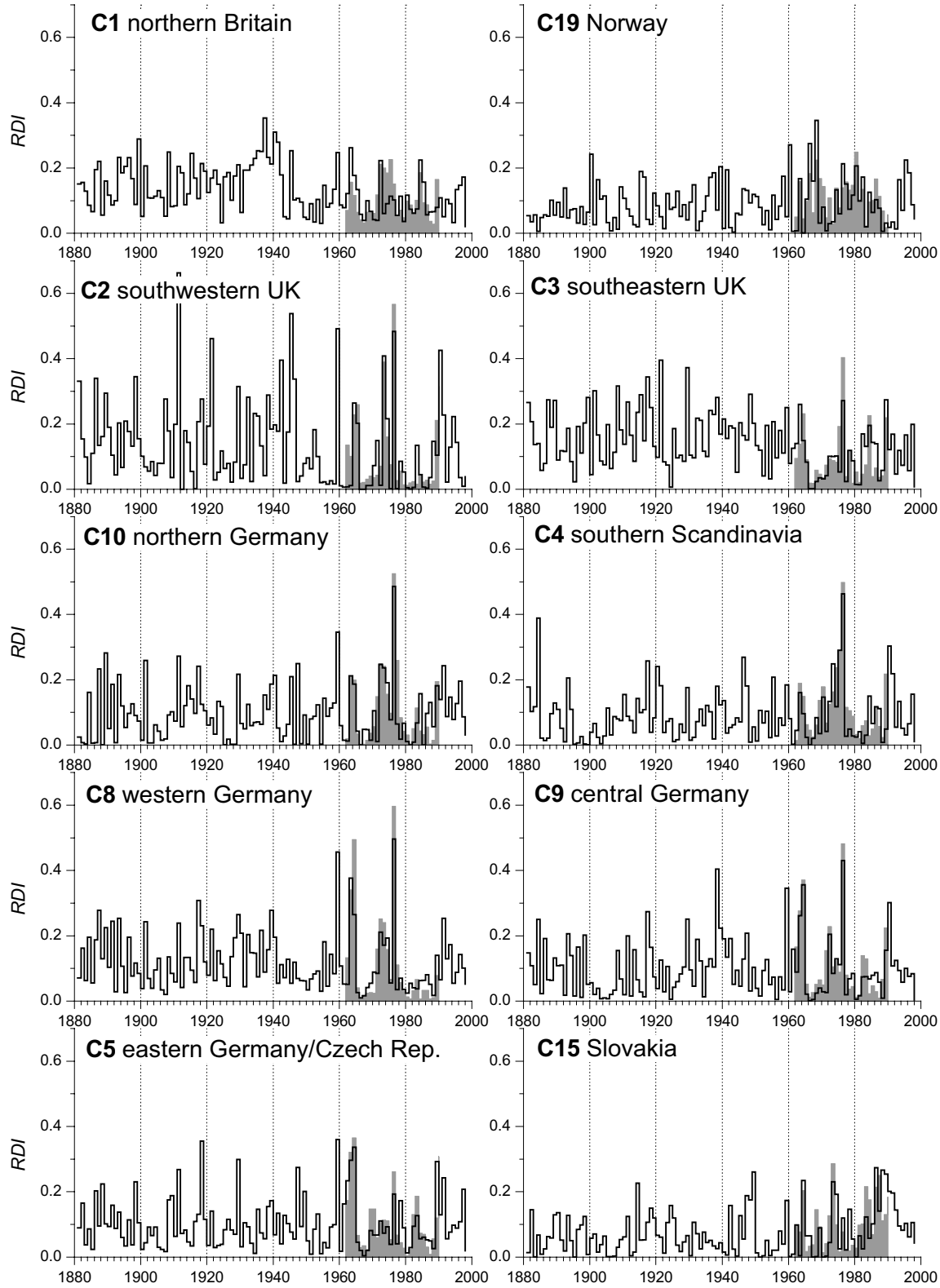

Fig. 8.1 *Reconstructed historic RDI series for the 19 European clusters*

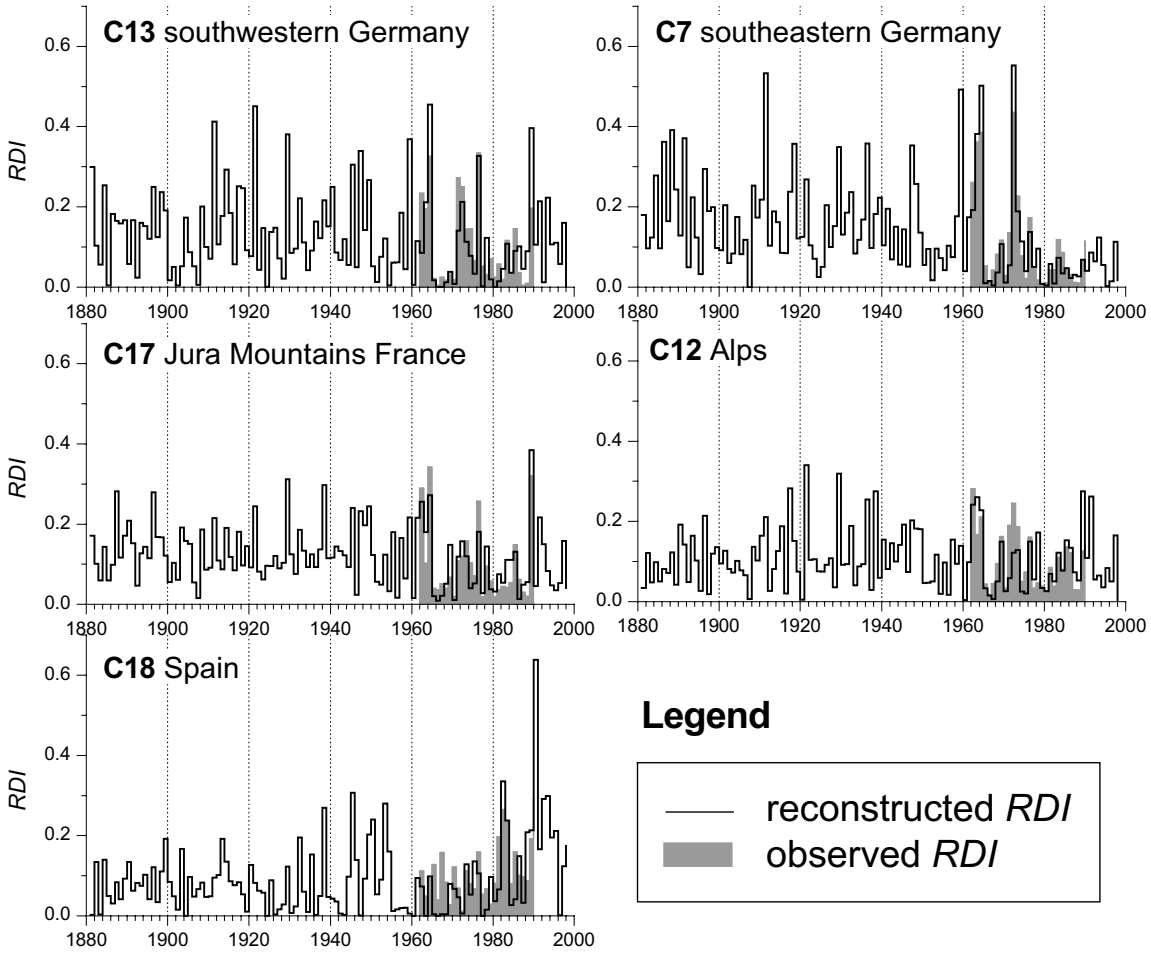

Fig. 8.1 *Reconstructed historic RDI series for the 19 European clusters (continued)*

Scandinavia (C4) show a change from a higher interannual variability in the beginning of the period to less but more severe events during the last 40 years. Less pronounced and not necessarily associated with larger events, this persistency change also occurred in southern UK (C2 and C3) and in southern Germany (C7, C13).

Even in the 110 years reconstructed series, the 1976 drought is still the largest event in many clusters (e.g. southern Scandinavia (C4), southeastern Germany (C7), and the northern half of Germany with C8, C9, C10), closely followed by a high peak in 1959, an event which affected all European clusters except Spain. Due to the lack of long hydrological series, a direct validation of the reconstructed series is not possible, but a comparison with documented historic events is partly feasible and reveals interesting information.

The reconstructed historic *RDI* series show a peak in 1921 in most clusters (Figure 8.1). The event is among the largest in the southern UK clusters (C2, C3), in southern Germany (C13, C7) and in the Alps (C12). A drought in 1921, which caused a great famine in eastern Europe, is documented in the OFDA/CRED disaster database (OFDA/CRED, 2001). Furthermore,

Santos et al. (2000) assigned a 100-year return period to the severity of a meteorological drought event, which occurred in 1921 in central Europe. The 1921 event was also ranked the most spatially extended summer drought event in a study by Briffa et al. (1994), who analysed summer moisture variability across Europe based on Palmer Drought Severity Indices from 1892-1991. This study is well suited for comparison, as their region delineation shows similarities with some of the 19 clusters. In fact, the 'northwestern European region' in Briffa et al. (1994) covers the UK (C1, C2, C3), southern Scandinavia (C4) and the northern part of Germany (C8, C9, C10). Besides the 1921 event in this region, the large events in 1929, 1945, 1938, 1947 and 1959 appear in both studies.

A very good agreement can further be found between the reconstructed historic *RDI* series for Spain (C18) and the northwest mediterranean region in Briffa et al. (1994). Most events correspond very well, in particular the peaks in the 1940s and 1950s (e.g. 1938, 1945, 1949/50, 1953). For the severity and covered area of the events in 1949/50 and 1953/54, Santos et al. (2000) obtained high return periods in a frequency analysis of areal meteorological drought.

Finally, the most recent period from 1991 to 1998, for which streamflow data was not available for all the stations in the clusters, should be mentioned. The most severe drought period in Spain (C18) lasting from 1990 to 1995 (Bradford, 2000, Álvarez & Estrela, 2000) was well reproduced by the model (Figure 8.1). In 1992, a severe drought caused crop losses in northeastern Germany (Bradford, 2000, Gierk & Jungfer, 1992). The event is well reproduced in the northern German clusters (C8, C9, C10) as one of the highest *RDI* peaks in the series. Southern UK and Scandinavia (C2, C3, C4) and the southeast of central Europe (C5, C15) were also affected.

8.3.2 Implications for climate change impact assessment

The reconstructed *RDI* series now cover the same period as the synoptic meteorological information, which is the basis of many climate change studies. However, a comparison with the documented changes in CP frequencies (Chapter 8.2.2) is difficult because climate change studies mostly consider series, which were smoothed over decades. Extreme streamflow events occur at considerably shorter time scales. Short severe events are even difficult to detect in annual parameters, but the comparison with historic droughts documented in the literature presented in the previous section proves that the peaks in the annual *RDI* series are a reliable estimator for exceptional large-scale drought events in Europe.

Despite the different time resolutions, some features in the reconstructed series may be related to observed changes in CP series summarised in Chapter 8.2.2. For instance, the observed variability pattern with a change to lower frequency fluctuations in the long *RDI* series might be a result of the increased persistency of certain circulation patterns since the mid-sixties (Klaus, 1993). A longer persistency in the CP sequences will most likely cause longer wet periods and longer dry periods. In southern Scandinavia (C4) and northern Ger-

many (C8, C9, C10), the fewer but more severe *RDI* peaks in the last three decades of the 20th century suggest an impact of this variability change on streamflow drought.

The increase of the west cyclonic CP (Wz) during wintertime is a result of the discussed changes towards higher NAOI phases. As the CP Wz was shown to have a strong negative frequency anomaly during streamflow deficiency in most clusters, the slightly negative trend of the average *RDI* level in northern Britain (C1) and less pronounced in southwestern UK (C3) might be a response to this change. Similarly, the drier conditions across Spain, which were also well reproduced by the reconstruction experiment, originate from the same driving force: high winter NAOI phases are associated with dry winter conditions in Spain, because the cyclones from the frontal zone move into Europe farther to the north.

8.4 Prediction of changes in regional streamflow deficiencies

8.4.1 Scenario of changed circulation pattern frequencies

Another possible application of the CP-*RDI* link model (Chapter 7) is the prediction of *RDI* series for assumed climate change scenarios. To create a scenario for this application, the assumed CP changes have to be expressed as a time series of CP occurrence, as this is the required input to the model. The occurrences, persistency, and transitions of CP sequences depend on complex continental-scale atmospheric circulation mechanisms and the generation of arbitrary climate change scenario CP-series would consequently require a complex model beyond the scope of this study. However, by modifying the existing CP-series of the reference period Period 1 (1962-90), a pragmatic method for scenario generation was found (Hassler, 2001). To actually generate the scenario series, CP types were chosen, for which the frequency and persistency during the reference period were increased by adding days to existing runs of the chosen CP in the time series. In a second step, days of the CP types chosen to be reduced were removed from existing runs. Hence, the new scenario series consists of the same sequences of CP runs as the reference period, but with increased and respectively decreased durations (and thus frequencies) of the chosen CP types.

The basic approach was to change the frequencies of CPs, which in their historic time series exhibit significant trends or changes that have been attributed to climate change (Chapter 8.2.2). As many studies have argued about the extraordinary conditions observed since the 1980s representing the beginning of climatic change due to increased greenhouse gas forcing, the scenario was based on the main CP characteristics of these two decades. Wintertime occurrence of the west cyclonic CP Wz was increased by 5.6% while meridional circulation with blocking continental high pressure patterns (HFa, HFz, etc.) was decreased

(Bardossy & Caspary, 1990, Gerstengarbe & Werner, 1999). Furthermore, the CPs with southern airflow were increased by 20% over the whole year, while the CPs with northern airflow were decreased. The amount of increase was roughly adjusted to the change rates observed by Klaus (1993) (Chapter 8.2.2). The modifications carried out on the CP series of the reference period (chosen CPs and the number of changed days) to create the 29-year long CP scenario period are summarised in Table 8.1.

Table 8.1 *Modifications on the CP series of the reference period for scenario creation*

Season	Increased CP	Decreased CP	Number of changed days
winter	Wz	HFa, HFz, HNFa, HNFz, SEa, SEz	200
whole year	SWa	HB	60
	SWz	TRM	80
	BM	HNa, HNz, HM	200
	SEa	NEz	35
	SEz	NEa	30
	Sa	NWa	35
	Sz	Na	20
	TB	Nz	46
	TRW	NWz	100

8.4.2 Results and discussion

The *RDI* series predicted by the scenario are best assessed by a comparison with the simulated *RDI* of the reference period, because the climate change fingerprint was imposed on this period. Figure 8.2 compares the *RDI* of the scenario to the reference series by plotting the changes for each cluster. For most clusters, the mean *RDI* for the scenario is lower than for the reference period (Figure 8.2a). Only for for the Alps (C12) and for Spain (C18), the value has slightly increased towards drier conditions. The strongest decrease occurs in northern Britain (C1) while Germany (C7, C8, C9, C10, C13) and the UK show moderate decreases.

The particular changes in extreme events are compared by the maxima of 3-month and 6-month moving averages of the *RDI* series (Figure 8.2b). For the British clusters, the result again indicates a negative change to less severe events. Only in southeastern UK (C2), has the maximum *RDI* only slightly decreased. In Norway (C19), eastern Germany (C7) and the Czech Republic (C5), the events also decrease. In contrast, southern Scandinavia (C4) and the northern part of Germany (C8, C9, C10) show an increase in their maximum *RDI* values. This change is even more pronounced for the long averaging period. The result that for the scenario conditions, the mean *RDI* can decrease while the maximum *RDI* values increase suggests a strong influence of the change in the durations of CP sequences. A look at the orig-

inal daily predictions shows, that during winter time the events tend to be interrupted due to the increased durations of the West cyclonic (Wz) CP (not shown). However the long dry spells in summer tend to be more persistent due to the increased duration of many CPs.

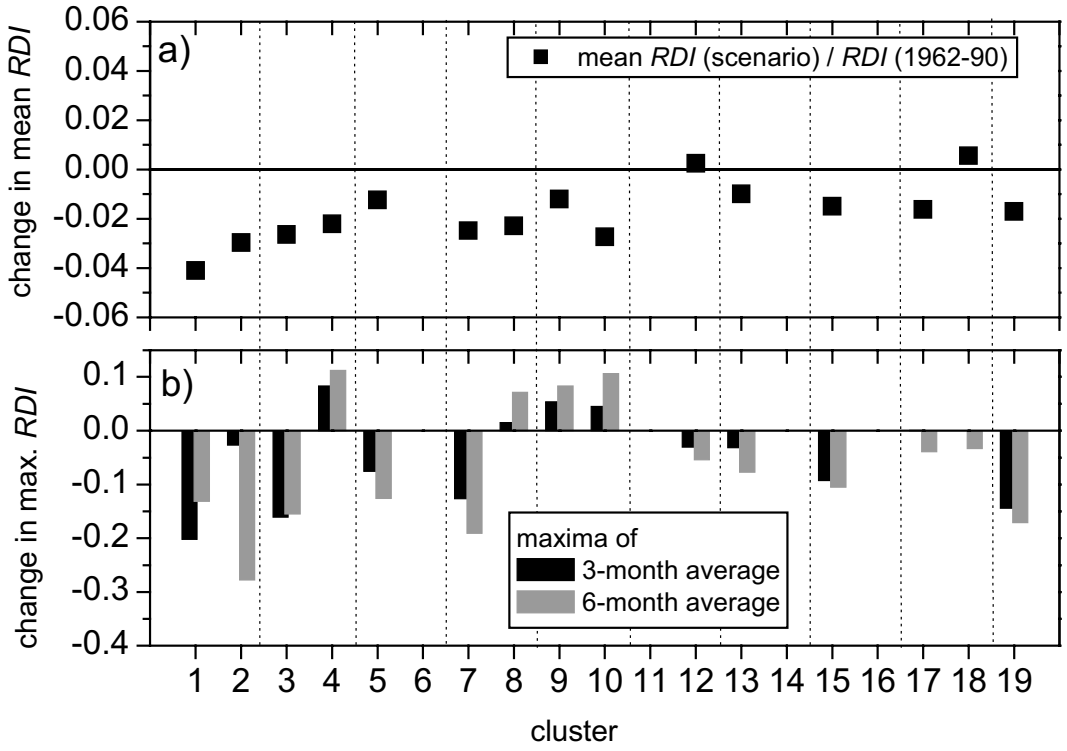

Fig. 8.2 *Results of the scenario - changes compared to the reference period*

Nevertheless, the absolute changes in the mean *RDI* of the whole period are quite small. In fact, a cross-check with the 29-year moving averages over the reconstructed long *RDI* series shows that in the past, most clusters have experienced periods with stronger changes than the change for the scenario period. Only northern UK (C1) has never experienced such a low mean *RDI* as for the scenario, which underpins the strong influence of the west cyclonic CP in northern Europe. The same effect is predicted by many studies for Norway. However, the hydrological response was found to be not as pronounced. In a region with snow dominated regimes, the impact of climate change is certainly more complex. Although through the CP-grouping, the model considers the seasonal differences in the CP influence, an assessment of the inter-seasonal influences is not possible, as the model does not include long term memory. However, climate change studies in Europe show the largest influence in winter. Therefore, for further applications the inclusion of a possible longer memory in the model approach should be considered.

The CP changes included into the scenario only cover a small part of the changes commonly associated to climate change. The results for the scenario period are therefore highly tentative. Future applications could consider a thorough assessment of the uncertainties of the pre-

dictions running several replicates of a certain climate change scenario, and further possible scenarios. Nevertheless, the experiment shows a sensitivity of the drought events to changes in CP occurrence, which shows a potential for an improved assessment of climate changes on drought impact.

8.5 Conclusion

In this chapter, two applications of the model linking CP occurrence to regional streamflow deficiency indices were presented: the reconstruction of historic *RDI* series since 1881 and the prediction of *RDI* changes in response to a given scenario of changed circulation pattern frequencies. Both applications were designed to evaluate the potential of the CP-*RDI* link to assess the impact of climate change on drought across Europe.

The reconstruction of the historic *RDI* series yields good results. A validation using documented historic drought records and analyses of long meteorological drought series in the literature revealed, that in particular severe drought events are well reproduced by peaks of the simulated mean annual *RDI*. Despite the different averaging intervals of all the different studies, some major features reported from observational climate change studies are reflected in the reconstructed streamflow deficiency series. The increasing persistency of most CPs in the last decades of the 20th century is reflected in a variability shift in the *RDI* series, particularly in central Europe. For some of the clusters fewer but more severe *RDI* peaks in the last three decades of the 20th century suggest an impact of this change on streamflow deficiency and thus on drought. The wetter conditions recently observed in northern Europe and commonly attributed to increased zonal circulation are reflected in a slight trend of the mean *RDI* level in northern and western UK. The drier conditions across Spain, which were also well reproduced by the reconstruction experiment, originate from the same atmospheric driving force: dry winter conditions in Spain occur when cyclones from the frontal zone move into Europe too far north during high NAOI phases.

These widely discussed atmospheric climate change indicators were then implemented into a scenario with increased duration and frequency of the West cyclonic CP (Wz). Additionally, the observed compensating trends of increasing southern CPs and decreasing northern CPs were implemented. The results indicate generally wetter conditions across most of Europe except Spain, but increasing regional streamflow deficiency peaks for southern Scandinavia and northern Germany. Although the ideas for scenario creation were obtained from very likely changes, extrapolating trends is a problematic approach to independently investigate climate change impact. Slonosky et al. (2001) for instance showed instationarities in the relationship of long series of atmospoheric circulation to temperature across Europe at the timescale of a few decades. They conclude that care should be taken extrapolating current rela-

tionships for future climate predictions based on downscaling or paleoclimatic reconstruction.

However, the main aim of the experiment was to test the model for the potential of such applications. The experiments served the analysis of the sensitivity of drought to short-term fluctuations in the atmospheric system. In fact, the shown sensitivity of the regional hydrologic response suggests a high potential for further applications and allows a first tentative regional assessment of the impact of climate change on drought across Europe.

9 Conclusion on Drought across Europe

9.1 Assessment of the drought impact in Europe

Covering different aspects of streamflow deficiencies and droughts, the presented study elucidates the regional impact of these hazards across Europe. With the availability of a large streamflow database, the varying threshold level approach could be elaborated to obtain a dataset of parameters indicating extreme dry periods comparable across Europe's range of climatic regions and hydrological regimes. The final assessment of the impact of drought in Europe can be based on three levels covered by this study (Figure 9.1): a general regional vulnerability can be derived from the results of the most detailed investigations of space-time characteristics of streamflow deficits. These were carried out for the *reference period* 1962-90. With the shown strong link to atmospheric circulation patterns, it was further possible to reconstruct historic regional drought series with the CP-*RDI* link model. The long *reconstructed period* since 1881 has great value for clarifying the representativeness of the vulnerability determined from the shorter reference period. Finally, a further modification of this assessment for a future drought impact can be based on the response to a *climate change scenario* together with information from the climate change literature.

The basic assessment of a general regional vulnerability to drought can be made using typical space-time characteristics of extreme droughts determined throughout the study. A rough indicator is the typical space-time persistency behaviour of dry spells. A tendency for long spatially extended events was found for regions covering southeastern UK, southern Scandinavia and northern Germany. There are indications from literature that the same behaviour extends into northern France and eastern Europe, but the scarce or short streamflow records prevented further analysis. These regions are governed by rainfed streamflow regimes with a high inter-annual variability and their behaviour can be ranked as highly vulnerable, because drought flows tend to persist and do not easily recover once they fell below a certain level. On the other hand, regions have been characterised which tend to experience only very short events, as noted for northern Britain, which is exposed to north Atlantic cyclonic activity, and snow influenced mountainous regimes in the Alps, Slovakia, and northern Austria. A transition with some quite long also spatially homogeneous events that last more than a few weeks

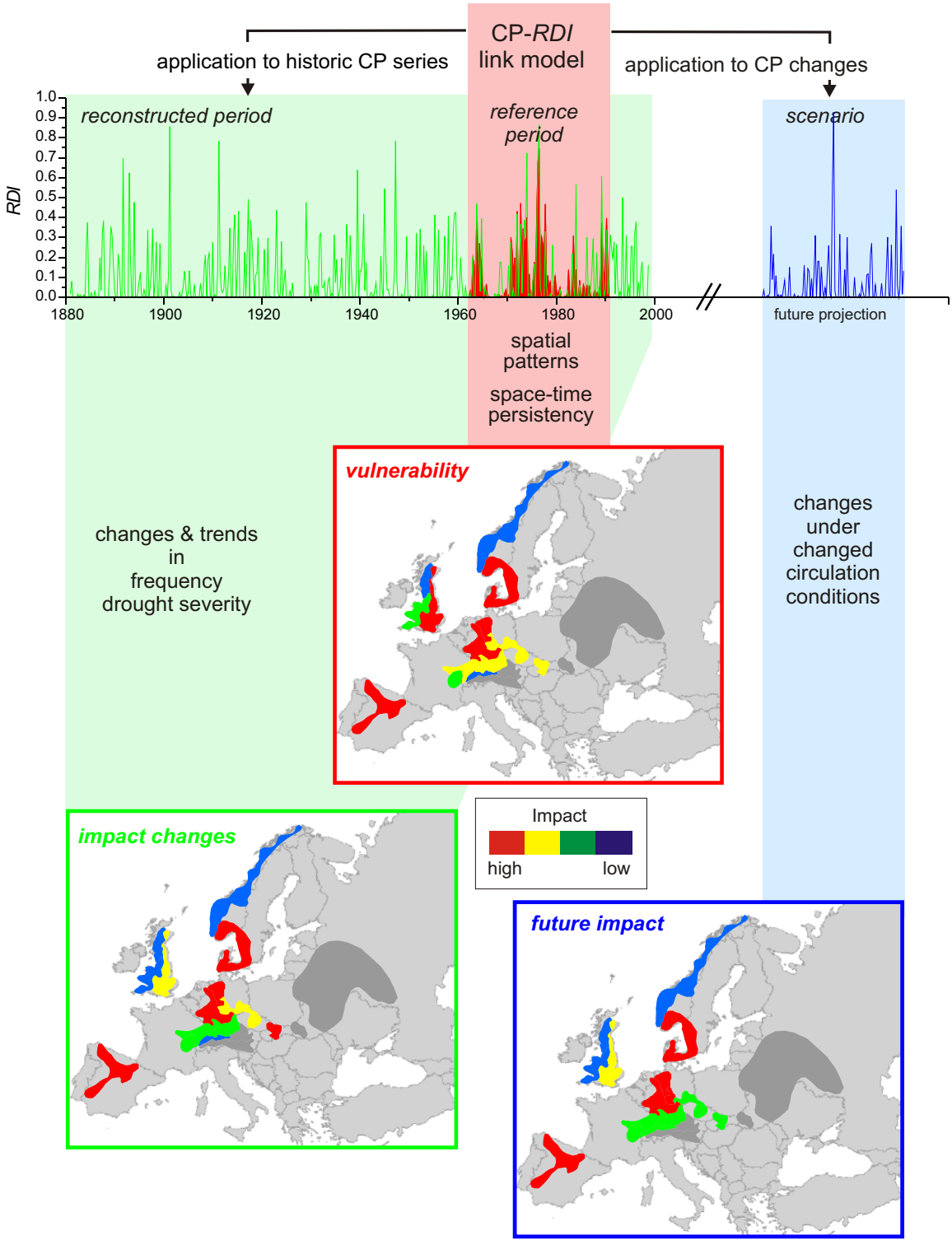

Fig. 9.1 *Scheme for three levels of drought impact assessment*

are found in southwestern UK and a region from southern Germany into the Czech Republic. Here mountain regimes with a high seasonal variability as well as regimes with a higher inter-annual persistence can be found. The investigation for Norway and Spain both suffered from the classification of all their stations into one region, due to scarce data compared to central Europe and strongly differing occurrence times of streamflow deficiencies. The considered part of Spain certainly tends to longer events, which are here more due to the climatic conditions than to the hydrogeological conditions. Norway includes regimes with different degrees of snow influence but dry periods seem to be rather fluctuating.

With the determination of a model linking drought to atmospheric circulation patterns, long series were reconstructed that allow to confirm or reject the vulnerability assessment by characteristics of the time series. Increasing drought conditions in Spain towards the end of the 20th century indicate an aggravation of the impact. The common opinion that the atmospheric processes of the last two centuries indicate the conditions in a changed, warmer climate further underline this appraisal. Another trend was found for Slovakia. Also related to a change in the variability of atmospheric circulation is the tendency for some regions as northern Germany and southern Scandinavia towards infrequent but longer dry periods. In southeastern UK, large droughts were also found in the historic series, and for southwestern UK, even a decrease of the dry periods was determined. All these findings are based on visual inspection of the reconstructed series, partly supported by the trend analysis of the shorter period (Hisdal et al,. 2001a). Although the comparison with documented historic events give great confidence in the reconstructed series their reliability for statistical trend or frequency analyses must first be evaluated in more detail.

The same methodological constraints apply to the prediction of a scenario of changed circulation pattern frequencies and persistencies. Motivated by a number of climate change studies predicting a continuation of the enhanced zonal circulation over Europe during winter time and trends of increasing southern flow circulation patterns compared to decreasing northern flow circulation patterns, the scenario was generated accordingly. The response across Europe is basically in line with the assessment from the historic series. Less dry conditions were predicted for most regions except Spain. However, for southern Scandinavia and northern Germany despite the generally less dry conditions, an increase in the extreme drought peaks was predicted, which adds some uncertainty to the regional impact pattern. As for most climate change impact studies in the literature, signals are most lucid in northern Britain and Spain. For other European regions the atmospheric signal is modified depending on regional scale topography, catchment properties and the regime characteristics.

The study on streamflow deficiency and drought and thus the assessment of the impact of drought solely considered natural conditions. A global definition of vulnerability however should include more aspects than just the natural space-time drought characteristics. Nevertheless, the comparison with documented drought records suggest that in the regions which have been identified as vulnerable due their tendency to persistent dry spells, large historic events as discussed throughout the study affected not only the environment but also many

aspects of water resources. The Intergovernmental Panel on Climate Change warns that changes in precipitation patterns, particularly over regions that already are sensitive (e.g., the Mediterranean basin), may lead to increased demand for water for irrigation purposes, especially for soils with low water-storage capacities (IPCC, 2001). They further mention that despite projected wetter winters, drier summers and increased evaporation may cause a deterioration of groundwater reservoirs in regions with heavy withdrawals such as the Netherlands and southeastern England. Scenarios with a global hydrological model, which takes into account water use, predict water stress in 2025 for southern Spain, southeastern UK, the Netherlands and northeastern Germany into Poland (Alcamo et al., 2000). These are about the same regions found to be vulnerable for drought in the results of this study.

It can be concluded that there is a considerable impact of drought on several regions in Europe. In addition to the natural hazard, increasing water demand and thus withdrawal will aggravate this impact. Consequently, further research should be directed towards a better understanding in particular of the interaction of seasonal changes in order to elaborate adequate strategies to prevent and mitigate undesirable effects.

9.2 Prospects for drought management in Europe

Finally, the question arises how the improved knowledge on large scale characteristics and atmospheric driving forces can contribute to drought management, particularly in regions identified as vulnerable. Wilhite (2000) strongly stresses the need to move from crisis to risk management. Important components of an active risk management are drought prediction and forecasting. *Forecasting* herein relates to a specific time in future and is important for warning and short-term preventive actions. *Prediction* relates to mean statistical characteristics of drought sometime in the future such as recurrence intervals, changes under different climatic conditions, etc. Hence, improved prediction allows to plan and prepare for drought on the long range.

The presented study addresses the important topic of *prediction* and *forecast* in the chapters dealing with the link to atmospheric circulation. A model linking drought to CPs can serve both applications. The lead time for forecasting will depend on the derivation of probable circulation pattern sequences from the medium range weather forecast. Such an application could also run several short-range to medium-range scenarios to assess the possible drought development. However, some improvements of the model, particularly relating to a better seasonal forecast should be considered by introducing a longer memory into the link function and by using additional predictors such as the NAOI or sea surface temperatures.

A simple example of a prediction of the regional streamflow deficiency index distribution was demonstrated in this study by applying changes of circulation pattern frequencies to the observed series and running the CP-*RDI* link model with the changed conditions. To obtain

estimates including uncertainties for the response to such scenariosr, the generation of independent CP scenarios should be considered in a future application. Replicates using Monte Carlo simulations will further improve such an application, which will then be very valuable for planning purposes and for the assessment of future changes.

Currently, operational drought forecasting and prediction is best implemented by continuous drought monitoring and early warning techniques. The US National Drought Mitigation Center (NDMC), for instance, issues a weekly drought monitor, which is a map showing current drought conditions as an index derived from different climatological and hydrological data (NDMC, 2001). For Europe, CEH Wallingford presented a pilot monitoring application elaborated in the framework of the ARIDE project (Rees & Gustard, 2001). This data visualisation system, which displays real-time conditions and historic series for the World Wide Web, could be the core of a European Drought Watch System as outlined by Demuth & Stahl (2001). Unfortunately, the implementation of such a system at the European scale is complicated by political restrictions concerning data provision in many countries (Rees & Gustard, 2001). The CP-*RDI* link model will even gain in performance, if near-real-time data is continuously assimilated to adjust the current conditions. Furthermore, the good performance of the model with a calibration period of only 17 years, suggest a test with a shorter period than the reference series, which would considerably improve the spatial coverage of the analysis across Europe. A medium-range forecast of the regional drought conditions based on the relationship to atmospheric circulation patterns will be a great improvement to drought management and a valuable accomplishment to the proposed drought analysis and public information system for Europe.

References

Abbaspour, K. C., van Genuchten, M. T. , Schulin, R. & Schläppi, E (1997) A sequential uncertainty domain inverse procedure for estimating subsurface flow and transport parameters. Water Resources Research, 33: 1897-1892.

Adler, M.-J., Busuioc, A., Ghioca, M. (1999) Atmospheric processes leading to droughty periods in Romania. In: L. Gottschalk, J.-C. Olivry, D. Reed, D. Rosbjerg (Eds). Hydrological Extremes: Understanding, Predicting, Mitigating. IAHS Publication no. 255: 29-35.

Ager, D. V. (1980) The Geology of Europe. McGraw Hill. London. 535pp.

Alcamo, J., Henrichs, T. & Rösch, T. (2000) World Water in 2025 - Global modeling and scenario analysis for the World Commission on Water for the 21st Century. Report A0002. Center for Environmental Systems Research, University of Kassel. Germany.

Aldenderfer, M.S. & Blashfield, R. K. (1984) Cluster analysis. Quantitative applications in the social sciences. 87pp. Sage Publications. Newbury Park.

Álvarez, J. & Estrela, T. (2000) Regionalization and drought characterisation in Europe. ARIDE Tech. Report no. 9. CEDEX, Madrid, Spain.

Arnell, N.W., Krasovskaia, I. & Gottschalk, L. (1993) River flow regimes in Europe. In: Flow Regimes from International Network Data (FRIEND). Volume I - Hydrological Studies. Institue of Hydrology. Wallingford. UK.

Arnell, N.W. & Reynard, N.S. (1996) The effects of climate change due to global warming on river flows in Great Britain. Journal of Hydrology, 183: 397-424.

Arnell, N.W. (1992) Factors controlling the effects of climate change on river flow regimes in a humid temperate environment. Journal of Hydrology, 132: 321-342.

Arnell, N.W. (1994) Variations over time in European hydrological behaviour: a spatial perspective. In: FRIEND: Flow Regimes from International Experimental and Network Data (ed. by P. Seuna, A. Gustard, N.W. Arnell & G.A. Cole), 179-184. IAHS Publ. no. 221.

Arpe, K. & Roecker, E. (1999) Simulation of the hydrological cycle over Europe: Model validation and impacts of increasing greenhouse gases. Advances in Water Resources, 23: 105-119.

Bardossy, A. & Caspary, H. (1990) Detection of climate change in Europe by analysing European circulation patterns from 1881 to 1989. Theor. Appl. Climat., 42: 155-167.

Bardossy, A. & Plate, E.J. (1992) Time-space model for daily rainfall using atmospheric circulation patterns. Water Resources Research, 28: 1247-1259.

Baur, F., Hess, P., Nagel, H. (1944) Kalender der Großwetterlagen Europas 1881-1939. Bad Homburg v. d. H.

Beran, M. & Rodier, J.A. (1985) Hydrological aspects of drought. Studies and reports in hydrology, 39. UNESCO-WMO, Paris, France.

Bogardi, I., Matyasovszky, I., Bardossy, A., Duckstein, L. (1994): A hydroclimatological model of areal drought. Journal of Hydrology,153: 245-264.

Bradford, R.B. (2000) Drought events in Europe. In: Drought and Drought Mitigation in Europe (ed. by J.V. Vogt & F. Somma), 7-20. Kluwer Academic Publishers, Dordrecht, The Netherlands.

Briffa, K.R., Jones, P.D., Hulme, M. (1994) Summer moisture variability across Europe, 1892-1991: An analysis based on the Palmer Drought Severity Index. International Journal of Climatology, 14, 475-506.

Cappel, A. (1975) Die Großwetterlagen in extremen Naß- und Trockenmonaten. Meteorologische Rundschau, 28: 71-82.

CEH (2001) Centre for Ecology and Hydrology, Walllingford. FRIEND. An International Collaborative Study in Regional Hydrology. http://www.nwl.ac.uk/ih/www/research/mfriend.html

Chiew, F. H. S., Piechota, T. C., Dracup, J.A., McMahon, T.A. (1998) El Nino/Southern Oscillation and Australian rainfall, streamflow and drought: Links and potential for forecasting.

CRU (2001) http://www.cru.uea.ac.uk.

Demuth S., & Heinrich, B. (1997) Temporal and spatial behaviour of drought in south Germany. In: FRIEND'97 - Regional Hydrology. Concepts and Models for Sustainable Water Resources Management (ed. by Gustard A., Blazkova, S., Brilly, M., Demuth, S., Dixon, J., Van Lanen, H., Llasat, C., Mkhandi, S., Servat, E.), 151-157. IAHS Publ. no. 246.

Demuth, S. & Stahl, K. (Eds) (2001) ARIDE - Assessment of the Regional Impact of Droughts in Europe. Final Report to the European Commission. Freiburg, Germany, 170 pp.

Demuth, S. (1993) Untersuchungen zum Niedrigwasser in West-Europa. Freiburger Schriften zur Hydrologie. B 1. Professur für Hydrologie an der Universität Freiburg i. Br., Germany.

Demuth, S., Lehner, B., Stahl, K. (2000) Assessment of the vulnerability of a river system to drought. In: Drought and Drought Mitigation in Europe (ed. by J.V. Vogt & F. Somma), 209-219. Kluwer Academic Publishers, Dordrecht, The Netherlands.

Dracup, J.A. & Kahya, E. (1994) The relationship between U.S. streamflow and La Niña events. Water Resources Research, 30: 2133-2141.

Dracup, J.A., Lee, K.S. & Paulson, E.G. Jr. (1980) On the definition of droughts. Water Resources Research, 16(2), 297-302.

Duckstein, L., Bardossy, A. & Bogardi, I. (1993): Linkage between the occurence of daily atmospheric circulation patterns and floods: an Arizona case study. Journal of Hydrology, 143: 413-428.

DVWK (Deutscher Verband für Wasserwirtschaft und Kulturbau e. V.) (1998) How to work out a drought mitigation strategy. Guidelines for water management 309/1998. An ICID (Int. Commission on Irrigation and Drainage) Guide. Bonn, Germany.

EC - European Commission - Environment Water Task Force (1998) Freshwater. A Challenge for Research and Innovation. A Concerted European Response, European Communities, July 1998, EUR 18098 EN.

EEA (1999) Sustainable Water Use in Europe – Part 1: Sectoral Use of Water. Environmental assessment report No 1. European Environment Agency. Copenhagen.

Gerstengarbe, F.-W. & Werner, P.C. (1999) Katalog der Großwetterlagen Europas nach Paul Hess und Helmuth Brezowsky 1881-1998. 5. verbesserte und ergänzte Auflage. Potsdam, Offenbach a. M., Germany.

Gierk, M. & Jungfer, E. (1992) Das Trockenjahr 1992 im Land Brandenburg. Studien- und Tagungsberichte Band 3, Landesumweltamt Brandenburg, 1-23.

Good P. (1994) Permutation Tests, A Practical Guide to Resampling Methods for Testing Hypothesis. Springer-Verlag. New York.

Greatbatch, R.J. (2000) The North Atlantic Oscillation. Stochastic Environmental Research and Risk Assessment 14, 213-242.

Gustard & Irving (1993) Classification of the low flow response of European soils. In: Gustard, A. (ed.) (1993) Flow Regimes from International Experimental and Network Data (FRIEND). Institute of Hydrology, Wallingford, Oxfordshire, UK.

Gustard, A., Bullock, A. & Dixon, J.M. (1992) Low Flow Estimation in the United Kingdom. Report no. 108. Institute of Hydrology, Wallingford, UK.

Gustard, A., Rees, H.G., Croker, K.M. & Dixon, A. R. (1997). Using regional hydrology for assessing European water resources. In: FRIEND'97-Regional Hydrology: Concepts and Models for Sustainable Water Resource Management (ed. by A. Gustard, S. Blazkova, M. Brilly, S. Demuth, J. Dixon, H. van Lanen, C. Llasat, S. Mkhandi & E. Servat), 107-115. IAHS Publ. no. 246.

Hassler, B. (2001). Der Einfluss von Klimavariabilitäten auf hydrologische Dürre in Europa - Szenarien. Diplomarbeit. Institut für Hydrologie. Albert-Ludwigs-Universität Freiburg. (unpublished thesis)

Hess, P., Brezowsky, H. (1977) Katalog der Großwetterlagen Europas 1881-1976. 3. verbesserte und ergänzte Aufl.. Ber. Dt. Wetterd. 15 (113).

Hisdal, H. & Tallaksen, L.M. (eds.) (2000) Drought event definition. ARIDE Tech. Report no. 6. University of Oslo, Oslo, Norway.

Hisdal, H., Stahl, K., Tallaksen, L.M. & Demuth, S. (2001a) Have streamflow droughts in Europe become more severe or frequent? International Journal of Climatology, 21:317-333.

Hisdal, H., Stahl, K., Tallaksen, L.M. & Demuth, S. (2001b) Initial time series analyses. In: Demuth, S. & Stahl, K. (eds) (2001) ARIDE - Final Report to the European Union. Institute of Hydrology. Freiburg. Germany.

Hurrel, J.W. & van Loon, H. (1997) Decadal variations in climate associated with the North Atlantic Oscillation. Climate Change, 36: 301-326.

Hurrel, J.W. (1995) Decadal trends in the North Atlantic Oscillation: Regional temeratures and precipitation. Sience, 269: 676-679.

IPCC (2001) Climate Change 2001: Impacts, Adaptation, and Vulnerability. A report of the working group II of the Intergovernmental Panal on Climate change.

Jones, P. (1998) It was the best of times, it was the worst of times. Science 280: 544-545.

Klaus, D. (1993) Zirkulations- und Persistenzänderungen des Europäischen Wettergeschehens im Spiegel der Grosswetterlagenstatistik. Erdkunde, 47: 85-104

Krasovskaia, I., Arnell, N.W., Gottschalk, L. (1994) Flow regimes in northern and western Europe: development and application of the procedures for classifying flow regimes. In: FRIEND: Flow Regimes from International Experimental and Network Data (ed. by P. Seuna, A. Gustard, N.W. Arnell & G.A. Cole), 179-184. IAHS Publ. no. 221.

Lamb, H.H. (1972) British Isles Weather types and a register of daily sequence of circulation patterns, 1861-1971. Geophysical Memoir 116, HMSO, London, 85pp.

Lanen, H.A.J. van & Peters, E. (2000) Definition, effects and assessment of groundwater droughts. In: Drought and Drought Mitigation in Europe (ed. by J.V. Vogt & F. Somma), 49-61. Kluwer Academic Publishers, Dordrecht, the Netherlands.

Maheras, P. (2000) Synoptic situations causing drought in the mediterranean basin. In: Vogt, J.V. & Somma, F. (eds.) (2000) Drought and drought mitigation in Europe. Kluwer Academic Publishers, Dordrecht.

Morell, M. (2001) MED-HYCOS. http://medhycos.com.

Murphy, J. (2000) Predictions of climate change over Europe using statistical and dynamical Downscaling techniques. International Journal of Climatology, 20: 489-501.

NDMC (2001) National Drought Mitigation Center. http://enso.unl.edu/ndmc/impacts/compare.htm.

NOAA (2001) Reanalysis Data. http://wesley.wwb.noaa.gov/reanalysis.htm.

Norius M.J. (1995) SPSS for Windows. Professional Statistics. Release 6.1, SPSS Inc. Chicago.

OFDA/CRED (2001) EM-Dat. http://www.cred.be/emdat/intro.html

Odziomek, A. (2000) Visualisation of large-scale droughts in Europe - a multimedia approach. Diplomarbeit. Institut für Hydrologie. Albert-Ludwigs-Universität Freiburg. (unpublished thesis)

Osborn, T. (2000) NAOI. http://www.cru.uea.ac.uk/~timo/projpages/nao_update.htm.

Pardé (1933) Fleuves et rivières. Collins. Paris.

Pesti, G., Shrestha B.P., Duckstein, L., Bogardi, I. (1996) A fuzzy rule-based approach to drought assessment. Water Resources Research, 32: 1741-1747.

Piechota, T.C. & Dracup, J.A. (1996) Drought and regional hydrologic variation in the United States: Associations with the El Niño-Southern Oscillation. Water Resources Research, 32, 1359-1373.

Pongracz, R. Bogardi, I. & Duckstein, L. (1999) Application of fuzzy rule-based modeling technique to regional drought. Journal of Hydrology 224:100–114.

Redmont, K.T. & Koch, R.W. (1991) Surface climate and streamflow variability in the Western United States and their relationship to large-scale circulation indices. Water Resources Research 27: 2381-2399.

Rees, H.G. & Gustard, A. (2001) Near-real-time monitoring of droughts in Europe. In: Demuth, S. & Stahl, K. (eds) (2001) ARIDE - Final Report to the European Union. Institute of Hydrology. Freiburg. Germany.

Rees, H.G., Croker, K. M., Reynard, N. S. & Gustard, A. (1997) Estimation of renewable water resources in the European Union In: FRIEND'97-Regional Hydrology: Concepts and Models for Sustainable Water Resource Management (ed. by A. Gustard, S. Blazkova, M. Brilly, S. Demuth, J. Dixon, H. van Lanen, C. Llasat, S. Mkhandi & E. Servat), 31-38. IAHS Publ. no. 246.

Rees, H.G. & Demuth, S. (2000) The application of modern information system technology in the European FRIEND project. Wasser & Boden, 52(3): 9-13.

Rees, H.G. (2001) Database. In: Demuth, S. & Stahl, K. (eds) (2001) ARIDE - Final Report to the European Union. Institute of Hydrology. Freiburg. Germany.

Rind, D. (2000) Drought, variability, and climate change in the twenty-first century. In: Wilhite, D.A. (ed.) (2000) Drought a global assessment. Volume II. Routledge Hazards and Disasters Series. Routledge, London, UK.

Roald, L.A., Wesselink, A.J., Arnell, N.W., Dixon, J.M., Rees, H.G., Andrews, A.J. (1993) European Water Archive. In: Flow Regimes from International Experimental and Network Data (FRIEND), vol. 1, Gustard A (ed.). Institute of Hydrology: Wallingford: 7–20.

Ropelewski C.F. & Folland, C.K. (2000) Prospects for prediction of meteorological drought. In: Wilhite, D.A. (ed.) (2000) Drought a global assessment. Volume I. Routledge Hazards and Disasters Series. Routledge, London, UK.

Salas, J.D. (1993) Analysis and modelling of hydrologic time series. In: Handbook of Hydrology. (ed. by D.R. Maidment). McGraw-Hill, New York, USA.

Santos, M.J., Veríssimo, R., Fernandes, S., Orlando, M. & Rodrigues, R. (2000) Overview of regional meteorological drought analysis on Western Europe. ARIDE Tech. Report no. 10. INAG, Lisbon , Portugal.

Schmid, R.E. (1998) More wet, dry areas in recent decades. Associated Press (August 20 1998), Washington, USA.

Schönwiese, C. D., Claussen, M., Cubasch, U., Fischer, H., Graßl, H, Rahmstorf, S. u.a. (2001) Stellungnahme zur Klimaänderung. Deutsche Meteorologische Gesellschaft.

Schwarzmaier, G. & Mayer, H. (1992) Regionalization of global runoff data. Meteorol. Zeitschrift, 6: 269-275.

Sen, Z. (1980) Regional drought and flood frequency analysis: Theoretical consideration. Journal of Hydrology, 46: 265-279.

Shorthouse, C.A. & Arnell, N.W. (1997) Spatial and temporal variability in European river flows and the Northern Atlantic Oscillation. In: FRIEND'97-Regional Hydrology: Concepts and Models for Sustainable Water Resource Management (ed. by A. Gustard, S. Blazkova, M. Brilly, S. Demuth, J. Dixon, H. van Lanen, C. Llasat, S. Mkhandi & E. Servat), 77-85. IAHS Publ. no. 246.

Slonosky, V. C., Jones, P.D. & Davies, T.D. (2001) Atmospheric circulation and surface temperature in Europe from the 18th century to 1995. International Journal of Climatology, 21: 63-75.

Stahl, K. & Demuth, S. (1999) Linking streamflow drought to the occurrence of atmospheric circulation patterns. Hydrological Sciences Journal, 44(3), 467-482.

Stahl, K. & Demuth, S. (2001) Atmospheric Circulation and Drought. In: Demuth, S. & Stahl, K. (eds) (2001) ARIDE - Final Report to the European Union. Institute of Hydrology. Freiburg. Germany.

Stahl, K., Demuth, S., Hisdal, H., Tallaksen, L., Santos, M.-J., Verissimo, R. & Rodrigues, R. (2001) The North Atlantic Oscillation and Drought. In: Demuth, S. & Stahl, K. (eds) (2001) ARIDE - Final Report to the European Union. Institute of Hydrology. Freiburg. Germany.

Tallaksen, L. M. & Hisdal, H. (1997) Regional analysis of extreme streamflow drought duration and deficit volume, In: FRIEND'97-Regional Hydrology: Concepts and Models for Sustainable Water Resource Management (ed. by A. Gustard, S. Blazkova, M. Brilly, S. Demuth, J. Dixon, H. van Lanen, C. Llasat, S. Mkhandi & E. Servat), 141-150. IAHS Publ. no. 246.

Tallaksen, L.M., Madsen, H. & Clausen, B. (1997) On the definition and modelling of stream-flow drought duration and deficit volume. Hydrological Sciences Journal, 42(1), 15-33.

Tate, E. & Gustard, A. (2000) Drought definition: a hydrological perspective. In: Drought and Drought Mitigation in Europe (ed. by J.V. Vogt & F. Somma), 23-48. Kluwer Academic Publishers, Dordrecht, The Netherlands.

Ulbrich, U. & Christoph, M. (1999) A shift of the NAO and increasing storm track activity over Europe due to anthropogenic greenhouse gas frocing. Climate Dynamics, 15: 551-559.

USGS (2001) Drought Watch. http://md.water.usgs.gov/drought/us.html

Vogel, R.M. & Fennessey, N.M. (1994) Flow Duration Curves. I: New Interpretation and Confidence Intervals, Journal of Water Resources Planning and Management, 120 (4): 485-504.

Watson, R.T., Zinyowera, M.C. & Moss, R.H. (eds.) (1998) The Regional Impacts of Climate Change: An Assessment of Vulnerability. IPCC, Cambridge University Press, Cambridge, UK.

Weatherald, R.T. & Manabe, S. (1999) Detectability of summer dryness by greenhouse warming. Climatic Change, 43(3): 495-511.

Weischet, W. (1991) Einführung in die allgemeine Klimatologie. Teubner Studienbücher Geographie. Teubner Stuttgart. 275 pp.

Werner, P.C., Gerstengarbe, F.-W., Fraedrich, K. & Oesterle, H. (2000) Recent climate change in the North Atlantic/European Sector. International Journal of Climatology, 20: 463-471.

Wilby, R., Greenfield, B. & Glenny, C. (1994) A coupled synoptic-hydrological model for climate change impact assessment. Journal of Hydrology, 153: 265-290.

Wilby, R.L. (1993) The influence of variable weather patterns on river water quantity and quality regimes. International Journal of Climatology, 13: 447-459.

Wilhite, D.A. & Glantz, M.H. (1985) Understanding the drought phenomenon: The role of definitions. Water International, 10 (3), 111-120.

Wilhite, D.A. (ed.) (2000) Drought a global assessment. Volume I and Volume II. Routledge Hazards and Disasters Series. Routledge, London, UK.

Wilhite, D.A., Hayes, J.M., Knutson, C. & Smith, K.H. (2000) Planning for drought: Moving from crisis to risk management. J. Am. Wat. Res. Assoc., 36: 697-710.

Willmott, C.J. (1981) On the validation of models. Physical Geography, 2:184-194.

WMO (1988) Analyzing long time series of hydrological data with respect to climate variability. TD-No. 224, Geneva, Switzerland.

Yevjevich, V. (1967) An objective approach to definition and investigations of continental hydrologic droughts. Hydrology papers 23. Colorado State University, Fort Collins, USA.

Young, A. R., Round, C.E. & Gustard, A. (2000) Spatial and temporal variations in the occurrence of low flow events in the UK. Hydrology and Earth System Sciences, 4: 35-45.

Zaidman, M.D. & Rees, H.G. (2000) Spatial patterns of streamflow drought in Western Europe 1960-1995. ARIDE Tech. Report no. 8. Centre for Ecology and Hydrology, Wallingford, UK.

Zaidman, M.D., Rees, H.G. & Gustard, A. (2000) An electronic atlas for visualisation of streamflow drought. ARIDE Tech. Report no. 7. Centre for Ecology and Hydrology, Wallingford, UK.

Annex

Seasonal CP frequency anomalies

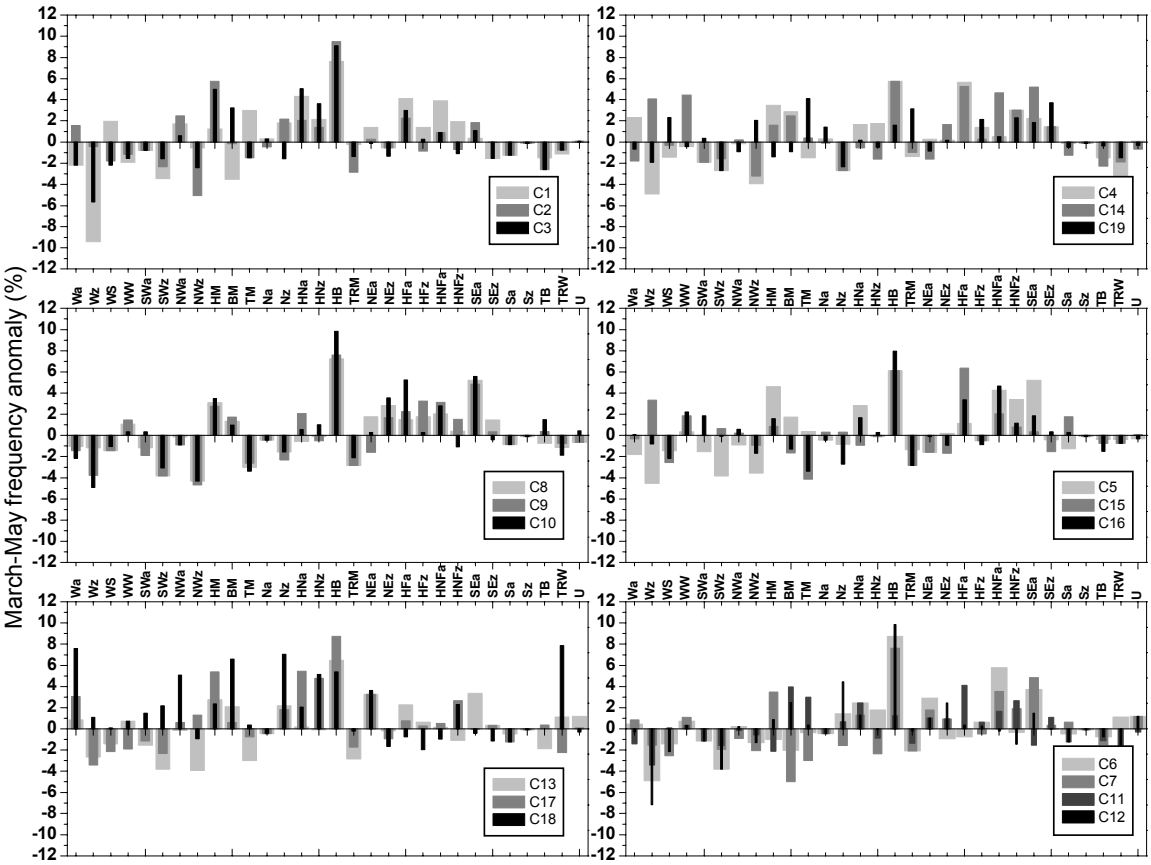

Fig. A.1 *Spring CP frequency anomalies during severe RDI periods*

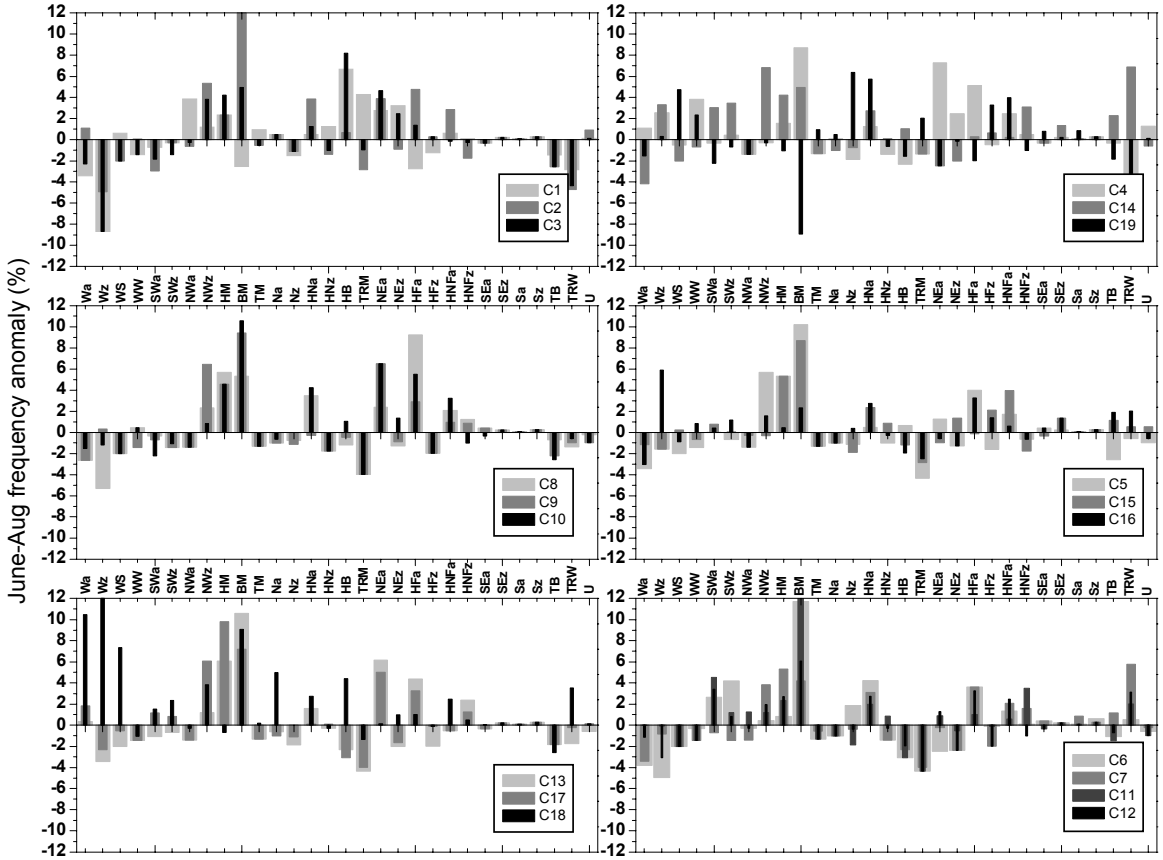

Fig. A.2 *Summer CP frequency anomalies during severe RDI periods*

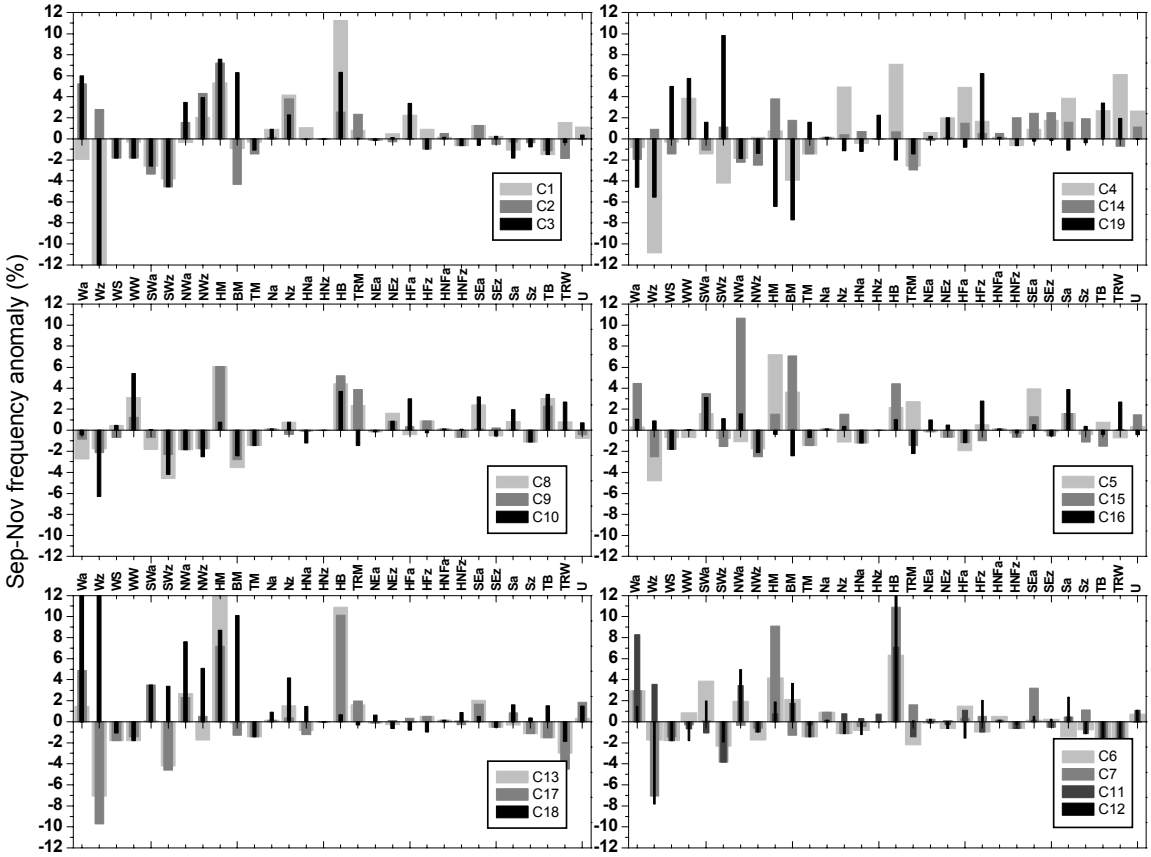

Fig. A.3 *Autumn CP frequency anomalies during severe RDI periods*

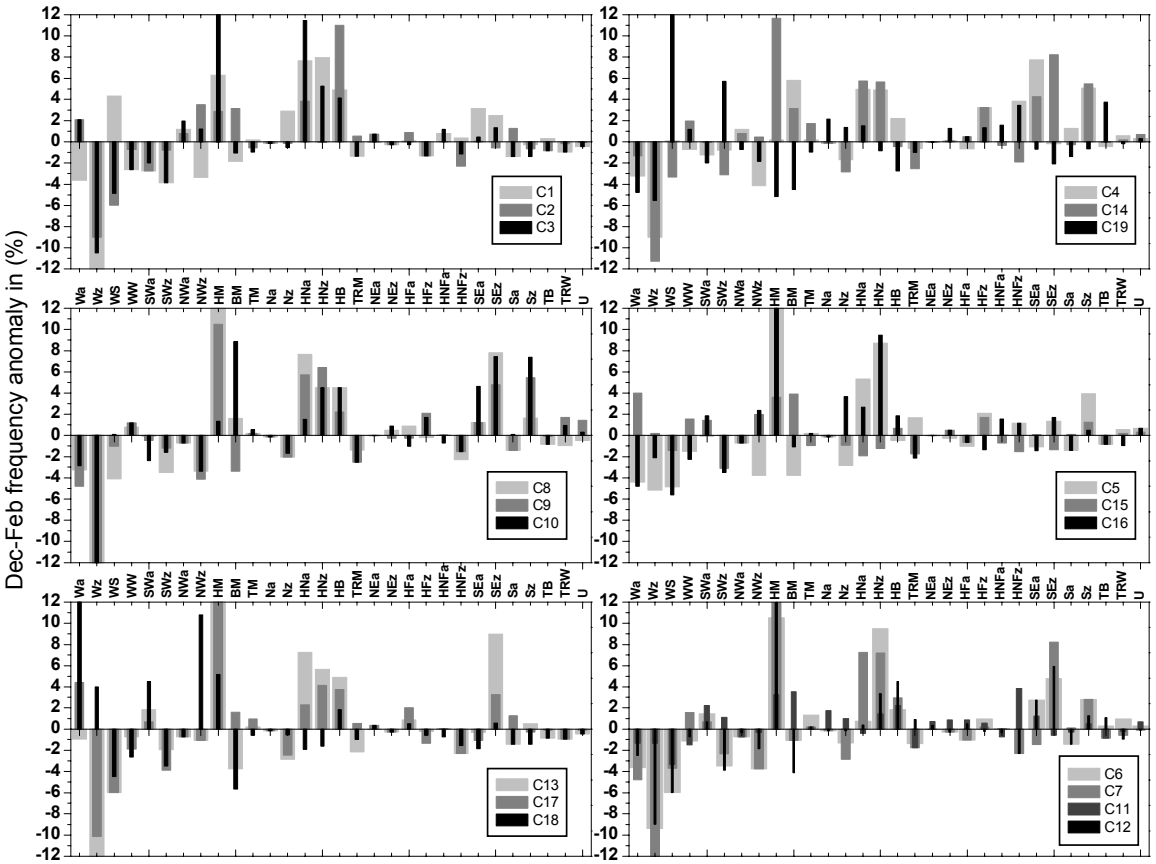

Fig. A.4 *Winter CP frequency anomalies during severe RDI periods*

Seasonal CP groups

Table A.1 *CP groups for spring*

GWL	Cluster																		
	1	**2**	**3**	**4**	**5**	**6**	**7**	**8**	**9**	**10**	**11**	**12**	**13**	**14**	**15**	**16**	**17**	**18**	**19**
Wa	7	4	7	3	6	5	4	6	6	7	6	5	4	6	5	5	3	2	6
Wz	8	5	8	7	7	7	6	6	7	7	7	8	7	3	3	6	7	4	6
WS	4	6	7	6	6	6	7	6	6	6	5	7	6	5	7	7	7	5	3
WW	6	6	6	5	5	4	4	4	4	5	5	5	4	3	4	3	6	4	5
SWa	6	6	6	6	6	6	5	6	6	5	6	6	6	6	5	4	6	4	5
SWz	7	7	6	7	7	7	6	7	7	7	6	7	7	6	4	5	7	3	7
NWa	4	3	4	5	6	5	6	5	6	6	5	5	5	5	5	4	4	2	6
NWz	6	8	7	7	7	6	7	7	7	7	6	6	7	7	6	6	4	6	3
HM	4	2	3	3	3	6	3	3	3	3	7	4	3	4	4	4	2	3	6
BM	7	5	3	3	4	7	8	4	4	4	3	3	3	3	6	6	4	2	6
TM	3	6	6	6	5	5	7	7	7	7	3	5	7	5	7	7	6	5	3
Na	5	5	5	5	5	5	5	5	5	5	5	5	5	5	5	5	5	5	4
Nz	4	3	6	7	6	4	6	6	7	6	4	3	3	7	5	7	4	2	7
HNa	3	3	2	4	3	3	4	6	3	4	3	4	5	6	6	4	2	3	5
HNz	3	4	3	4	5	4	7	5	5	4	6	5	5	6	5	5	3	2	5
HB	2	2	2	2	2	2	2	2	2	2	4	2	2	2	2	2	2	2	4
TRM	5	7	6	6	6	7	7	7	7	7	6	5	7	6	7	7	6	5	3
NEa	4	5	5	5	6	3	4	4	6	5	4	4	3	6	6	5	3	3	6
NEz	6	6	6	5	5	6	4	3	4	3	4	3	5	4	6	6	6	6	5
HFa	3	3	3	2	4	6	5	4	3	2	3	5	3	2	2	3	4	6	5
HFz	4	6	5	4	5	4	5	4	3	5	4	5	4	5	5	6	5	6	3
HNFa	3	4	4	4	3	2	3	3	3	3	4	5	5	3	3	3	4	6	4
HNFz	4	6	6	3	3	5	4	5	4	6	3	6	6	3	4	4	3	3	3
SEa	5	4	4	3	2	3	3	2	3	2	6	4	3	2	5	4	5	5	4
SEZz	6	5	6	4	5	5	5	4	5	5	4	5	5	4	6	5	5	6	3
Sa	6	6	6	5	6	5	4	6	6	6	6	6	5	6	4	5	6	6	5
Sz	5	5	5	5	5	5	5	5	5	5	5	5	5	5	5	5	5	5	5
TB	6	7	7	6	5	6	6	6	5	4	6	6	6	7	6	6	5	5	5
TRW	6	6	6	7	5	4	5	6	6	6	7	6	4	6	6	6	7	2	6
U	5	5	5	5	5	4	4	6	6	5	5	4	4	6	5	5	5	5	5

Table A.2 *CP groups for summer*

GWL	Cluster																		
	1	**2**	**3**	**4**	**5**	**6**	**7**	**8**	**9**	**10**	**11**	**12**	**13**	**14**	**15**	**16**	**17**	**18**	**19**
Wa	7	4	7	4	7	7	7	7	7	6	5	6	5	7	6	7	4	1	6
Wz	8	7	8	3	6	7	6	8	5	6	5	7	7	3	6	2	7	1	5
WS	4	7	7	6	7	7	7	7	7	7	7	7	7	7	5	6	6	2	3
WW	6	5	6	3	6	5	6	5	6	5	6	6	6	6	6	4	6	6	3
SWa	6	7	6	5	5	3	6	5	6	7	3	3	6	3	4	5	4	4	7
SWz	5	5	6	5	6	3	6	6	6	6	4	4	6	3	5	4	4	3	6
NWa	3	6	5	6	6	5	6	6	6	6	4	5	6	6	5	6	6	5	6
NWz	4	2	3	5	2	5	3	3	2	4	4	4	4	2	5	4	2	3	5
HM	3	3	3	4	2	4	2	2	3	3	3	3	2	3	2	5	2	6	6
BM	7	1	3	2	1	1	3	2	2	1	1	2	1	3	2	3	2	2	8
TM	4	6	6	6	6	6	6	6	6	6	6	6	6	6	6	6	6	5	4
Na	5	5	5	5	6	6	6	6	6	6	6	6	6	6	6	6	6	3	5
Nz	6	6	6	6	6	4	5	6	6	5	6	5	6	6	6	5	6	5	2
HNa	5	3	4	4	5	3	3	3	5	3	4	3	4	3	3	3	5	3	2
HNz	4	6	6	6	6	6	6	6	6	6	4	5	5	5	4	5	5	5	6
HB	2	4	2	7	4	7	7	6	5	4	7	6	7	4	6	6	7	3	6
TRM	3	7	6	6	7	7	7	7	7	7	7	7	7	6	7	7	7	6	3
NEa	3	3	3	2	4	7	5	3	2	2	4	4	2	7	6	6	2	5	7
NEz	3	6	3	3	6	7	7	6	6	4	6	7	7	7	4	6	6	4	5
HFa	7	3	4	2	3	3	3	2	3	2	4	3	3	5	5	3	3	4	6
HFz	6	5	5	5	6	5	6	6	6	6	5	6	6	4	3	4	5	5	3
HNFa	4	3	5	3	4	4	3	3	4	3	4	3	6	5	3	4	6	3	3
HNFz	5	6	5	5	6	5	4	4	4	6	3	6	3	3	6	6	4	5	6
SEa	5	5	5	5	5	5	5	5	5	5	5	5	5	5	5	5	5	5	4
SEZz	5	5	5	5	5	5	5	5	5	5	5	5	5	4	4	4	5	5	5
Sa	5	5	5	5	5	5	4	5	5	5	5	5	5	5	5	5	5	5	4
Sz	5	5	5	5	5	4	5	5	5	5	5	5	5	5	5	5	5	5	5
TB	6	7	7	5	7	6	4	6	7	7	6	6	6	3	4	4	6	7	6
TRW	7	7	7	7	6	4	2	6	6	6	3	3	6	2	4	3	5	3	7
U	5	4	5	4	6	6	5	5	6	6	6	6	6	6	4	6	5	5	5

Table A.3 *CP groups for autumn*

GWL	Cluster																		
	1	**2**	**3**	**4**	**5**	**6**	**7**	**8**	**9**	**10**	**11**	**12**	**13**	**14**	**15**	**16**	**17**	**18**	**19**
Wa	6	2	2	6	5	3	3	7	6	5	2	4	4	6	3	4	3	1	7
Wz	9	3	9	9	7	6	8	6	7	8	3	8	8	4	7	4	8	1	8
WS	5	6	6	5	6	6	6	5	6	5	6	6	6	6	6	6	6	6	2
WW	5	6	6	3	6	4	5	3	4	2	6	6	6	5	5	5	6	6	2
SWa	7	7	7	6	4	3	5	6	6	5	6	4	5	6	3	3	3	3	4
SWz	7	7	7	7	6	7	7	7	7	7	7	6	7	4	6	4	7	3	2
NWa	5	4	3	6	6	4	5	6	6	6	3	3	3	7	1	4	3	2	6
NWz	3	3	3	5	6	6	6	6	6	7	6	6	6	7	7	7	4	2	6
HM	2	2	2	4	2	3	2	2	2	4	4	4	1	3	4	5	2	2	8
BM	6	7	2	7	3	3	6	7	7	7	4	3	5	4	2	7	6	1	8
TM	5	6	6	6	6	6	6	6	6	6	5	6	6	6	6	6	6	6	4
Na	4	5	4	5	5	4	4	5	5	5	5	5	5	5	5	5	5	4	5
Nz	3	3	3	3	6	6	6	4	5	4	4	6	4	5	4	5	5	3	6
HNa	4	5	5	5	6	6	5	5	5	6	5	6	6	4	6	6	6	4	6
HNz	5	5	5	5	5	5	5	5	5	5	4	5	5	5	5	5	5	5	3
HB	1	3	2	2	3	2	1	3	2	3	2	1	1	4	3	4	1	4	7
TRM	4	3	5	7	3	7	4	3	3	6	6	5	4	7	6	7	4	5	6
NEa	5	5	5	4	5	5	5	5	5	5	5	5	5	5	5	4	5	4	5
NEz	5	5	5	3	6	6	5	4	4	4	5	6	5	5	6	5	5	6	3
HFa	3	5	3	3	6	4	5	5	5	3	4	6	5	4	6	6	5	6	6
HFz	4	6	6	4	4	6	4	4	4	5	6	3	4	4	6	3	4	6	2
HNFa	5	4	5	5	5	4	5	5	5	5	5	5	5	4	5	5	5	5	5
HNFz	6	6	6	6	5	6	6	6	6	5	6	5	5	3	6	5	5	4	6
SEa	4	4	6	4	3	5	3	3	5	3	5	4	3	3	4	4	4	4	5
SEZz	5	6	5	4	5	5	6	6	5	6	6	5	6	3	6	6	6	6	5
Sa	6	5	6	3	4	6	5	4	5	4	5	3	5	4	4	3	4	4	6
Sz	5	5	6	5	5	6	4	6	6	6	6	6	6	4	6	5	6	5	5
TB	6	6	6	3	4	6	6	3	3	3	6	6	6	5	6	5	6	4	3
TRW	4	6	5	2	6	7	7	4	5	3	7	7	7	6	5	3	7	6	4
U	4	5	5	3	5	4	5	6	5	4	4	4	5	4	4	5	4	4	5

Table A.4 *CP groups for winter*

GWL	Cluster																		
	1	**2**	**3**	**4**	**5**	**6**	**7**	**8**	**9**	**10**	**11**	**12**	**13**	**14**	**15**	**16**	**17**	**18**	**19**
Wa	7	3	3	7	7	7	7	7	7	7	6	7	6	6	3	7	3	1	7
Wz	9	8	9	8	8	8	9	9	9	9	6	8	9	9	5	7	9	3	8
WS	3	8	7	5	7	8	7	7	6	5	7	8	8	7	6	8	8	7	1
WW	7	6	7	6	6	6	4	4	4	4	6	6	6	4	4	7	6	7	4
SWa	7	7	6	6	5	4	4	5	5	7	3	4	4	5	4	4	4	3	6
SWz	7	6	7	6	5	7	7	7	6	6	4	7	6	7	7	7	7	7	2
NWa	4	4	4	4	6	6	6	6	6	6	6	5	6	4	6	6	6	6	6
NWz	7	3	4	7	7	7	7	7	7	7	5	6	6	5	4	3	6	1	6
HM	2	3	1	5	1	1	1	1	1	4	3	1	1	1	3	1	1	2	8
BM	6	3	6	2	7	6	6	4	7	2	3	7	7	3	3	6	4	8	7
TM	5	6	6	5	5	4	5	5	5	4	5	5	5	4	6	5	4	6	6
Na	5	5	5	5	5	5	5	5	5	5	4	5	5	5	5	5	5	5	3
Nz	3	5	6	6	7	6	7	7	7	6	4	5	7	7	6	3	7	6	4
HNa	2	3	1	3	2	4	2	2	2	4	5	5	2	2	6	3	3	6	4
HNz	2	5	2	3	2	2	2	3	2	3	4	3	2	2	6	2	3	6	6
HB	3	1	3	3	5	4	3	3	3	3	3	3	3	5	4	4	3	4	7
TRM	6	4	6	6	4	6	6	6	7	7	6	4	7	7	6	7	4	6	6
NEa	5	4	4	5	5	5	5	5	5	5	4	5	5	5	5	5	5	5	5
NEz	5	5	5	5	5	5	5	5	5	4	4	5	5	5	5	5	5	5	4
HFa	5	4	5	6	6	6	6	4	5	6	4	5	4	5	6	6	3	5	5
HFz	6	6	6	3	3	4	5	5	3	4	4	5	5	3	4	6	6	6	4
HNFa	4	5	4	5	5	5	5	5	5	6	6	5	5	5	6	4	5	6	4
HNFz	5	7	6	3	4	5	7	7	6	6	3	7	7	6	6	4	7	6	3
SEa	3	5	5	2	6	3	6	4	4	3	4	3	5	3	5	6	6	6	6
SEZz	3	6	4	5	4	3	2	2	3	2	6	2	2	2	6	4	3	4	7
Sa	6	4	6	4	6	6	5	6	6	5	5	6	6	5	5	6	4	6	6
Sz	5	6	6	2	3	3	3	4	2	2	5	4	5	2	4	5	5	6	6
TB	5	6	6	5	6	5	6	6	5	6	6	4	6	5	6	6	5	6	3
TRW	6	5	6	4	4	4	6	6	4	4	5	6	6	5	5	6	6	6	5
U	5	5	5	5	4	5	5	5	4	5	4	5	5	4	5	4	5	5	5

Finally,

I would like to express my gratitude to all my colleagues, friends and family, who have contributed to this thesis in different ways.

A sincere thanks goes to my supervisor, Siegfried Demuth, who asked me to join the ARIDE project in 1998. His advice and the co-operation with the ARIDE project participants have inspired my work, in fact have made work a pleasure throughout the entire project period. Funding by the European Community Framework Programme for Research and Technical Development under contract no. ENV4-CT97-0553 provided a safe position for research. My study on droughts across Europe enormously benefited from the European experience and input by (from west to east): Maria João Santos, Raquel Veríssimo (Portugal), Javier Álvarez, Teodoro Estrela (Spain), Alan Gustard, Gwyn Rees, Maxine Zaidman (UK), Henny van Lanen, Lies Peters (The Netherlands), Lena Tallaksen and Hege Hisdal (Norway) and all colleagues from the NE-FRIEND Low Flow Group. I am very grateful to Lena Tallaksen for taking over the 'Korreferat' of my thesis.

Still, the major part of my European research was carried out in front of my map of Europe in my office at the Institut für Hydrologie, Albert-Ludwigs-Universität, Freiburg, where I was working among the best colleagues one could imagine. Thanks to all of you! Working with Bernhard Lehner, Andreas Kaul, Achim Odziomek and Birgit Hassler during their thesis work (Diplomarbeit) was a pleasure and their input greatly improved my research. Furthermore, I have particularly appreciated the constant advice as well as last-minute proofreading by Jens Lange. My office colleagues Paul Königer and Stephen Schrempp also earn a special thanks for a nice work environment never lacking the mood for discussions, coffee, etc.

Thank you very much to John and Vickey for kindly reviewing my English writing.

I am deeply grateful for the continuous encouragement and loving care of my parents and my sister who made life for me easy and enjoyable throughout the busy PhD years. They even made sure, I never had to abstain from my (expensive) passion for skiing.

After all, the key to the successful completion of my thesis was the loving support from my husband Markus Weiler. The details of his support are too numerous to be named, and besides providing an amiable home also included motivating scientific discussions and the encouragement I sometimes needed to overcome the hesitation to implement my ideas.

Kerstin Stahl